

Table S1. Primers used in this study.

Primer	Sequence	Target
DdTPS9f	<u>GGATCC</u> CATGTATTCTCTTCAATGATTCAAATTC	pET32a::DdTPS9
DdTPS9r	CTCGAGTTATTTAATAAAAATTTATCAACAAATTTC	pET32a::DdTPS9
DpTPS10f	<u>GGATCC</u> CATGGAAGCTATAAACAAAAAGAAGT	pET32a::DpTPS10
DpTPS10r	CTCGAGTCATCGAAAAATGTTTTATGTTGGAC	pET32a::DpTPS10
DpTPS11f	<u>GGATCC</u> CATGGATATAAAACAAAAACCAAATG	pET32a::DpTPS11
DpTPS11r	CTCGAGTTAATTATTTTATTGATATAGTTTG	pET32a::DpTPS11
JR098f	CATTAACTGACCCTTACATTTTAC	DdTPS9-N236D
JR098r	GTAAAAAAATGTAAAGGGTCAGTTAAATG	DdTPS9-N236D
JR099f	CATTAACTGCCCTTACATTTTAC	DdTPS9-N236A
JR099r	GTAAAAAAATGTAAAGGGGCAGTTAAATG	DdTPS9-N236A
JR106f	GCTTATTGTGACACTTTTATTTTAC	DpTPS10-N236D
JR106r	GTAAAAAAATAAAAGTGTACAATAAGC	DpTPS10-N236D
JR107f	GCTTATTGTGCCACTTTTATTTTAC	DpTPS10-N236A
JR107r	GTAAAAAAATAAAAGTGGCACAAATAAGC	DpTPS10-N236A
JR110f	CCAGATACTATGGATTATGTAAAAATTATG	DpTPS11-N243D
JR110r	CATAATTTTACATAATCCATAGTATCTGG	DpTPS11-N243D
JR111f	CAGATACTATGGCTATGTAAAAATTATG	DpTPS11-N243A
JR111r	CATAATTTTACATAAGCCATAGTATCTG	DpTPS11-N243A
JR149f	GACAGCCCAGATCTG	pET32a start forward
JR149r	CAGATCTGGGCTGTC	pET32a start reversed
JR150f	CGAATTCGAGCTCCG	pET32a end forward
JR150r	CGGAGCTCGAATTCTG	pET32a end reversed

Strains and culture conditions

Dictyostelium discoideum strain AX4 (DBS0235552) and *Dictyostelium purpureum* strain AX1 (DBS0308472) were obtained from the Dictybase Stock Center (www.dictybase.org). Both *Dictyostelium* species were cultured with bacterium *Klebsiella pneumonia* on SM agar plates, which were incubated at 22 °C under continuous darkness.

Gene cloning

For both *D. discoideum* and *D. purpureum*, the cultured cells were harvested just prior to the formation of fruiting bodies and subject to RNA extraction. Total RNA was isolated using RNeasy mini kit (<https://www.qiagen.com>) and made into cDNAs using the First-strand cDNA synthesis kit (<https://www.gelifesciences.com>). Full-length cDNAs for *DdTPS9*, *DpTPS10* and *DpTPS11* were amplified using PfuUltra II fusion high-fidelity DNA polymerase (<https://www.agilent.com>) with modified gene specific-primers listed in Table S1. The amplified cDNAs were cloned into pGEM-T Easy vector (<https://www.promega.com>) and confirmed by sequencing. Next, each cDNA was excised from the pGEM-T vector with the digestion of restriction enzymes *BamHI* and *Xhol*, and the fragment was inserted into the *BamHI* and *Xhol* cloning sites of the pET32a vector.

For site-directed mutagenesis, a two-step PCR approach was pursued. In the first PCR reaction, two fragments for two target mutations were amplified from each of the three expression constructs in pET32a (first fragment using primers JR149f and JR098r or JR099r [*DdTPS9*], JR106r or JR107r [*DpTPS10*], JR110r or JR111r [*DpTPS11*]; second fragment using primers JR150r and JR098f or JR099f [*DdTPS9*], JR106f or JR107f [*DpTPS10*], JR110f

or JR111f [DpTPS11]). PCR conditions using Q5 DNA polymerase (NEB, Ipswich, MA, USA) were as follows: initial denaturation 30 s 98 °C, denaturation 10 s 98 °C, annealing 30 s between 60 °C and 65 °C, elongation 30 s 72 °C, cycle repeated 33 times, final elongation 5 min 72 °C. PCR products were obtained from gel slices. In a second PCR, the two fragments were combined using primers JR149f and JR150r to yield one mutation-containing fragment, which was homologously recombined to linear pET32a (obtained by PCR using JR149r and JR150f) using In-Fusion HD cloning kit (Takara Bio, Shimogyō-ku, Kyoto, Japan) following the manufacturers protocol. The resulting plasmids were isolated from single colonies and the correct insertion of the gene containing the desired mutation(s) was checked by analytical digest and sequencing. Correct plasmids were shuttled to *E. coli* BL21(DE3).

Gene expression and protein purification

E. coli BL21(DE3) transformants were grown in LB medium precultures containing ampicillin (100 µg/mL) overnight at 37 °C with shaking. Main cultures were inoculated by transferring the preculture (1/1000) to culture flasks with LB-ampicillin. The cells were grown at 37 °C until OD₆₀₀ = 0.4-0.6 was reached. The cultures were cooled to 18 °C, before protein expression was induced by addition of IPTG (400 µM). Incubation was continued overnight at 18 °C with shaking and the cells were harvested by centrifugation (10000 x g, 4 min). The cell pellet was suspended in binding buffer (10 mL L⁻¹ culture; 20 mM Na₂HPO₄, 500 mM NaCl, 20 mM imidazole, 1 mM MgCl₂, pH = 7.4, 4 °C). Ultra-sonification on ice (5x 0.5 min; 50% power) was used to lyse the cells, followed by centrifugation (15000 x g, 4 °C, 7 min). The soluble enzyme fractions were loaded onto Ni²⁺-NTA columns (Qiagen, Venlo, Netherlands) and the bound proteins were washed with binding buffer (2x 10 mL/L culture). The proteins were eluted by the addition of elution buffer (2x 6.25 mL/L culture; 20 mM Na₂HPO₄, 500 mM NaCl, 500 mM imidazole, 1 mM MgCl₂, pH = 7.4, 4 °C). Elution fractions were checked by SDS-PAGE (Figure S1) and the protein concentrations were estimated by Bradford assay¹ (typical concentrations: 1.0 mg/mL for DdTPS9, 0.34 mg/mL for DpTPS10 and 0.45 mg/mL for DpTPS11).

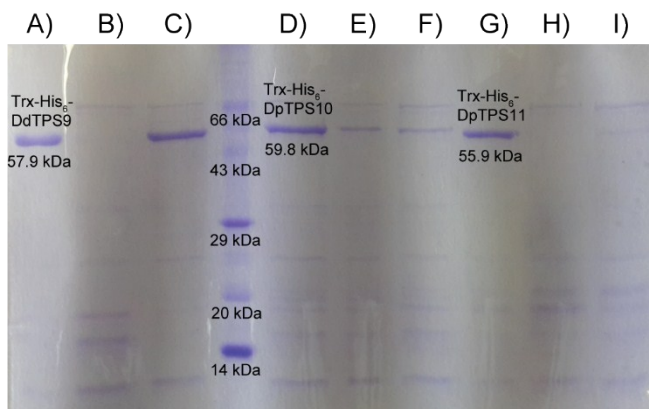


Figure S1. SDS-PAGE of recombinant protein preparations of A) (–)-β-barbatene synthase from *Dictyostelium discoideum* AX4 (DdTPS9), B) DdTPS9-N236D, C) DdTPS9-N236A, D) (–)-β-araneosene synthase from *Dictyostelium purpureum* AX1 (DpTPS10), E) DpTPS10-N249D, F) DpTPS10-N249A, G) (S)-(+) -nephthenol synthase from *D. purpureum* AX1 (DpTPS11), H) DpTPS11-N243D, and I) DpTPS11-N243A. Calculated molecular weights for the TrxA-fusion proteins are given.

GC/MS and GC/MS-QTOF analyses

GC/MS analyses were performed on a 7890B GC connected to a 5977A mass selective detector (Agilent, Santa Clara, CA, USA). The GC was equipped with a HP5-MS fused silica capillary column (30 m, 0.25 mm i. d., 0.50 μm film). Specific GC settings were 1) inlet pressure: 77.1 kPa, He at 23.3 mL min⁻¹, 2) injection volume: 2 μL , 3) temperature program: 5 min at 50 °C increasing at 5 °C min⁻¹ to 320 °C, 4) 60 s valve time, and 5) carrier gas: He at 1.2 mL min⁻¹. MS settings were 1) source: 230 °C, 2) transfer line: 250 °C, 3) quadrupole: 150 °C and 4) electron energy: 70 eV. Retention indices (*I*) were determined from retention times in comparison to the retention times of of *n*-alkanes (C₇-C₄₀).

A 7890B GC connected to a 7200 accurate-mass Q-TOF detector (Agilent) equipped with a HP5-MS fused silica capillary column (30 m, 0.25 mm i. d., 0.50 μm film) were used for GC/MS-QTOF analyses. MS parameters were 1) inlet pressure: 83.2 kPa, He at 24.6 mL min⁻¹, 2) transfer line: 250 °C, 3) electron energy 70 eV. GC parameters were 1) temperature program: 5 min at 50 °C increasing at 5 °C min⁻¹ to 320 °C, 2) injection volume: 1 μL , 3) split ratio: 50:1, 60 s valve time, and 4) carrier gas: He at 1 mL min⁻¹.

NMR spectroscopy

NMR spectra were recorded on a Bruker (Billerica, MA, USA) Avance I (300 MHz), Avance I (400 MHz), Avance I (500 MHz), Avance III HD Prodigy (500 MHz) or an Avance III HD Cryo (700 MHz) NMR spectrometer. Spectra were measured in C₆D₆ and referenced against solvent signals (¹H-NMR, residual proton signal: δ = 7.16; ¹³C-NMR: δ = 128.06).²

Incubation experiments with recombinant TPSs

Small scale incubations for testing the substrate scope, and labelling experiments were carried out by dissolving the diphosphate substrate(s) in substrate buffer (1 mL; 25 mM NH₄HCO₃). The solutions were diluted with incubation buffer (5 mL; 50 mM Tris/HCl, 10 mM MgCl₂, 20% glycerol, pH = 8.2), before adding enzyme elution fractions (1 mL each). The reactions were further diluted by binding buffer (to 10 mL total reaction volume) and incubated at 28 °C with shaking for 3 h. Extraction was done by hexane (150 µL) or C₆D₆ (650 µL, 300 µL) and the extracts were analysed by GC/MS and/or NMR.

For large scale product isolation, a solution of the corresponding diphosphate substrate (100 mg) in substrate buffer (20 mL) was dropped to a slowly stirred mixture of TPS elution fraction (100 mL), incubation buffer (200 mL) and binding buffer (100 mL) over 2 h at room temperature. Incubation was further continued for 4 h at 28 °C with shaking. The reaction was extracted with pentane (2x 300 mL) and the extracts were dried with MgSO₄, concentrated under reduced pressure and purified by column chromatography on silica gel ([pentane] for **4** and **5**, [pentane/Et₂O (5:1)] for **6**) to afford the target terpenes as colourless oils (**4**: 2.3 mg; **5**: 5.4 mg; **6**: 5.4 mg).

(–)-β-Barbatene, (3a*R*,4*R*,8*R*,8a*S*)-3a,4,8a-trimethyl-7-methylenedecahydro-4,8-methanoazulene (**4**). *R*_f (pentane) = 0.92. [α]_D²⁰ = –11.1° (c 0.25, C₆D₆). HRMS (QTOF): *m/z* = 204.1879 (calc. for [C₁₅H₂₄]⁺ 204.1873). GC (HP5-MS): *I* = 1456. MS (EI, 70 eV): *m/z* (%) = 204 (6), 189 (17), 175 (6), 161 (7), 148 (6), 133 (10), 119 (11), 111 (38), 108 (100), 96 (99), 93 (93), 81 (60), 69 (14), 55 (14), 41 (9), cf. Figure S2. NMR data are given in Table S2 and Figures S3–S9.

(–)-β-Araneosene, (3a*S*,6*E*,10*E*,12a*S*)-6,10,12a-trimethyl-3-(propan-2-ylidene)-1,2,3,3a,4,5,8,9,12,12a-decahydrocyclopenta[11]annulene (**5**). *R*_f (pentane) = 0.78. [α]_D²⁰ = –133.0° (c 0.64, C₆D₆). HRMS (QTOF): *m/z* = 272.2499 (calc. for [C₂₀H₃₂]⁺ 272.2499). GC (HP5-MS): *I* = 2025. MS (EI, 70 eV): *m/z* (%) = 272 (12), 257 (7), 229 (25), 216 (35), 201 (12), 189 (35), 175 (13), 161 (37), 147 (18), 136 (68), 135 (67), 121 (100), 107 (40), 93 (29), 79 (19), 67 (16), 55 (9), 41 (8), cf. Figure S15. NMR data are given in Table S3 and Figures S16–S22.

(+)-Nephthenol, 2-((*S*,3*E*,7*E*,11*E*)-4,8,12-trimethylcyclotetradeca-3,7,11-trien-1-yl)propan-2-ol (**6**). *R*_f ([cyclohexane/EtOAc (3:1)]) = 0.63. [α]_D²⁰ = +45.5° (c 0.68, C₆D₆). HRMS (QTOF): *m/z* = 272.2501 (calc. for [C₂₀H₃₂]⁺ 272.2499, [M-H₂O]⁺). GC (HP5-MS): *I* = 2164. MS (EI, 70 eV): *m/z* (%) = 272 (38), 257 (26), 229 (20), 215 (7), 202 (13), 201 (13), 189 (26), 175 (18), 161 (33), 147 (36), 136 (48), 135 (49), 133 (43), 121 (88), 107 (85), 93 (100), 81 (74), 79 (46), 69 (33), 68 (47), 67 (51), 59 (42), 55 (25), 53 (14), 43 (22), 41 (22), cf. Figure S26. NMR data are given in Table S4 and Figures S27–S33.

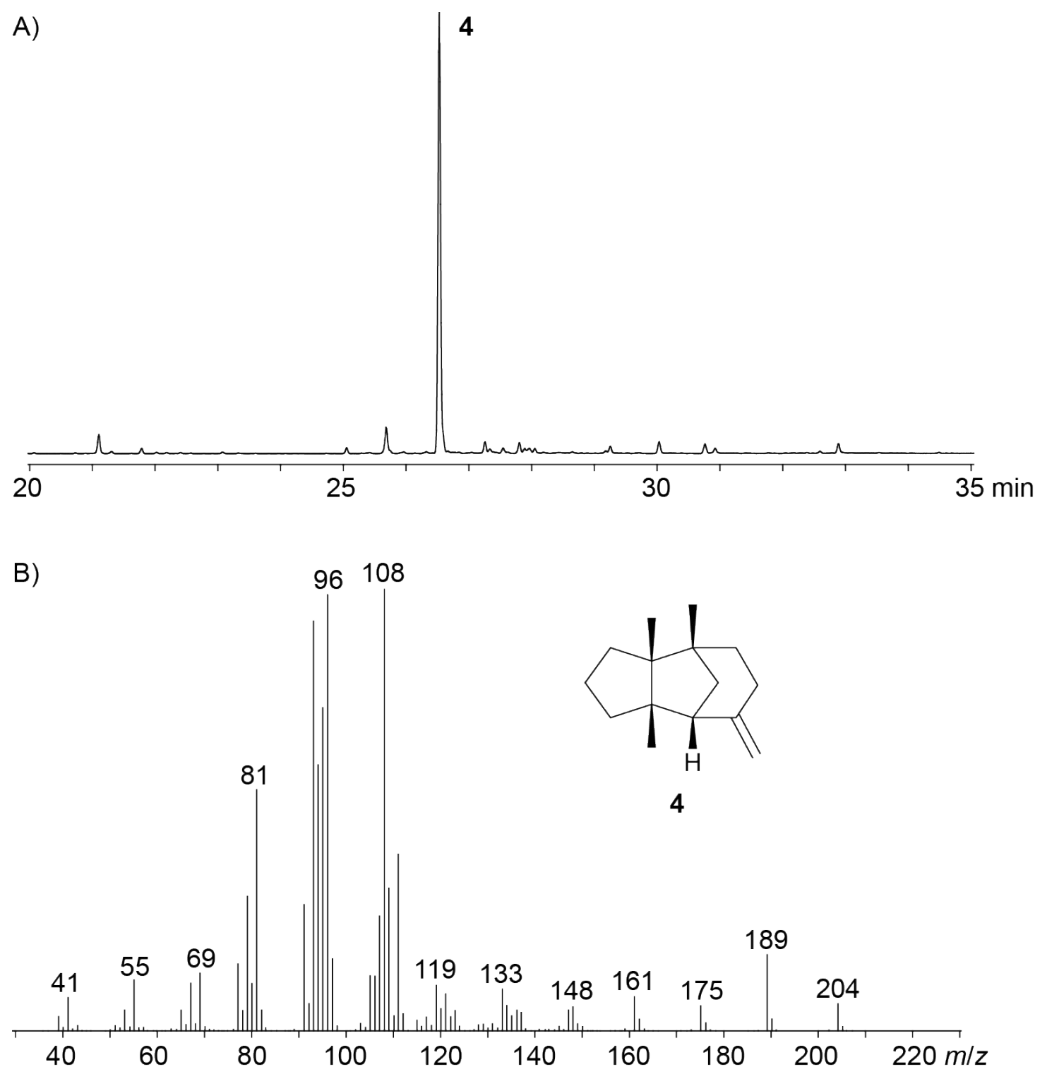
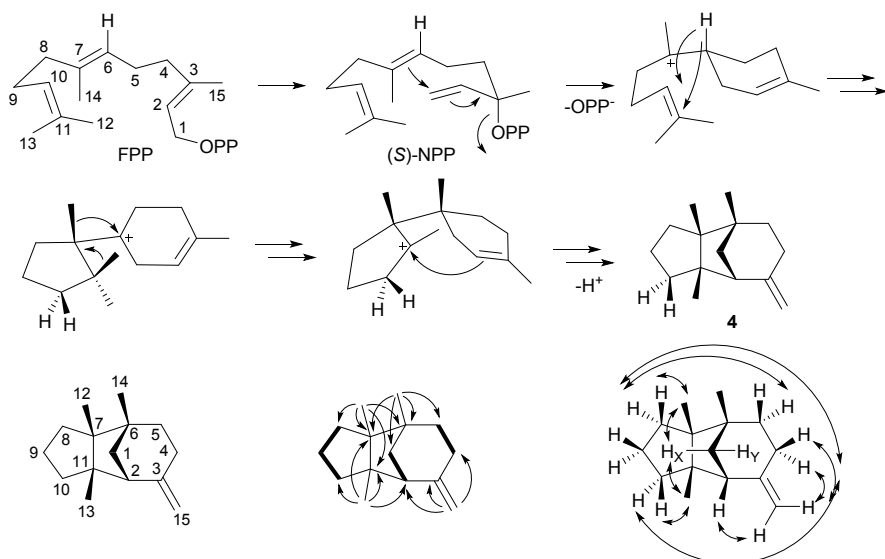


Figure S2. A) Total ion chromatogram of an extract from the incubation of FPP with DdTPS9. B) EI mass spectrum of β -barbatene (**4**).



Scheme S1. Short biosynthesis and structure elucidation of **4**. Carbon numbers refer to the corresponding positions in FPP. H,H-COSY spin systems are represented by bold bonds, single headed arrows show HMBC correlations and NOESY correlations are depicted by double headed arrows.

Table S2. NMR data of β -barbatene (**4**) in C_6D_6 recorded at 298 K.

C[a]		^{13}C [b]	1H [b]	^{13}C [c]
1	CH ₂	47.04	1.99 (ddd, $J = 11.4, 5.0, 3.1$, H _X) 1.35 (m, H _Y)	46.8
2	CH	56.44	2.20 (d, $J = 5.0$)	56.0
3	C _q	151.58	—	152.0
4	CH ₂	29.07	2.41 (m, H _{α}) 2.18 (dd, $J = 16.6, 8.1$, H _{β})	28.7
5	CH ₂	38.33	1.63 (ddd, $J = 13.7, 8.1, 2.5$, H _{α}) 1.34 (m, H _{β})	38.0
6	C _q	43.27	—	43.0
7	C _q	54.41	—	54.1
8	CH ₂	35.86	1.82 (m, H _{α}) 1.03 (m, H _{β})	35.5
9	CH ₂	27.85	1.75 (m, 2H)	27.5
10	CH ₂	37.45	1.87 (m, H _{α}) 1.21 (m, H _{β})	37.0
11	C _q	55.73	—	55.4
12	CH ₃	23.54	0.84 (s)	23.3
13	CH ₃	27.68	0.99 (s)	27.5
14	CH ₃	24.95	0.80 (s)	24.8
15	CH ₂	108.28	4.74 (m, 2H)	107.5

[a] Carbon numbering indicates the origin of each carbon from FPP by identical number as shown in Scheme S1. [b] Chemical shifts δ in ppm, multiplicity: s = singlet, d = doublet, m = multiplet, br = broad, coupling constants J are given in Hertz. [c] ^{13}C -NMR data in $CDCl_3$ from ref. [3].

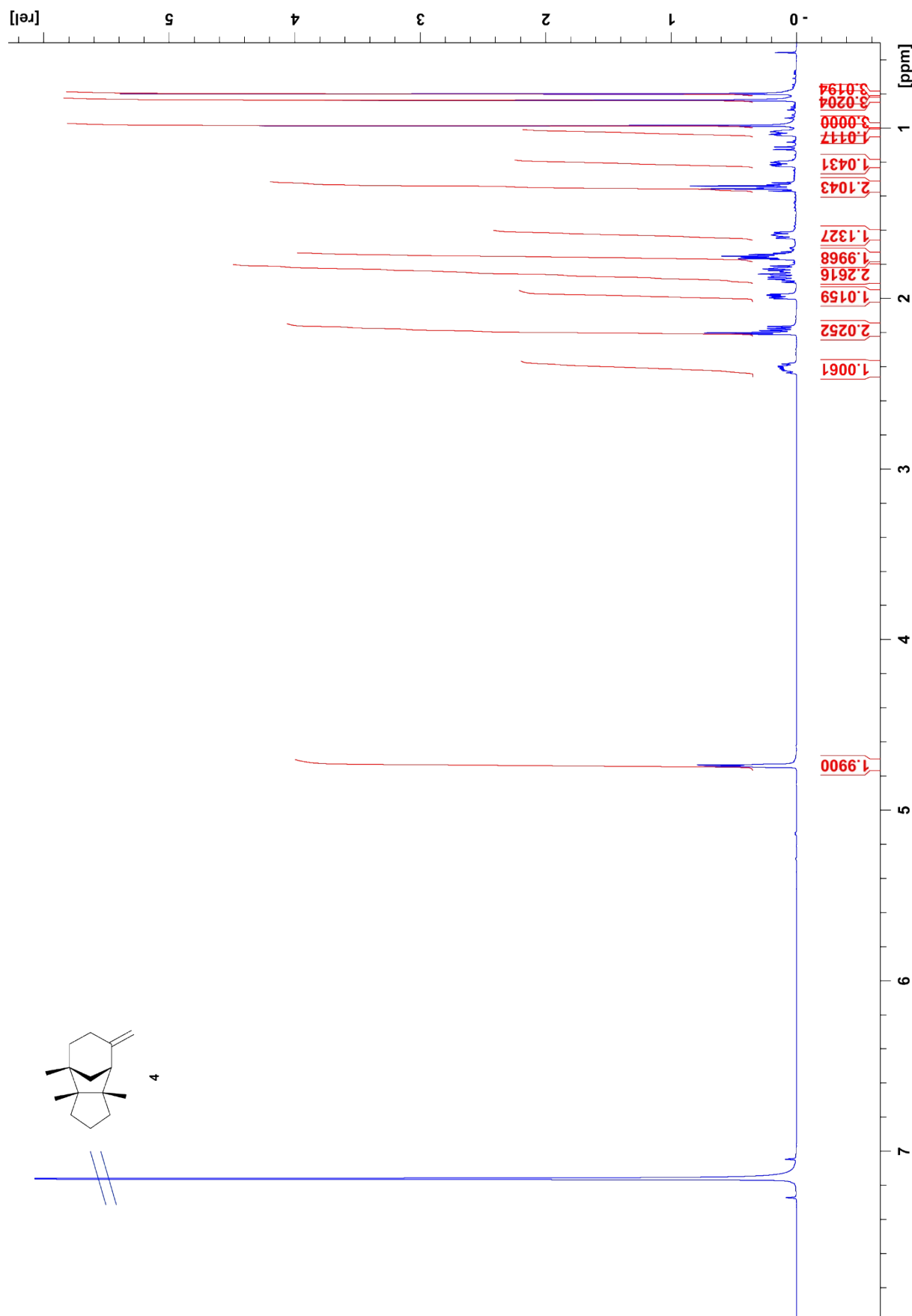


Figure S3. ^1H -NMR spectrum of **4** (700 MHz, C_6D_6).

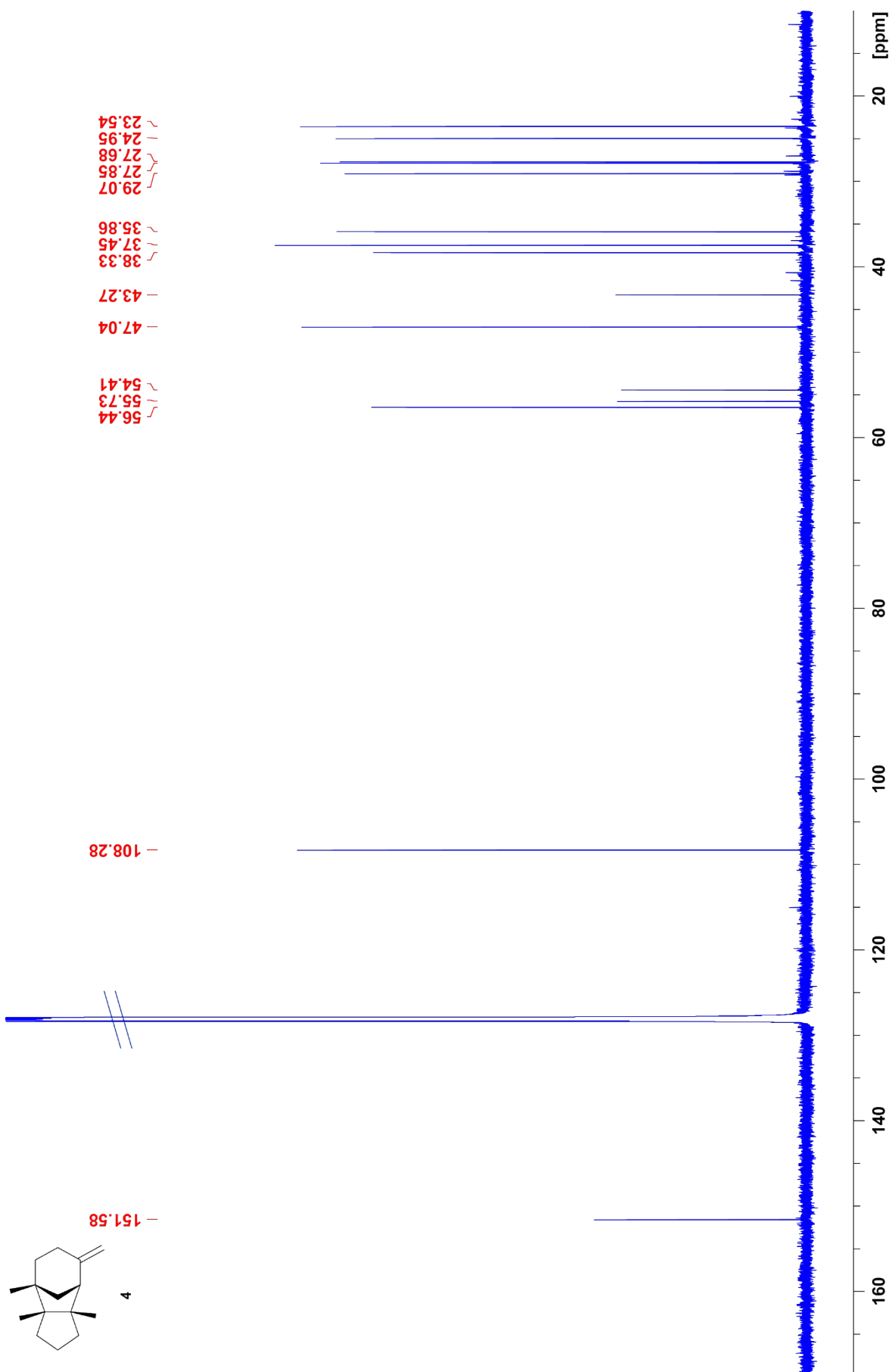


Figure S4. ^{13}C -NMR spectrum of **4** (175 MHz, C_6D_6).

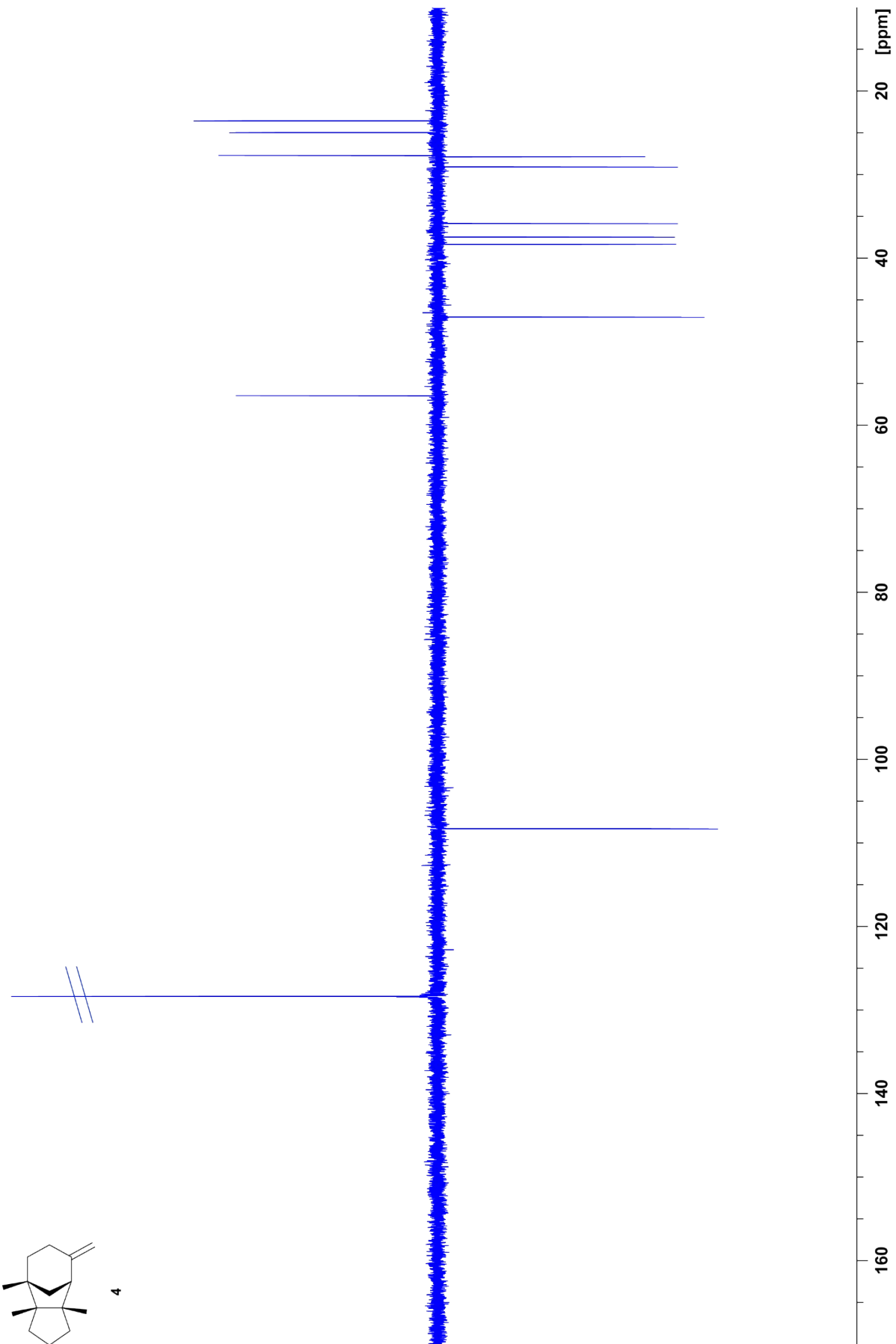


Figure S5. ¹³C-DEPT spectrum of **4** (175 MHz, C₆D₆).

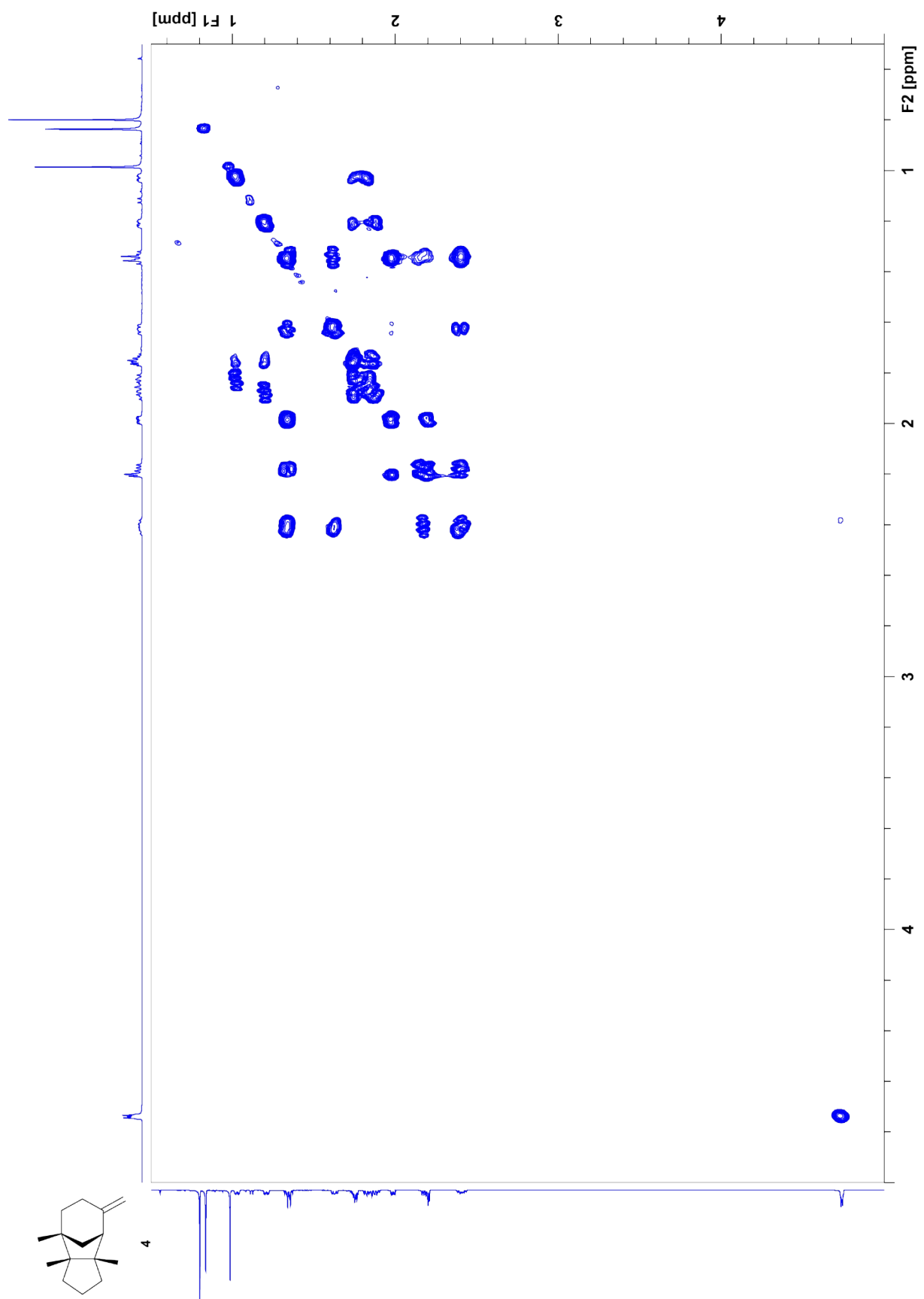


Figure S6. $^1\text{H},^1\text{H}$ -COSY spectrum of **4** (700 MHz, C_6D_6).

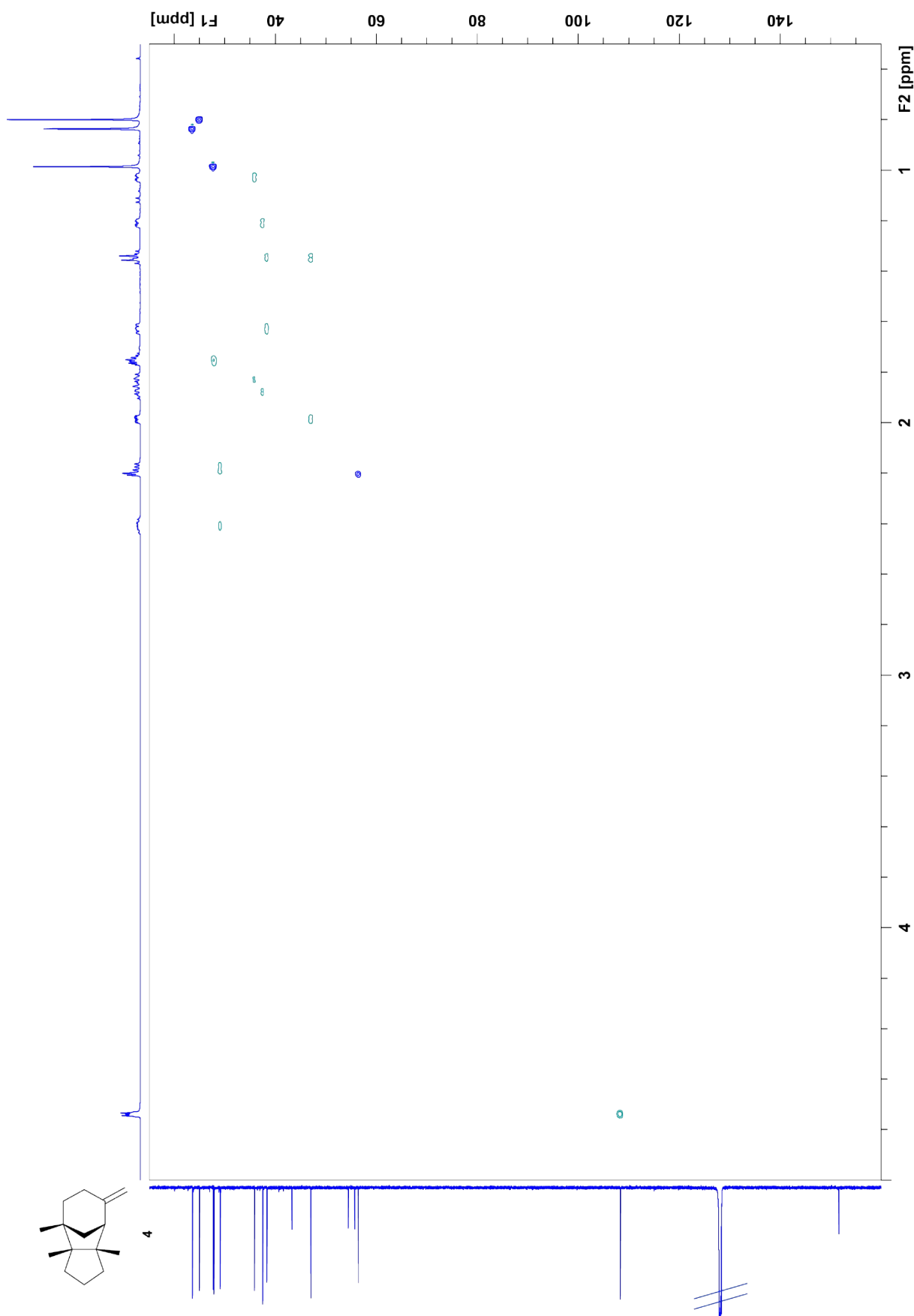
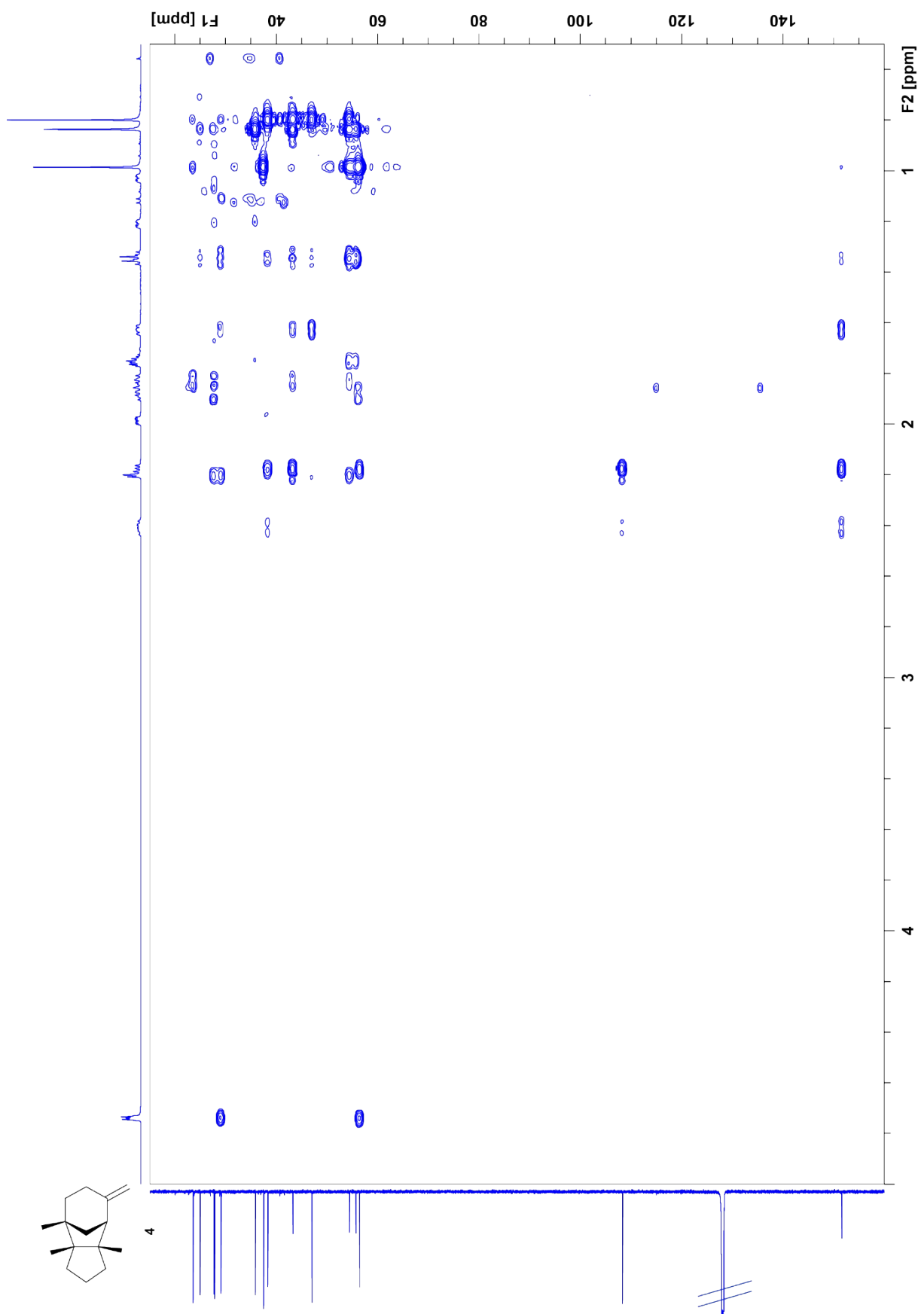


Figure S7. HSQC spectrum of **4** (700 MHz, C_6D_6).



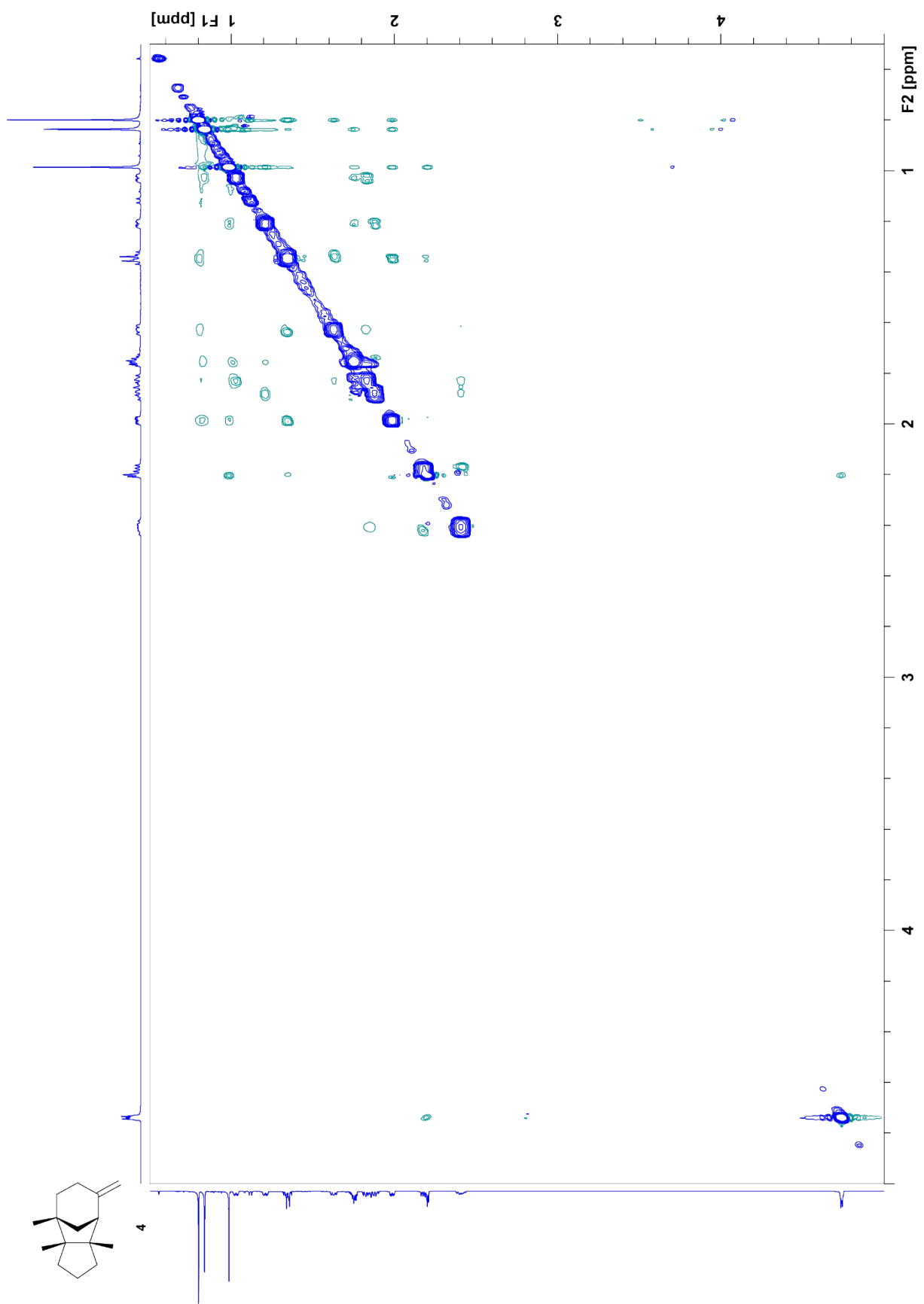


Figure S9. NOESY spectrum of **4** (700 MHz, C₆D₆).

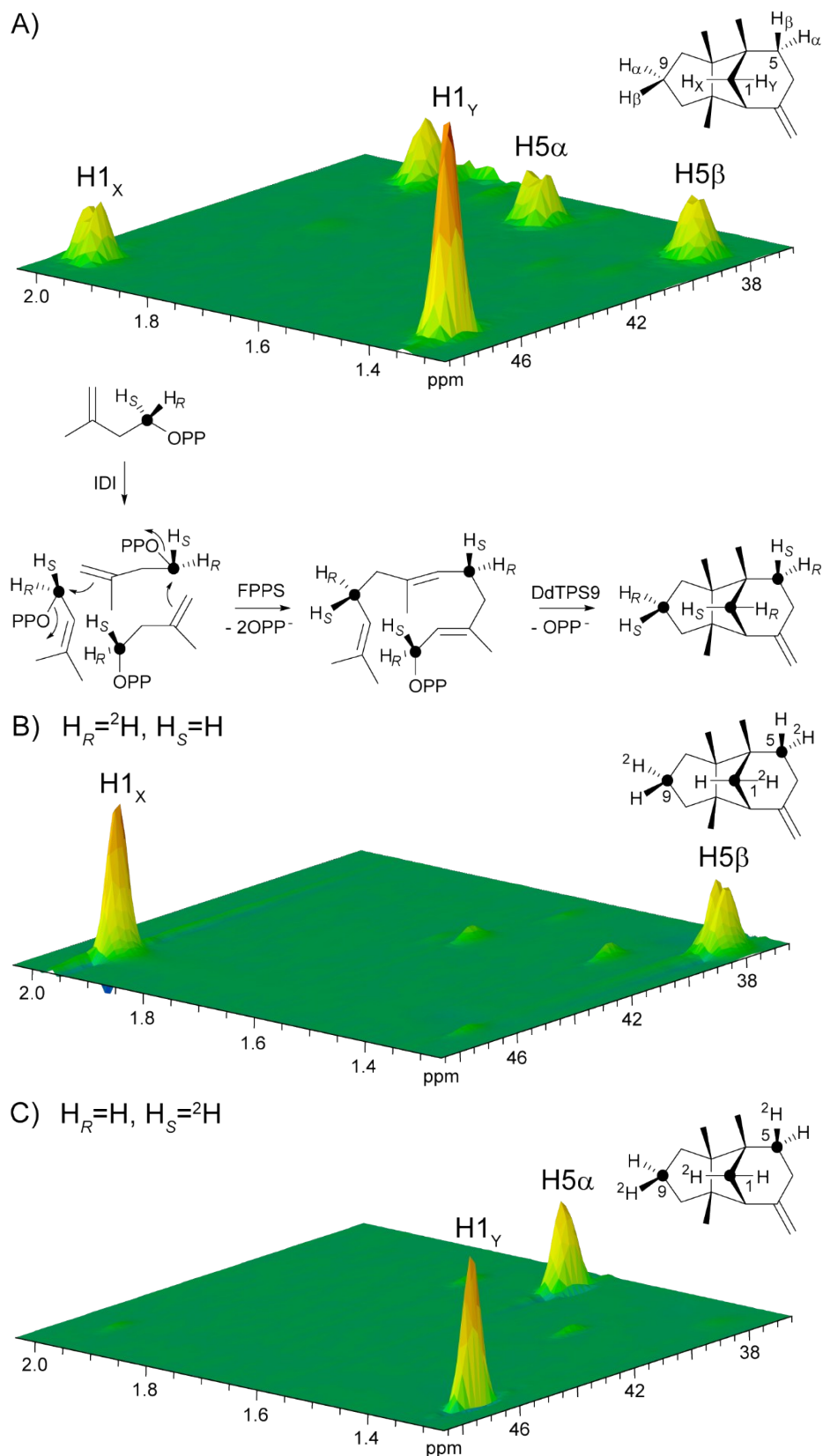


Figure S10. Partial HSQC spectra of A) unlabelled **4**, B) an incubation of (*R*)-(1-¹³C, 1-²H)IPP⁴ with IDI,⁴ FPPS⁵ and DdTPS9 and C) an incubation of (*S*)-(1-¹³C, 1-²H)IPP⁴ with IDI, FPPS and DdTPS9 showing the selective incorporation of deuterium into the methylene positions C1 and C5. The observed outcome is in line with the shown absolute configuration of **4**. Because of overlaying hydrogen signals, the labelled position C9 is not shown. Black dots represent ¹³C-labelled carbon atoms.

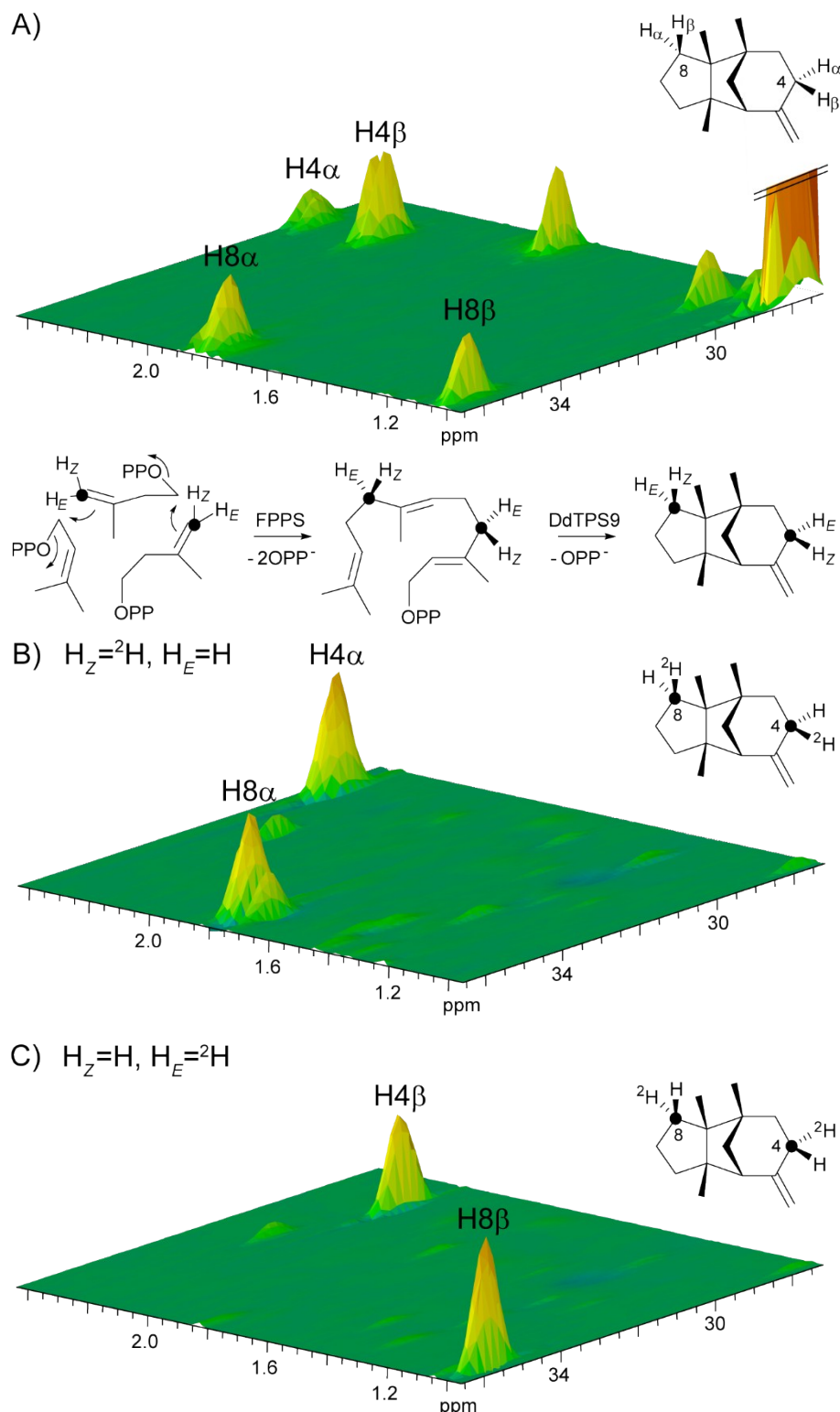


Figure S11. Partial HSQC spectra of A) unlabelled **4**, B) an incubation of (*Z*)-(4-¹³C,4-²H)IPP⁶ with DMAPP, FPPS and DdTPS9 and C) an incubation of (*E*)-(4-¹³C,4-²H)IPP⁶ with DMAPP, FPPS and DdTPS9 showing the selective incorporation of deuterium into the methylene positions C4 and C8. The observed outcome is in line with the shown absolute configuration of **4**. Black dots represent ¹³C-labelled carbon atoms.

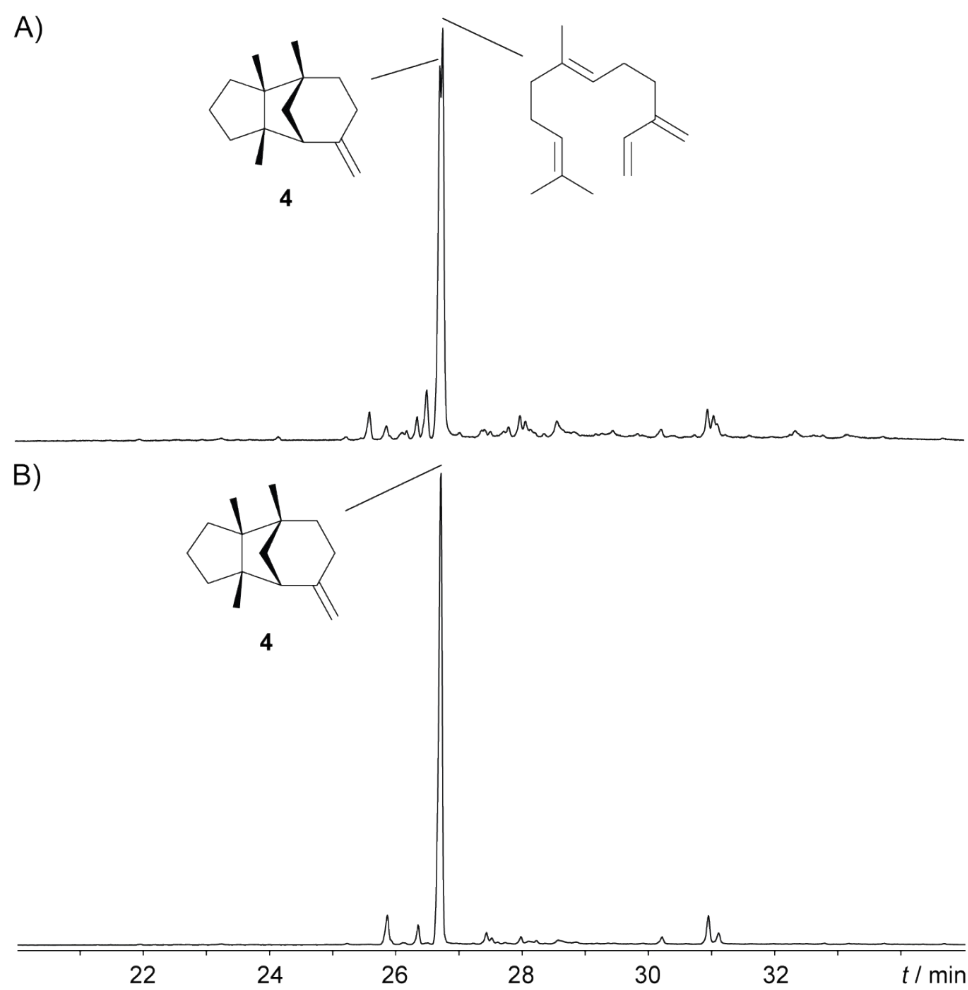
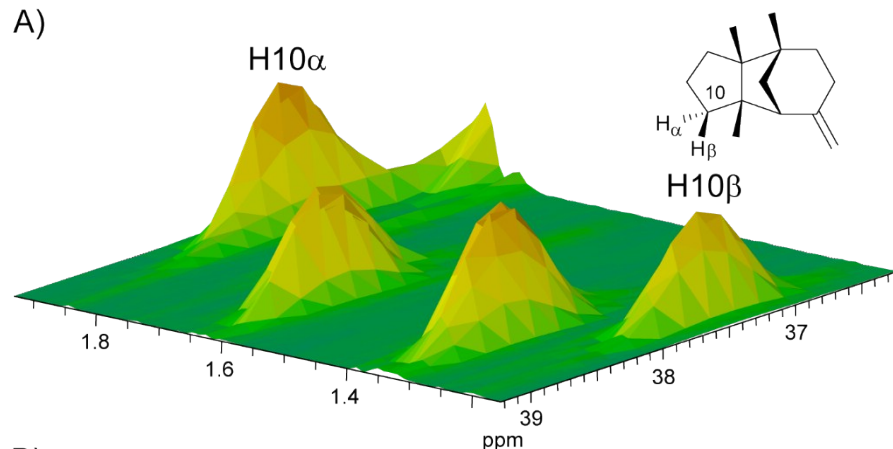


Figure S12. Total ion chromatograms of extracts from the incubation of DdTPS9 with A) (*R*)-NPP⁷ and B) (*S*)-NPP.⁷

Incubation experiment of DdTPS9 with (2-¹³C)DMAPP and (2-²H)DMAPP

(2-²H)DMAPP⁸ (1 mg) was dissolved in substrate buffer (100 µL), diluted with binding buffer (180 µL) and incubation buffer (500 µL), before IDI elution fraction was added (220 mL). The reaction was incubated at 37 °C for 30 min, before heat inactivation was performed by keeping the sample for 10 min at 90 °C with shaking. The mixture was centrifuged (1 min, 14000 × g) and the soluble fraction was added to a mixture of (2-¹³C)DMAPP⁹ dissolved in substrate buffer (1.12 mL), incubation buffer (5 mL), binding buffer (2 mL), FPPS elution fraction (440 µL) and DdTPS9 elution fraction (440 µL). The reaction was further incubated for 3 h at 28 °C, extracted with C₆D₆ (650 µL; 250 µL) and analysed by NMR.

A)



B)

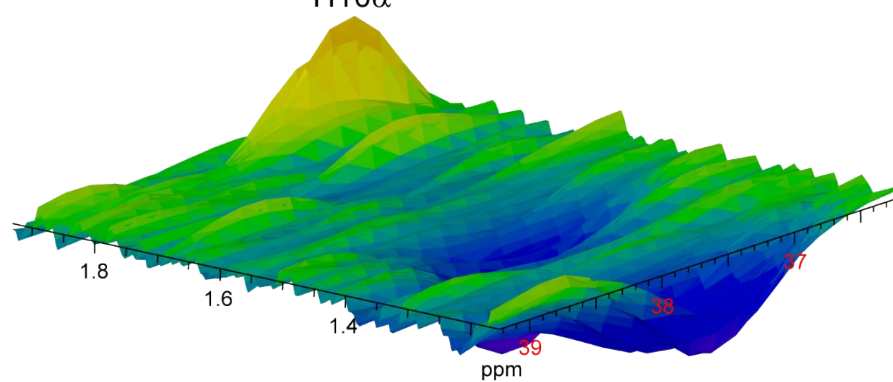
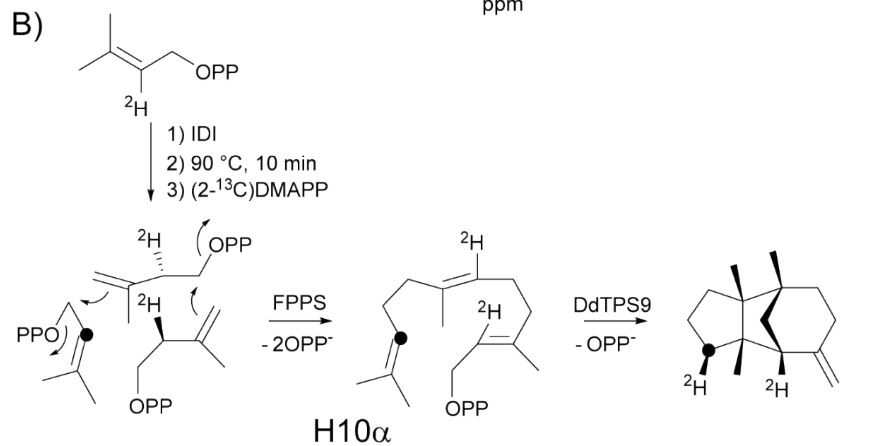


Figure S13. Movement of H6 to C10 in the cyclisation mechanism of **4**. Partial HSQC spectra of A) unlabelled **4** and B) an incubation experiment using (2-²H)DMAPP with IDI, followed by heat inactivation of IDI, addition of (2-¹³C)DMAPP, FPPS and DdTPS9. Note that HSQC B) was recorded in biphasic mode to differentiate between CH/CH₃ signals (positive crosspeaks, orange) and CH₂ signals (negative crosspeaks, blue, caused by contaminants in the extracted mixture and are not belonging to labelled **4**). Black dots represent ¹³C-labelled carbon atoms.

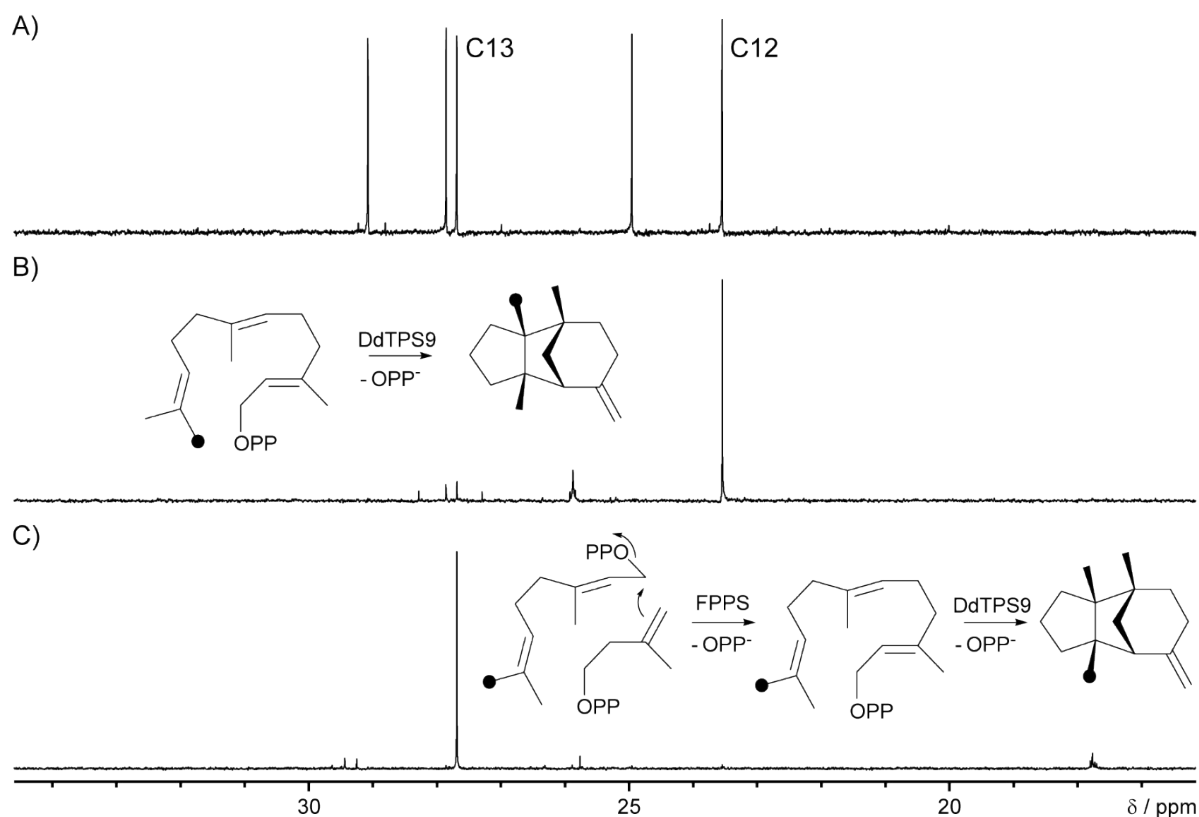


Figure S14. Partial ^{13}C -NMR spectra of A) unlabelled **4**, B) incubation of $(12\text{-}^{13}\text{C})\text{FPP}^{10}$ with DdTPS9 and C) incubation of $(9\text{-}^{13}\text{C})\text{GPP}^{11}$ FPPS and DdTPS9. Black dots represent ^{13}C -labelled carbon atoms. The minor peak of C13 in B) is caused by an impure labelling of the starting material.

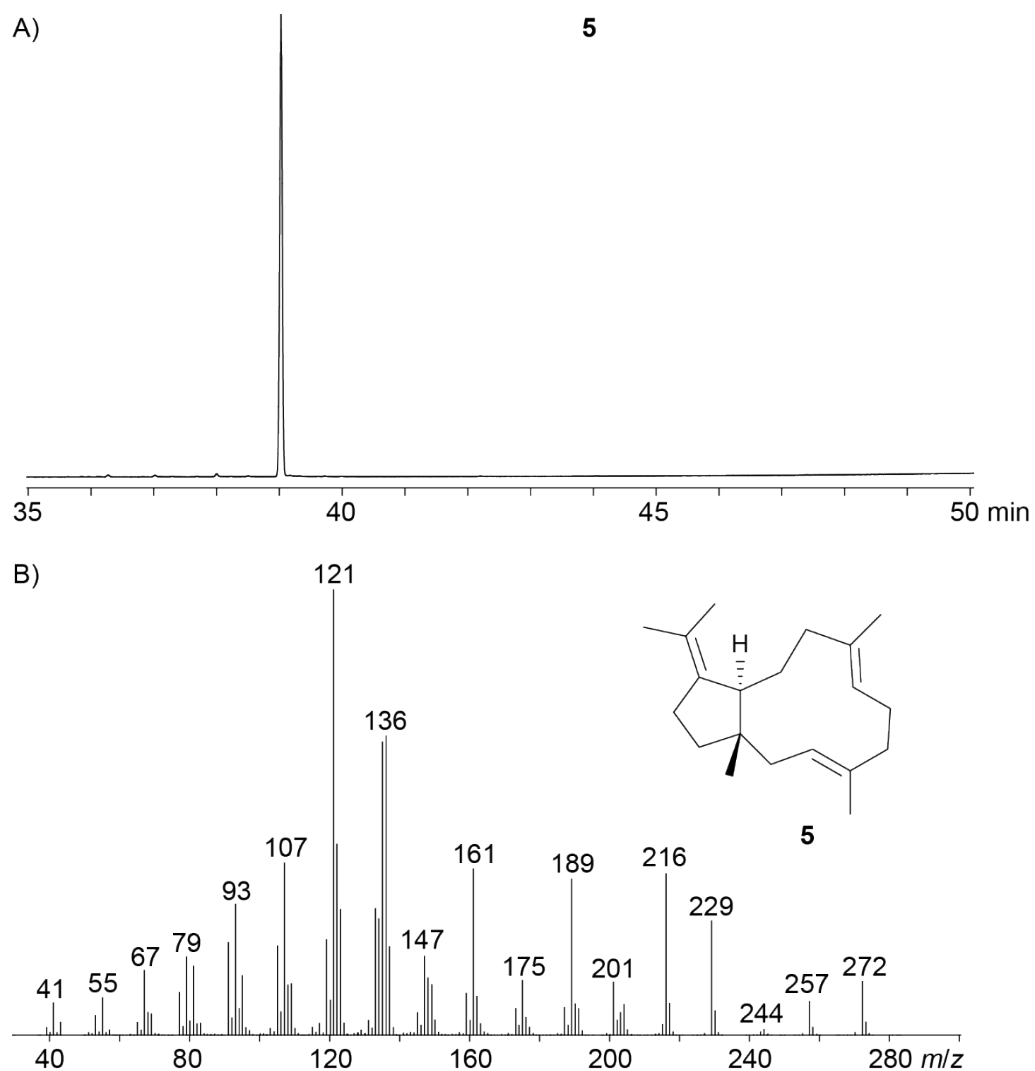
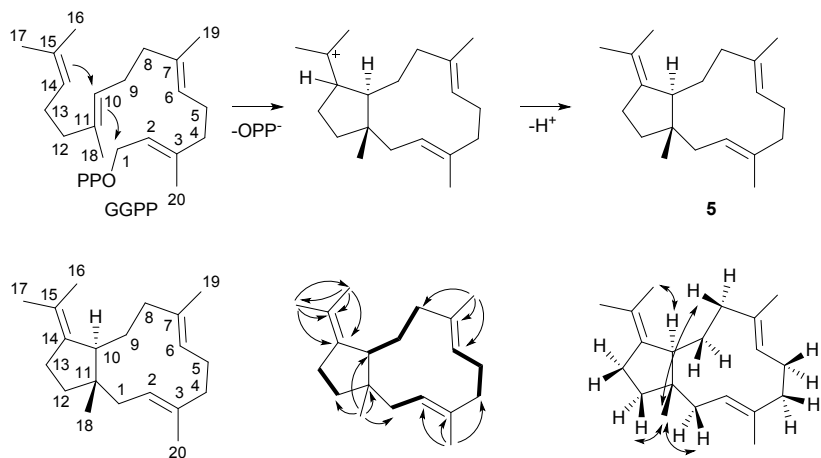


Figure S15. A) Total ion chromatogram of an extract from the incubation of GGPP with DPTS10. B) EI mass spectrum of β -araneosene (**5**).



Scheme S2. Short biosynthesis and structure elucidation of **5**. Carbon numbers refer to the corresponding positions in GGPP. H,H-COSY spin systems are represented by bold bonds, single headed arrows show HMBC correlations and NOESY correlations are depicted by double headed arrows.

Table S3. NMR data of β -araneosene (**5**) in C_6D_6 recorded at 298 K.

C[a]		^{13}C [b]	1H [b]	^{13}C [c]
1	CH_2	39.16	2.20 (dd, $J = 12.5, 11.5$, H_α) 1.52 (m, H_β)	38.7
2	CH	126.39	5.28 (ddm, $J = 11.3, 5.6$)	126.0
3	C_q	134.77	–	134.8
4	CH_2	40.30	2.16 (m, H_α) 2.08 (m, H_β)	40.0
5	CH_2	24.68	2.27 (m, H_α) 2.04 (m, H_β)	24.3
6	CH	129.93	4.92 (br d, $J = 10.8$)	129.3
7	C_q	132.27	–	132.5
8	CH_2	38.65	2.31 (ddd, $J = 12.7, 12.7, 5.7$, H_β) 2.07 (m, H_α)	38.2
9	CH_2	28.27	1.53 (m, H_β) 1.49 (m, H_α)	27.9
10	CH	42.43	2.52 (d, $J = 11.0$)	42.1
11	C_q	48.69	–	48.4
12	CH_2	40.63	1.66 (ddd, $J = 12.7, 10.3, 10.3$, H_β) 1.43 (dddd, $J = 12.7, 8.1, 3.0, 0.7$, H_α)	40.3
13	CH_2	28.67	2.26 (m, H_β) 2.24 (m, H_α)	28.3
14	C_q	143.05	–	142.5
15	C_q	122.11	–	122.0
16	CH_3	21.50	1.68 (br s)	21.2
17	CH_3	21.84	1.62 (br s)	21.7
18	CH_3	23.90	1.11 (s)	23.6
19	CH_3	16.43	1.63 (br s)	16.3
20	CH_3	15.47	1.46 (br s)	15.3

[a] Carbon numbering indicates the origin of each carbon from GGPP by identical number as shown in Scheme S2. [b] Chemical shifts δ in ppm, multiplicity: s = singlet, d = doublet, m = multiplet, br = broad, coupling constants J are given in Hertz. [c] ^{13}C -NMR data in $CDCl_3$ from ref. [12].

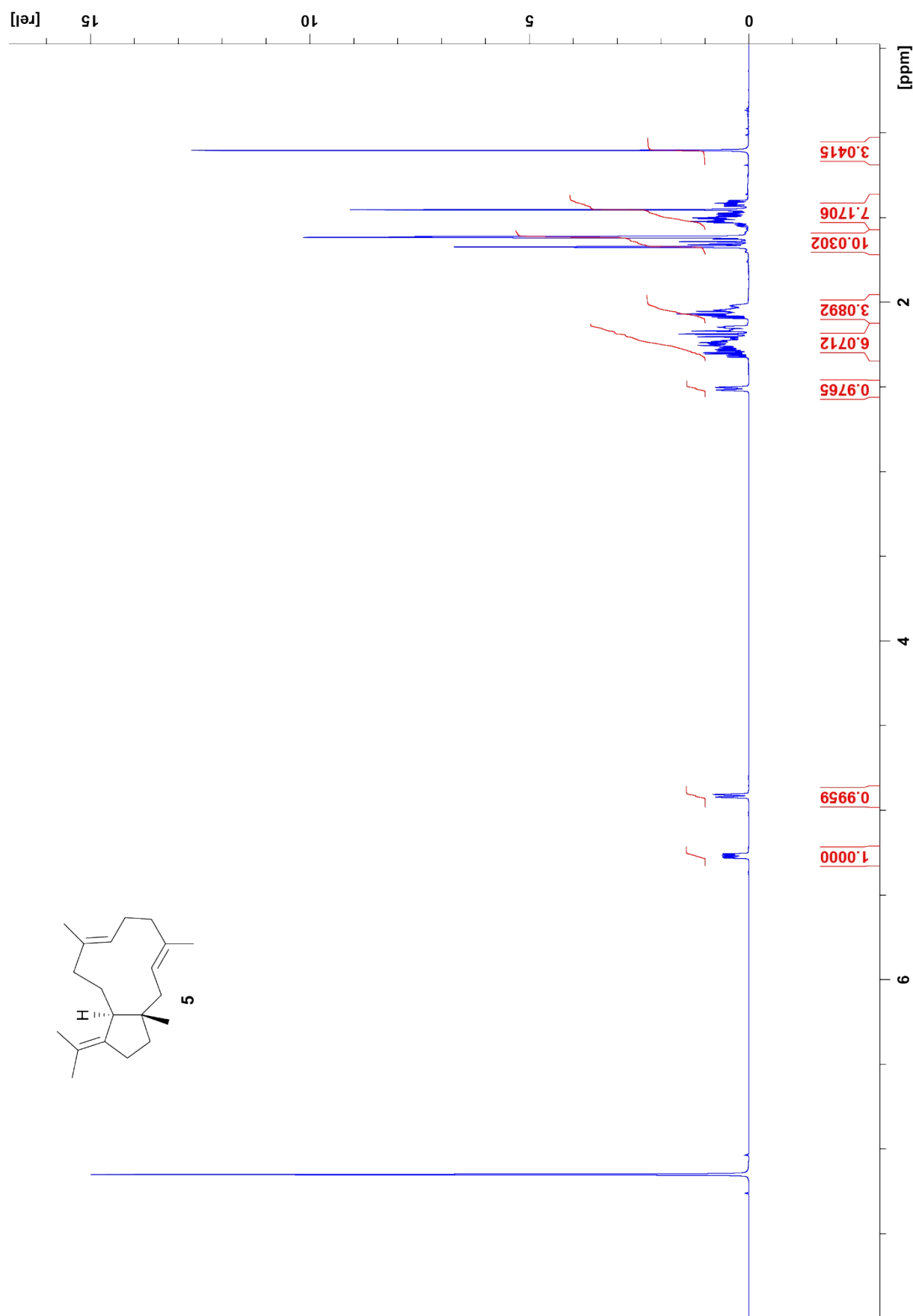


Figure S16. ¹H-NMR spectrum of **5** (700 MHz, C₆D₆).

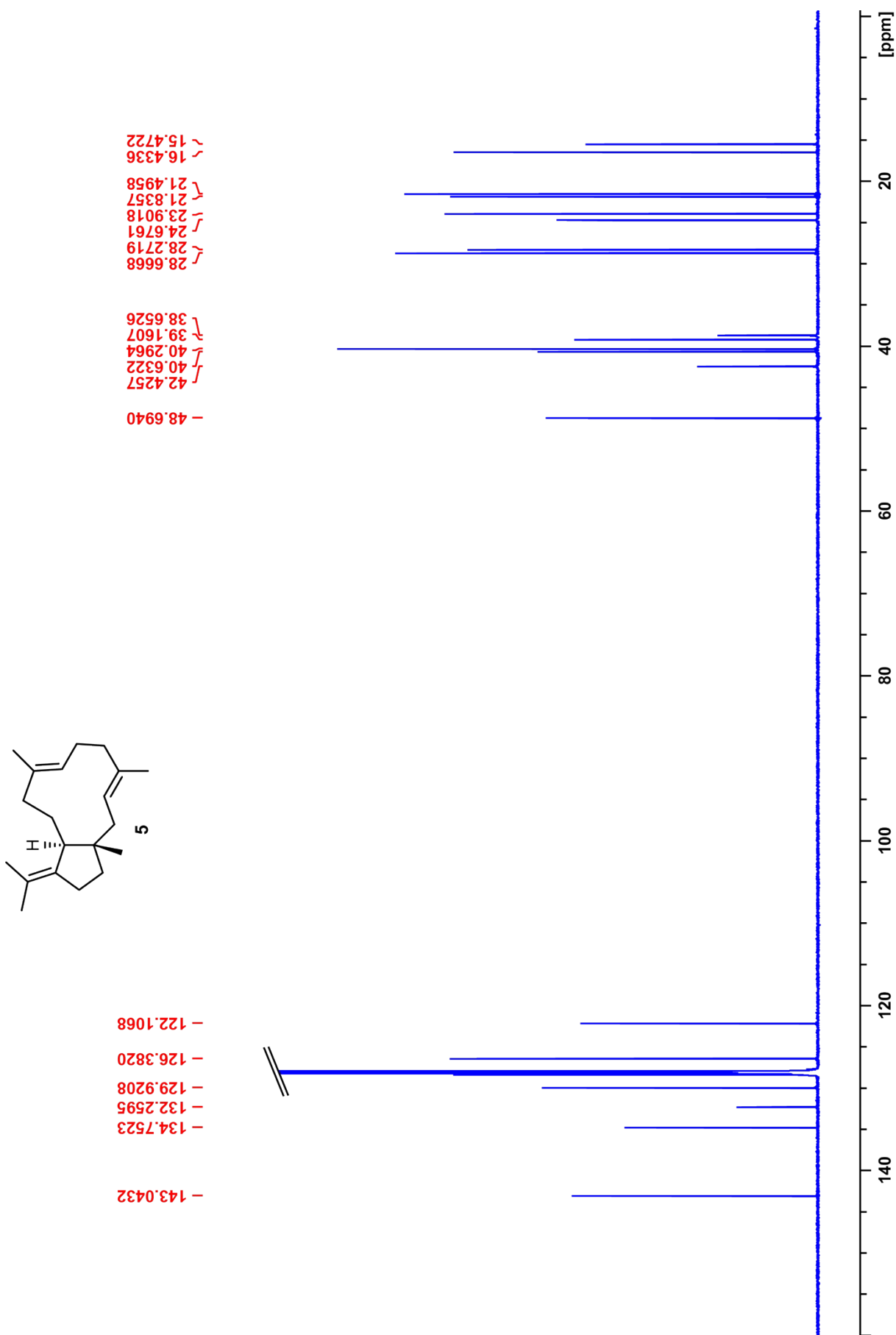


Figure S17. ^{13}C -NMR spectrum of **5** (175 MHz, C_6D_6).

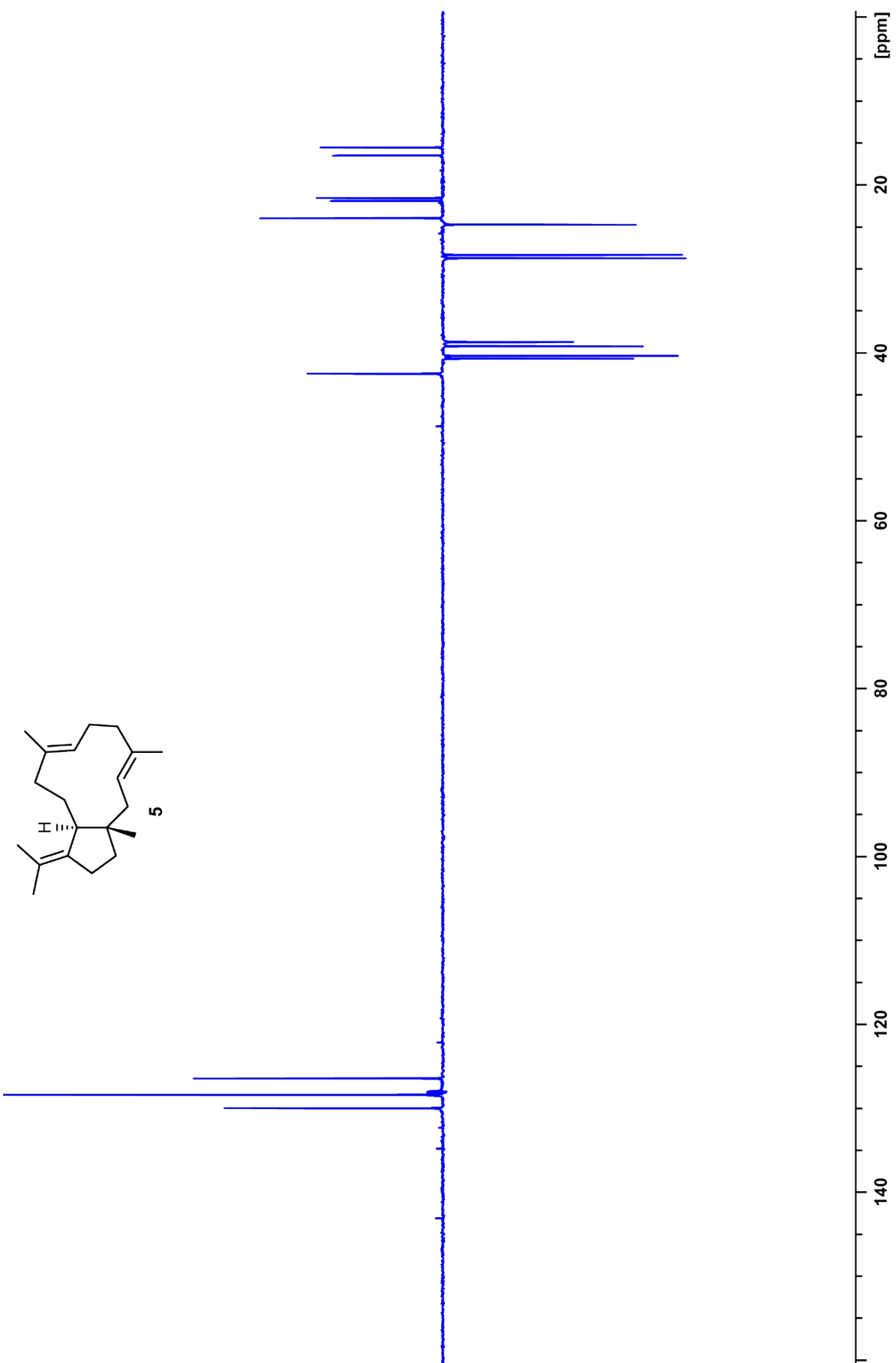


Figure S18. ^{13}C -DEPT spectrum of **5** (175 MHz, C_6D_6).

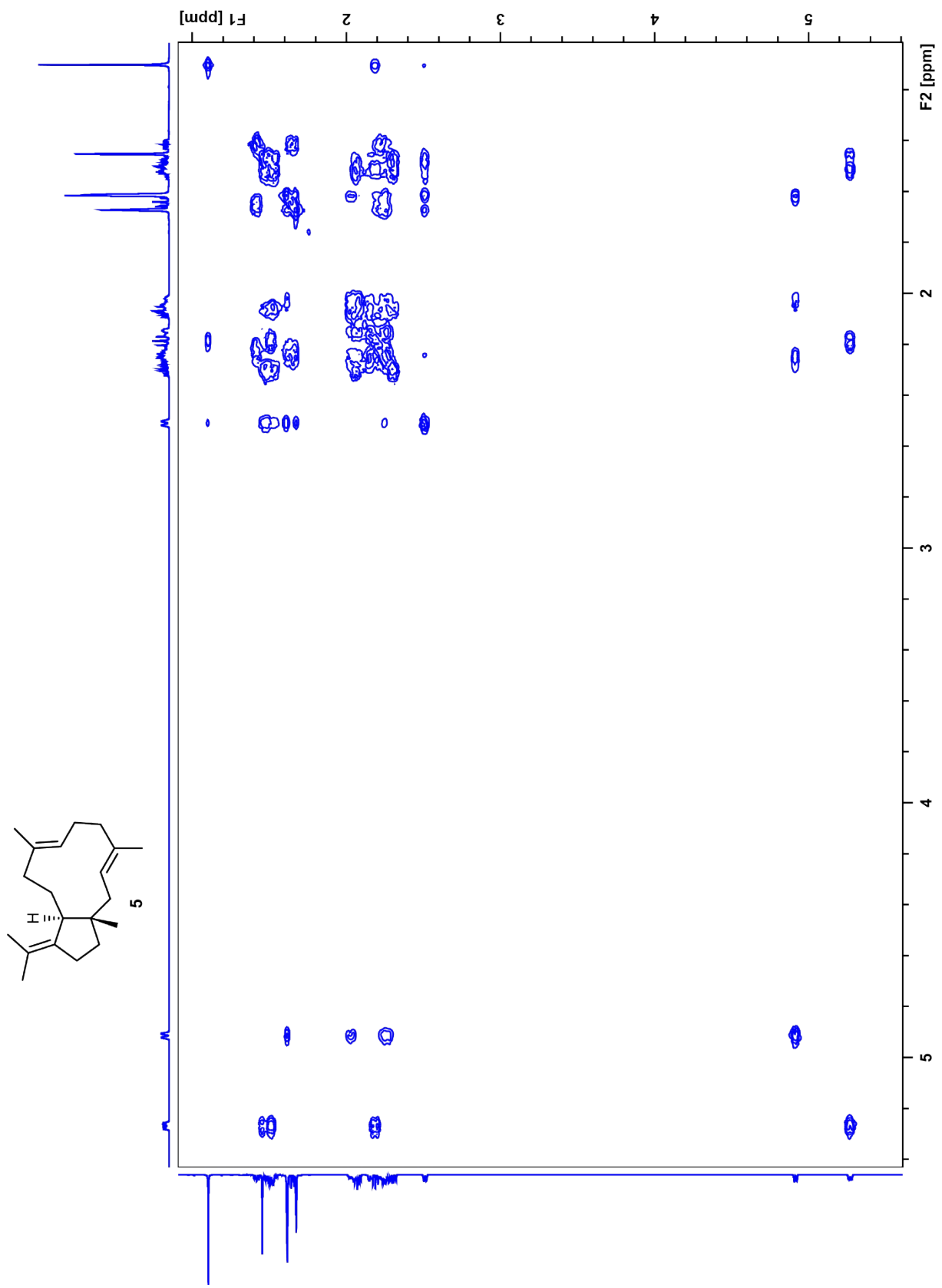


Figure S19. $^1\text{H},^1\text{H}$ -COSY spectrum of **5** (700 MHz, C_6D_6).

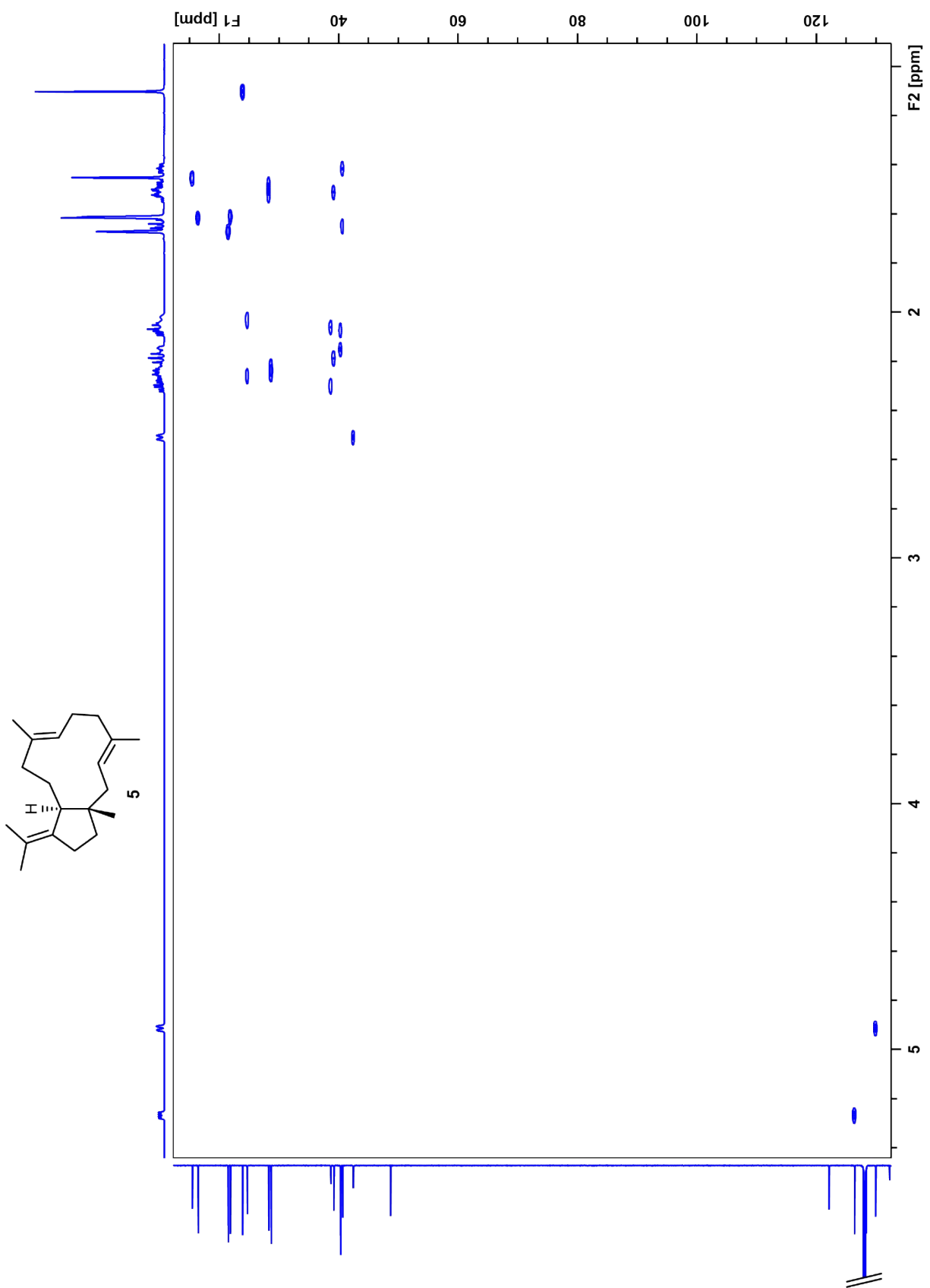


Figure S20. HSQC spectrum of **5** (700 MHz, C₆D₆).

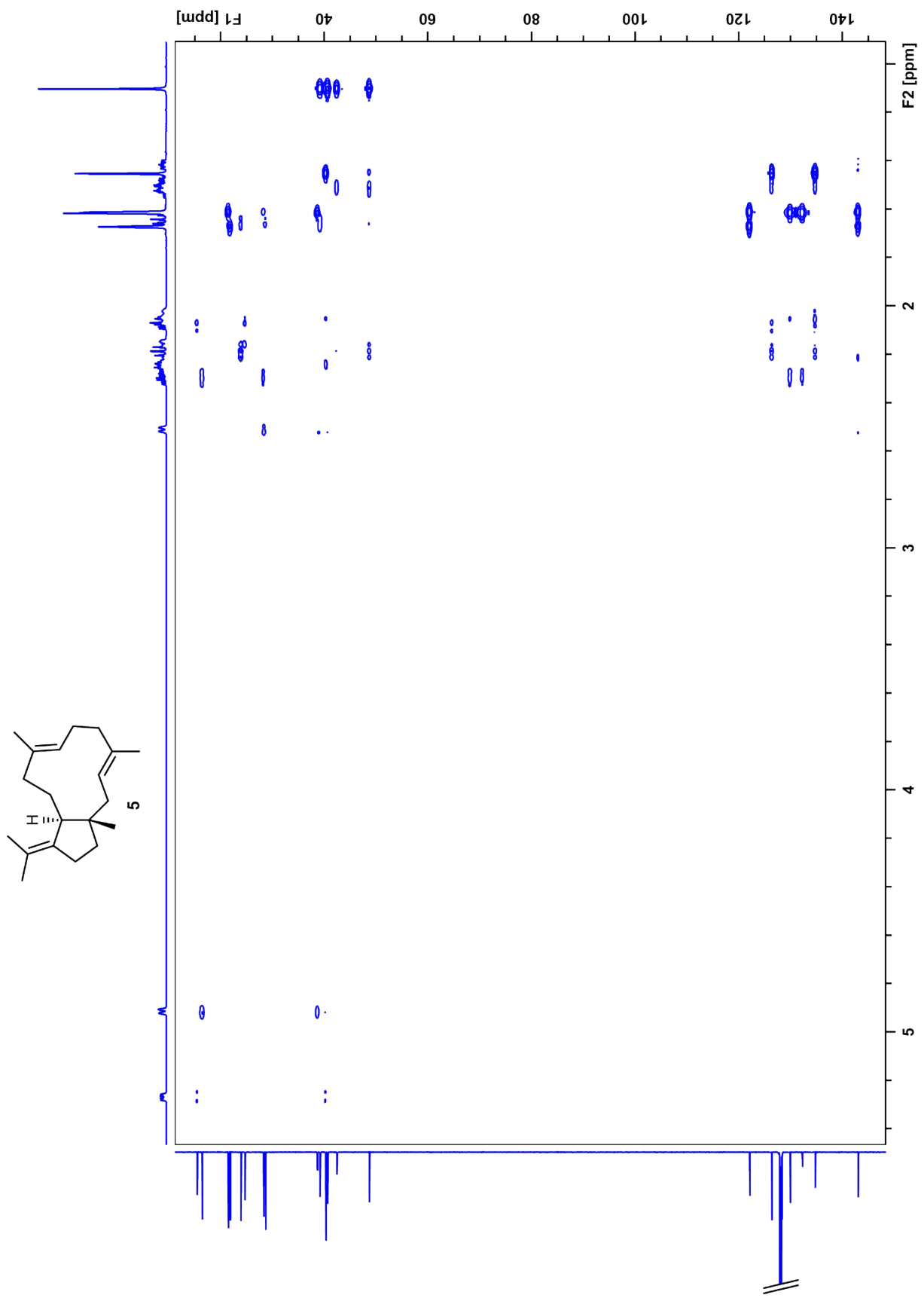


Figure S21. HMBC spectrum of **5** (700 MHz, C₆D₆).

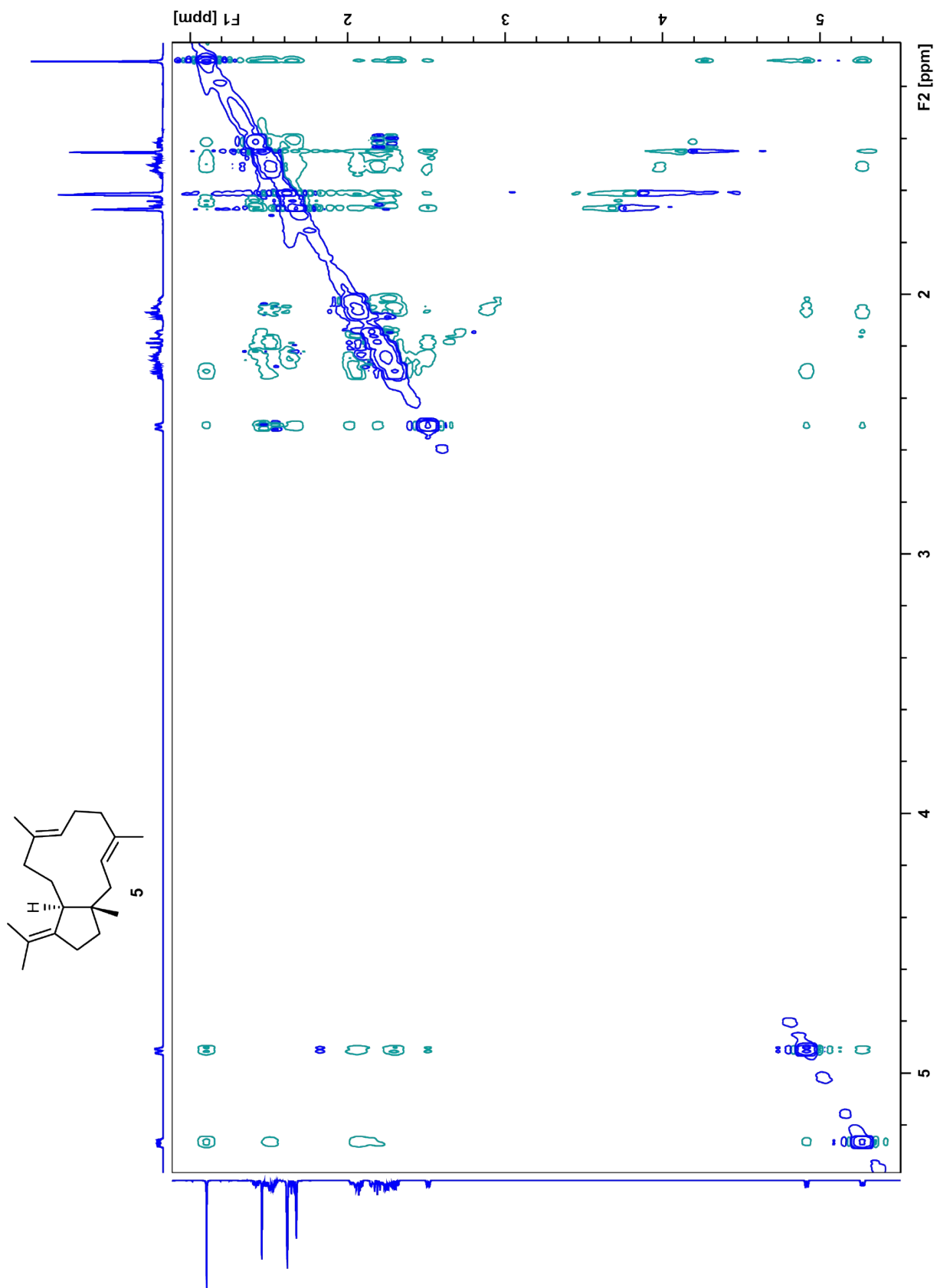


Figure S22. NOESY spectrum of **5** (700 MHz, C₆D₆).

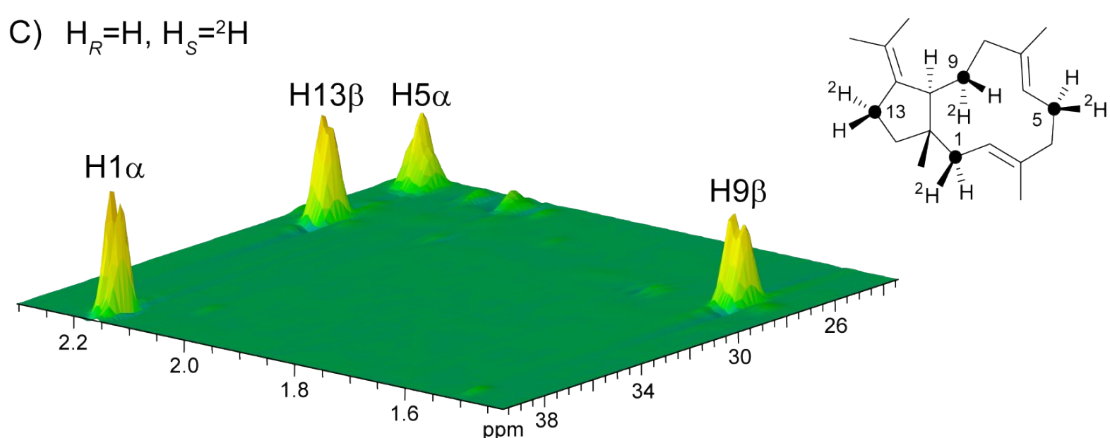
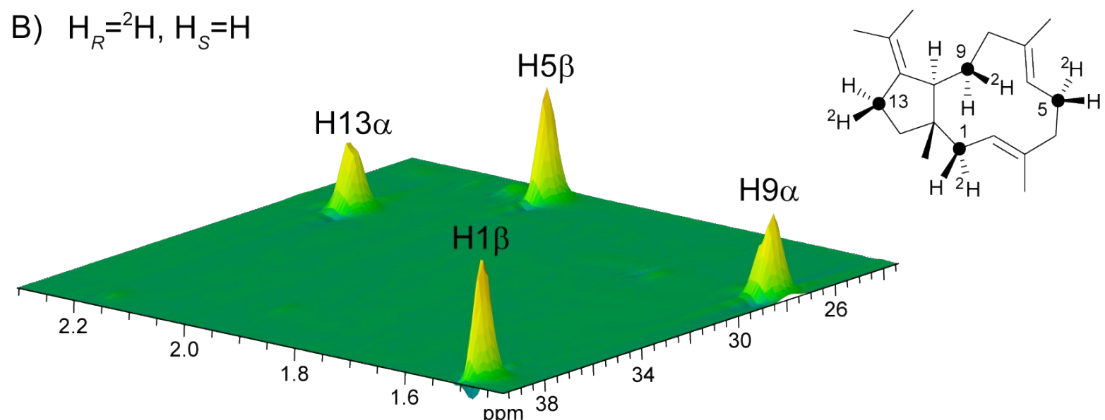
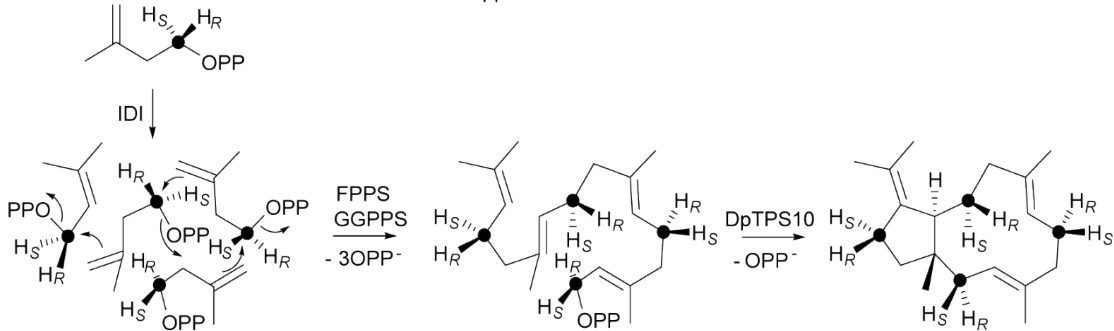
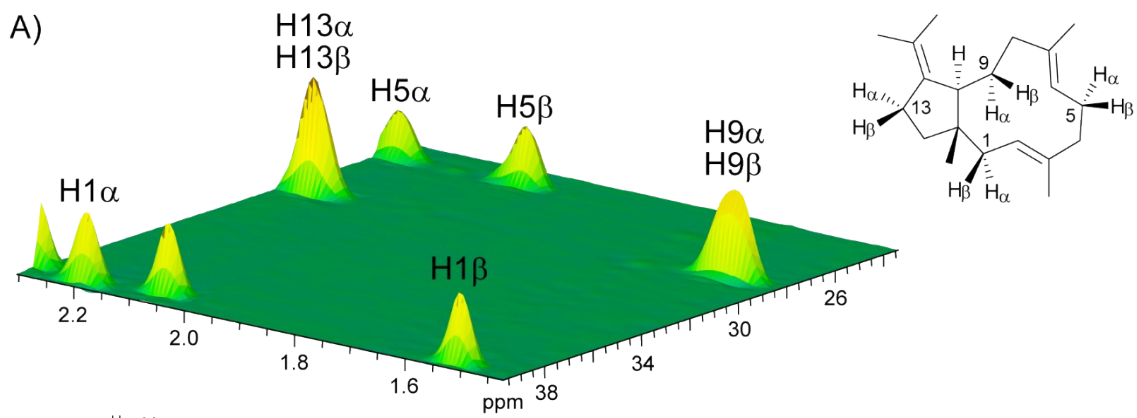


Figure S23. Partial HSQC spectra of A) unlabelled **5**, B) an incubation of (*R*)-(1-¹³C,1-²H)IPP with IDI, FPPS, GGPPS¹³ and DpTPS10 and C) an incubation of (*S*)-(1-¹³C,1-²H)IPP with IDI, FPPS, GGPPS and DpTPS10 showing the selective incorporation of deuterium into the methylene positions C1, C5, C9 and C13. The observed outcome is in line with the shown absolute configuration of **5** for C1, C9 and C13. Determination of the relative configuration of C5 by NOE correlations was not possible. Black dots represent ¹³C-labelled carbon atoms.

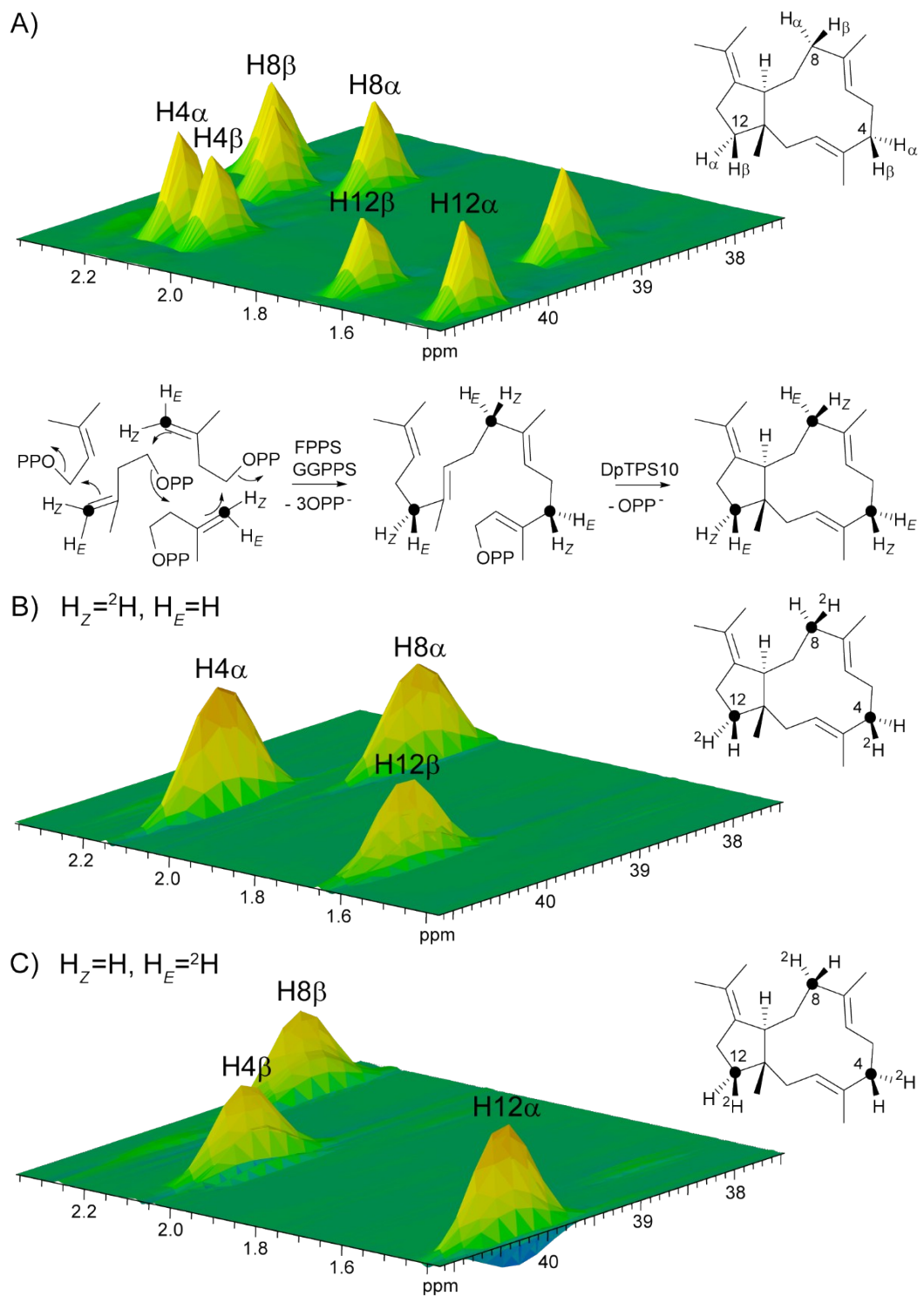


Figure S24. Partial HSQC spectra of A) unlabelled **5**, B) an incubation of (*Z*)-(4-¹³C,4-²H)IPP with DMAPP, FPPS, GGPPS and DpTPS10 and C) an incubation of (*E*)-(4-¹³C,4-²H)IPP with DMAPP, FPPS, GGPPS and DpTPS10 showing the selective incorporation of deuterium into the methylene positions C4, C8 and C12. The observed outcome is in line with the shown absolute configuration of **4** regarding C8 and C12. For C4, the relative configuration could not be obtained from the NOESY spectrum. Black dots represent ¹³C-labelled carbon atoms.

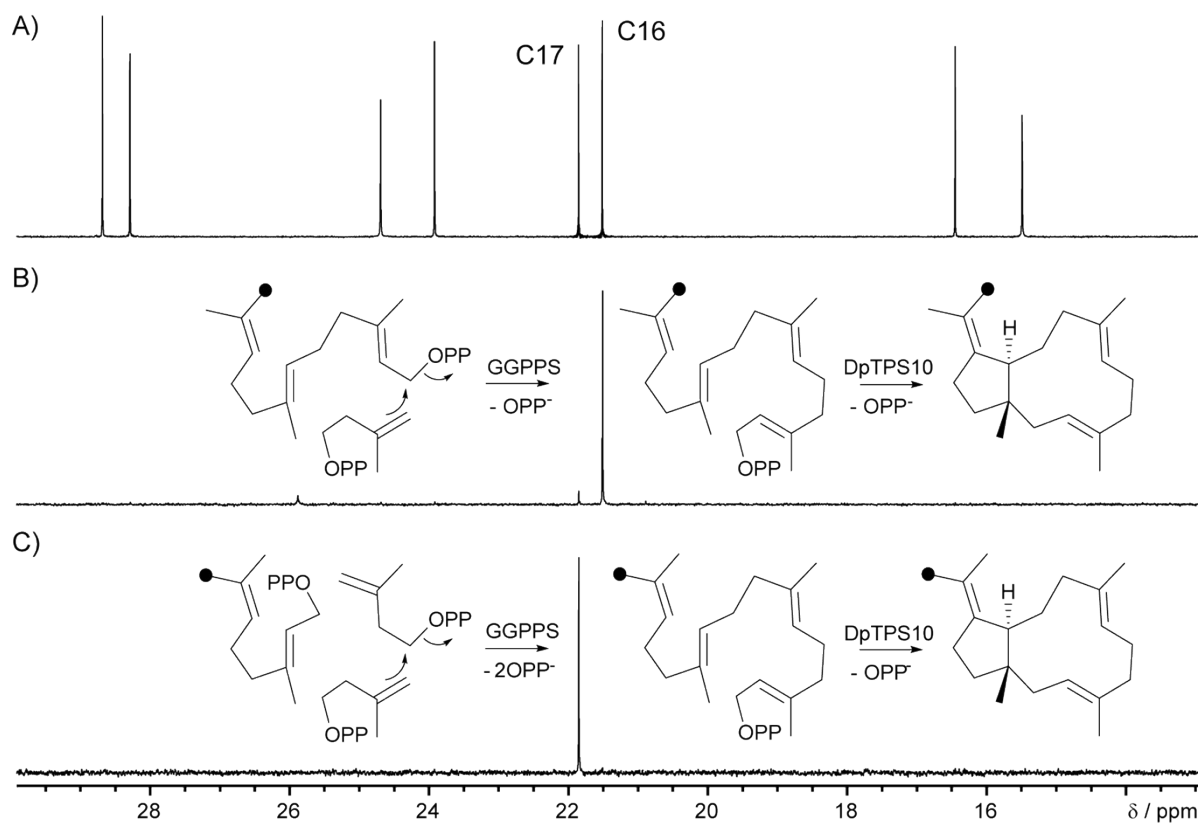


Figure S25. Partial ^{13}C -NMR spectra of A) unlabelled **5**, B) incubation of ($12\text{-}^{13}\text{C}$)FPP with IPP, GGPPS and DpTPS10 and C) incubation of ($9\text{-}^{13}\text{C}$)GPP, IPP, GGPPS and DpTPS10. Black dots represent ^{13}C -labelled carbon atoms. The minor peak of C17 in B) is caused by an impure labelling of the starting material.

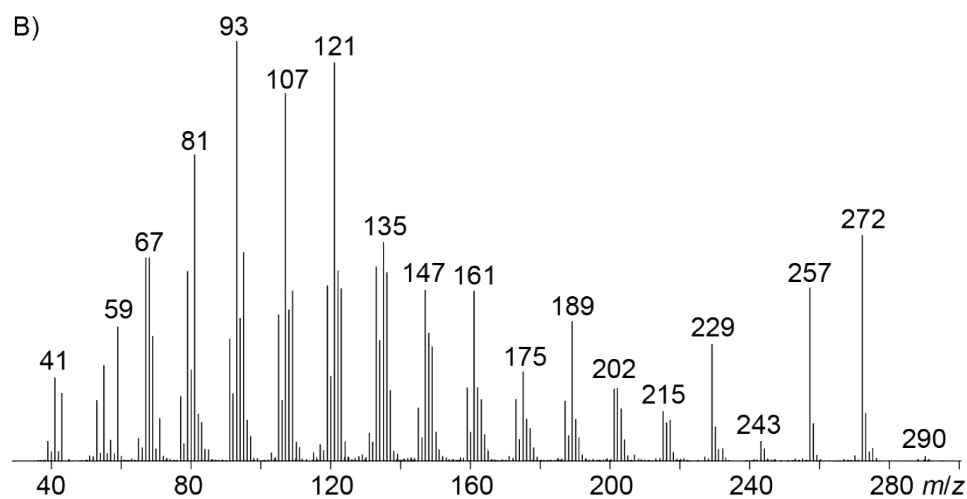
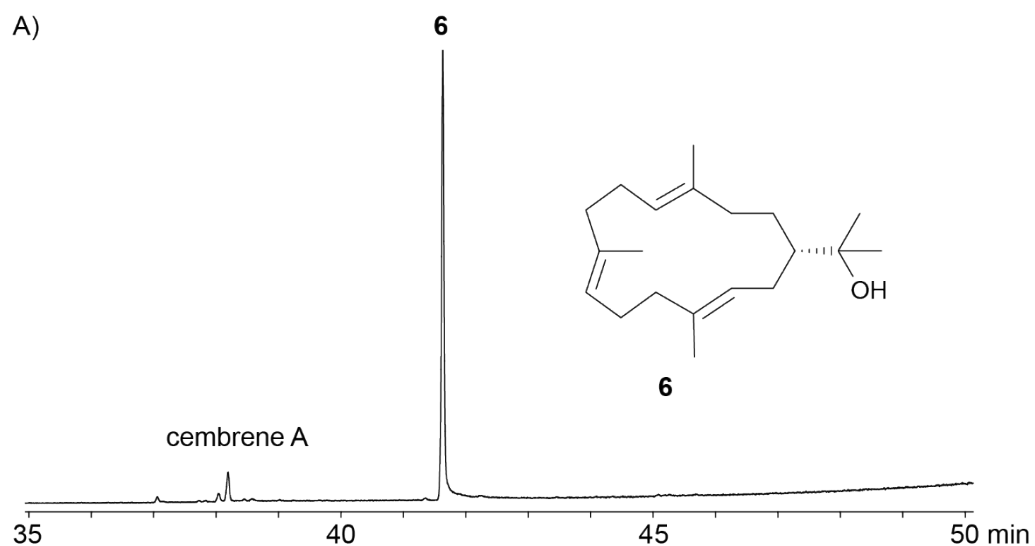
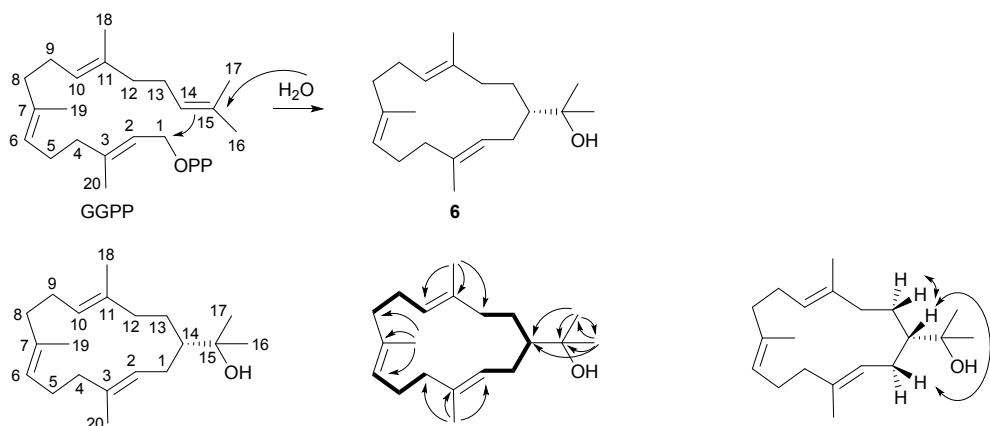


Figure S26. A) Total ion chromatogram of an extract from the incubation of GGPP with DpTPS11. B) EI mass spectrum of nephthenol (**6**).



Scheme S3. Short biosynthesis and structure elucidation of **6**. Carbon numbers refer to the corresponding positions in GGPP. H,H-COSY spin systems are represented by bold bonds, single headed arrows show HMBC correlations and NOESY correlations are depicted by double headed arrows.

Table S4. NMR data of nephthenol (**6**) in C_6D_6 recorded at 298 K.

C[a]		^{13}C [b]	1H [b]	^{13}C [c]
1	CH ₂	29.03	2.20 (m) 1.91 (dddd, $J = 7.6, 7.6, 7.6, 7.6$)	28.5
2	CH	126.92	5.26 (tm, $J = 7.0$)	125.9
3	C _q	133.03	—	134.4
4	CH ₂	39.30	2.13 (m, 2H)	38.8
5	CH ₂	25.15	2.18 (m, 2H)	24.7
6	CH	126.28	5.07 (tm, $J = 6.9$)	125.8
7	C _q	133.01	—	133.0
8	CH ₂	39.87	2.11 (m) 2.06 (m)	39.4
9	CH ₂	24.48	2.13 (m, 2H)	24.0
10	CH	125.32	5.16 (tm, $J = 6.6$)	125.0
11	C _q	134.27	—	134.0
12	CH ₂	38.21	2.16 (m) 2.08 (m)	37.7
13	CH ₂	28.76	1.66 (m) 1.24 (m)	28.3
14	CH	48.79	1.34 (m)	48.5
15	C _q	73.21	—	73.9
16	CH ₃	27.83 ^[d]	1.07 (s) ^[d]	27.7 ^[d]
17	CH ₃	27.86 ^[d]	1.06 (s) ^[d]	27.5 ^[d]
18	CH ₃	15.78	1.59 (s)	15.6
19	CH ₃	15.43	1.54 (s)	15.3
20	CH ₃	15.68	1.57 (s)	15.6

[a] Carbon numbering indicates the origin of each carbon from GGPP by identical number as shown in Scheme S3. [b] Chemical shifts δ in ppm, multiplicity: s = singlet, d = doublet, m = multiplet, br = broad, coupling constants J are given in Hertz. [c] ^{13}C -NMR data in $CDCl_3$ from ref. [14]. [d] Signals may be interchanged.

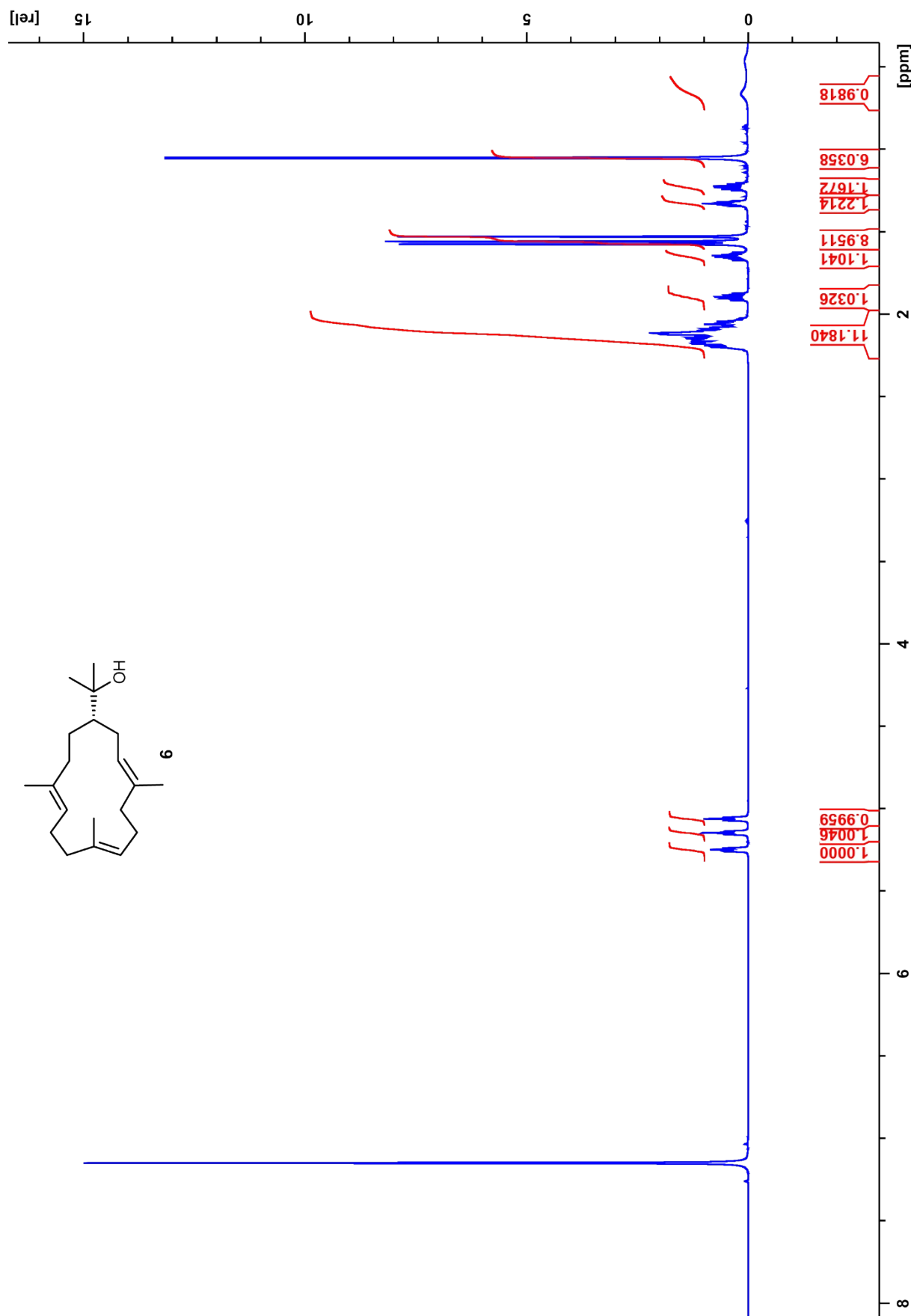


Figure S27. ¹H-NMR spectrum of **6** (700 MHz, C₆D₆).

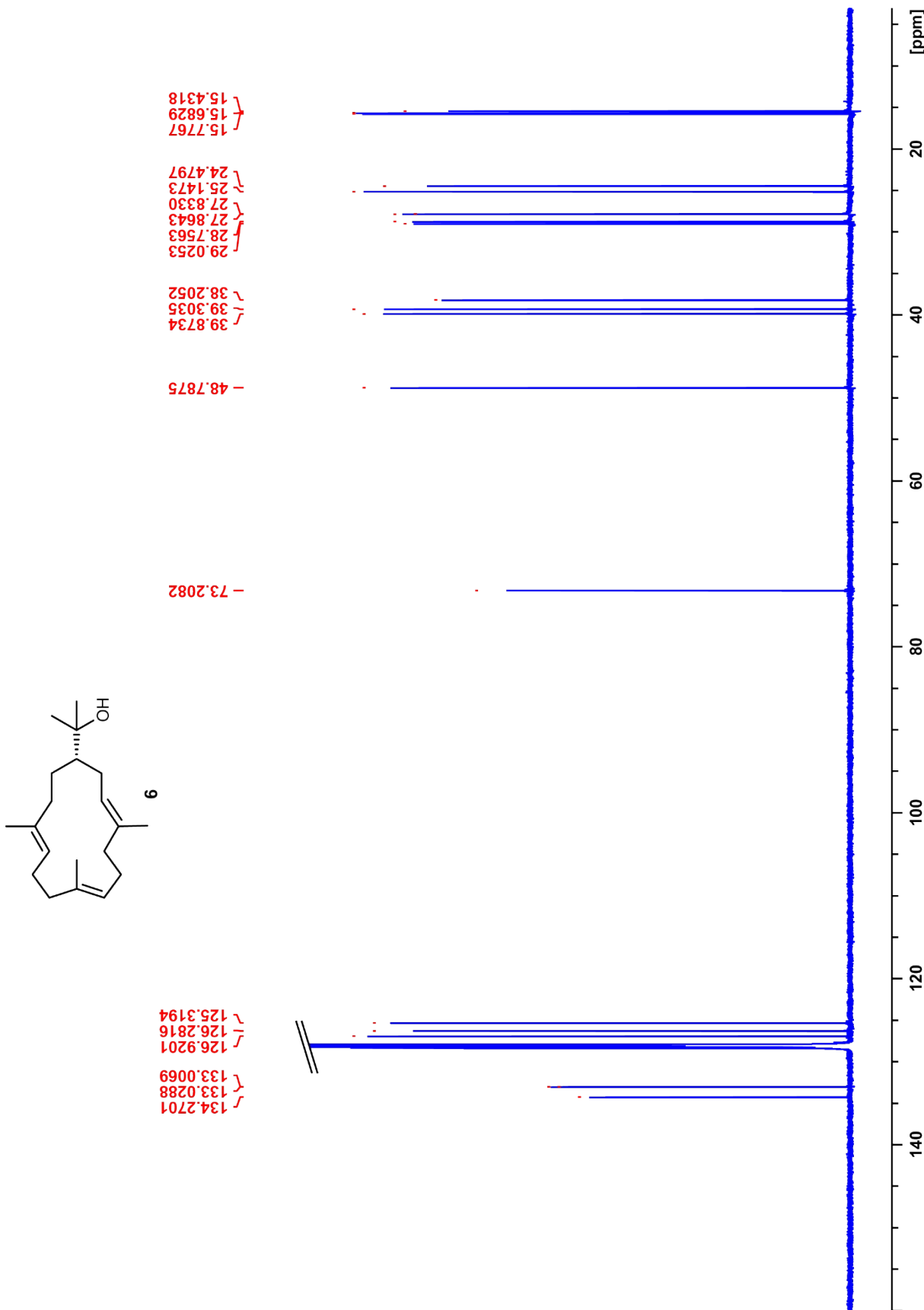


Figure S28. ^{13}C -NMR spectrum of **6** (175 MHz, C_6D_6).

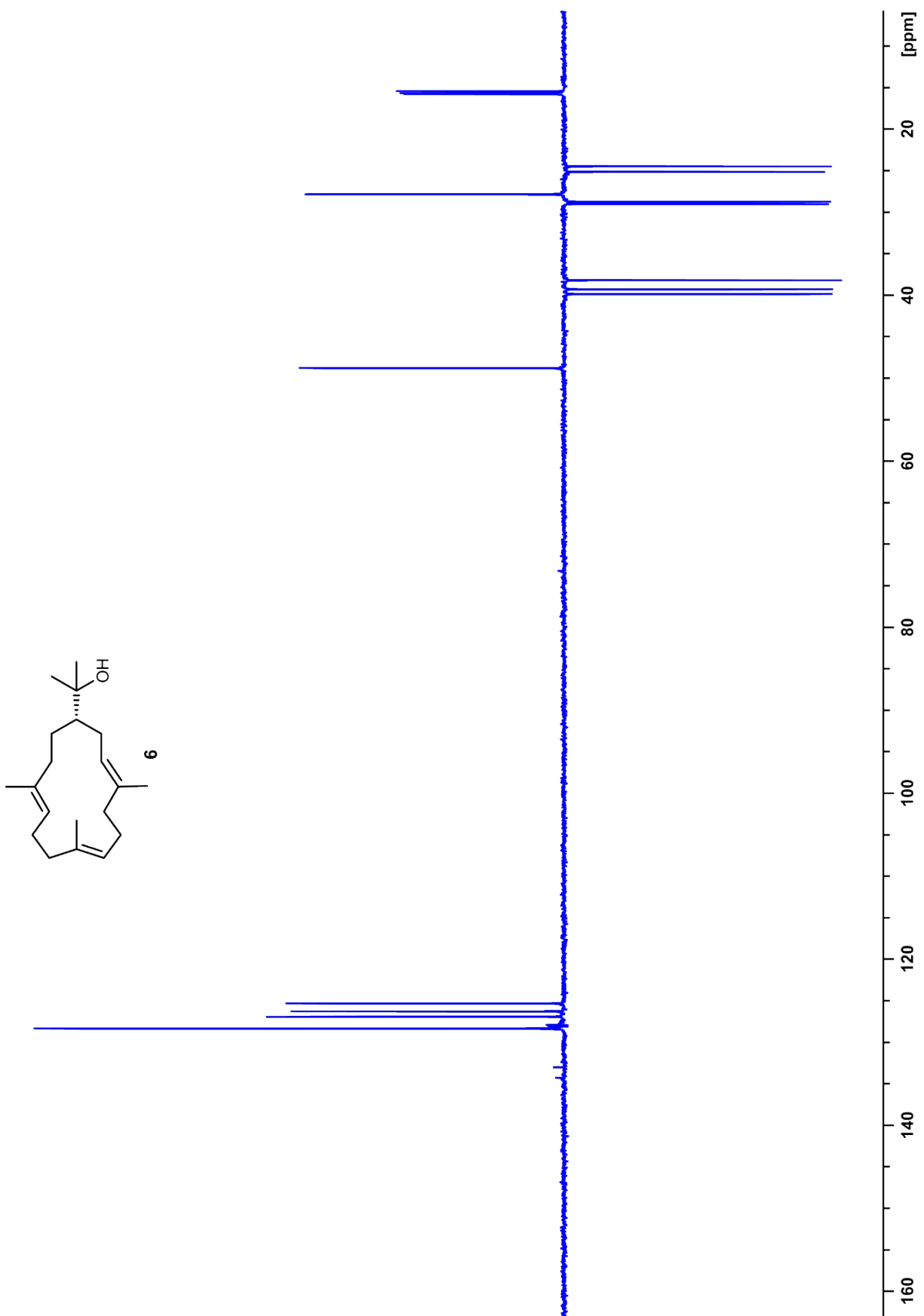


Figure S29. ^{13}C -DEPT spectrum of **6** (175 MHz, C_6D_6).

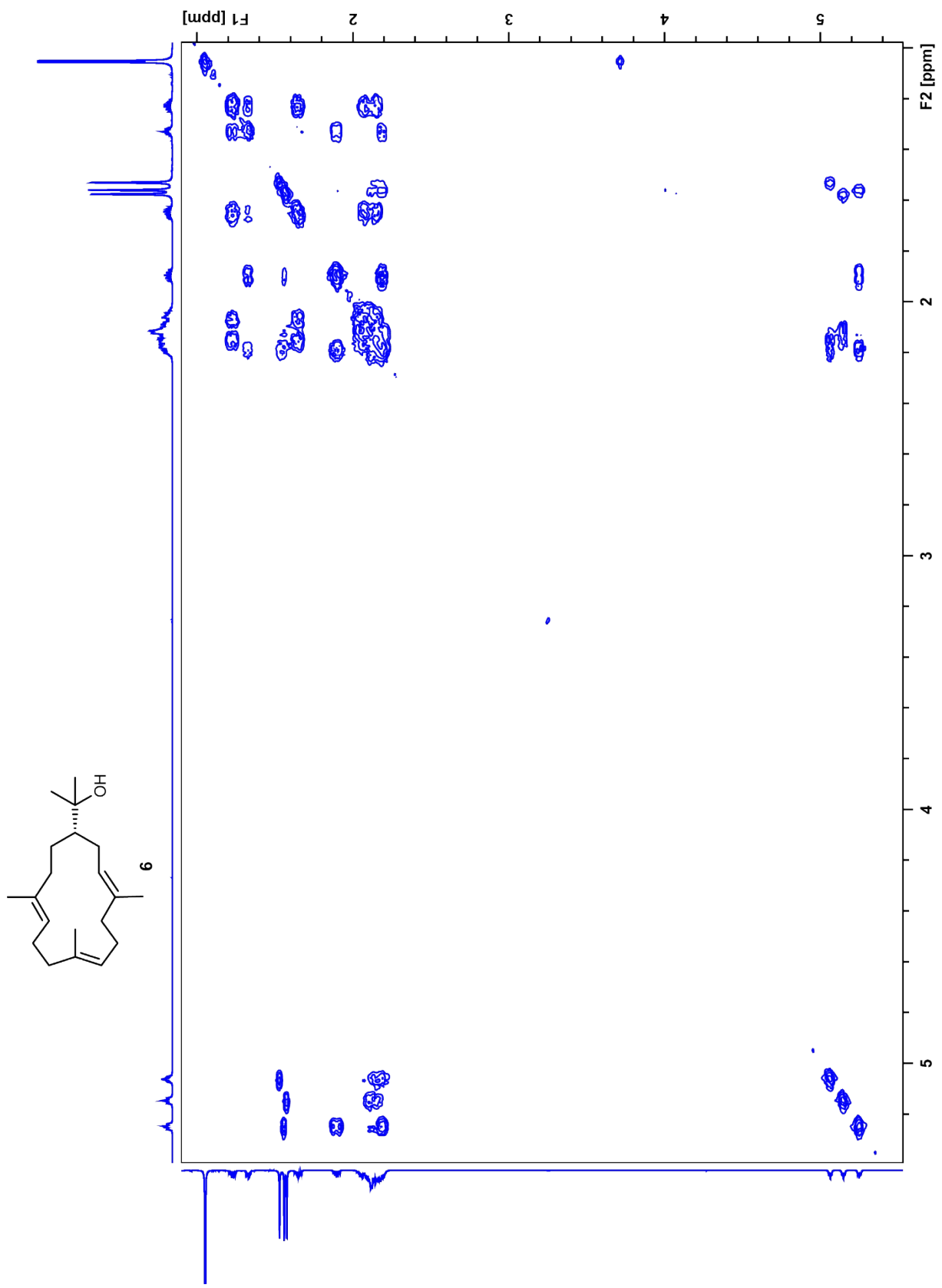


Figure S30. $^1\text{H},^1\text{H}$ -COSY spectrum of **6** (700 MHz, C_6D_6).

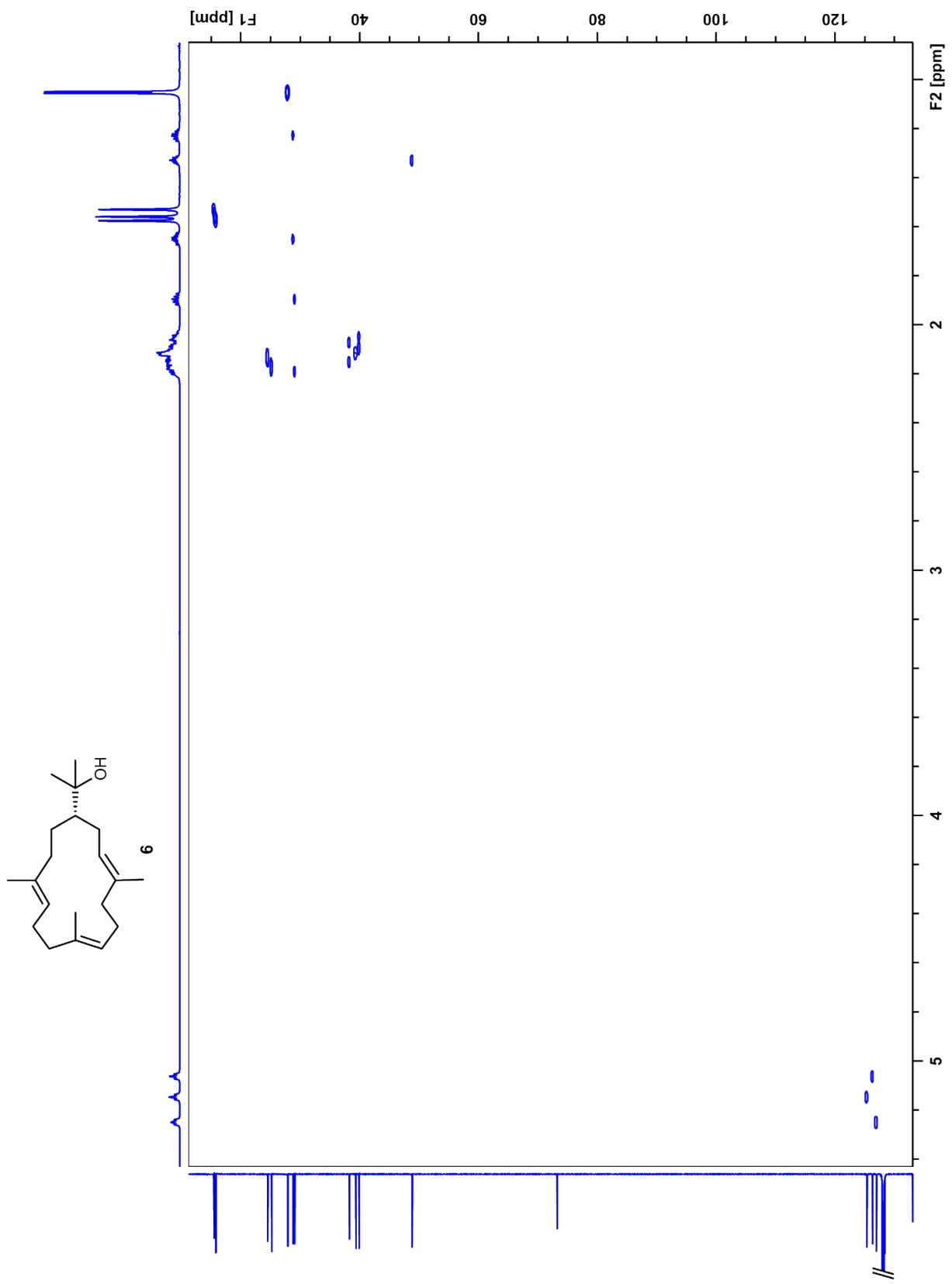


Figure S31. HSQC spectrum of **6** (700 MHz, C₆D₆).

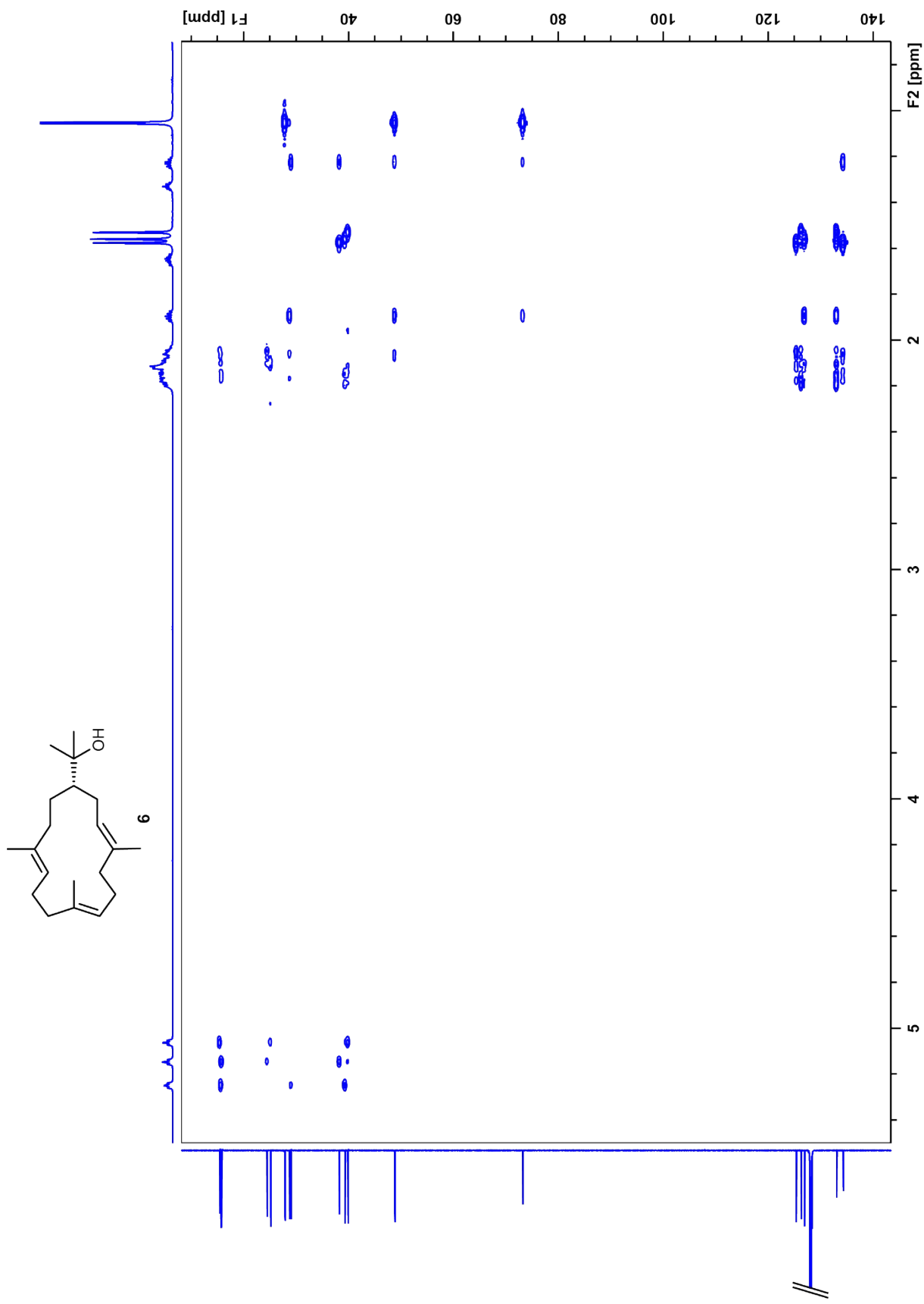


Figure S32. HMBC spectrum of **6** (700 MHz, C_6D_6).

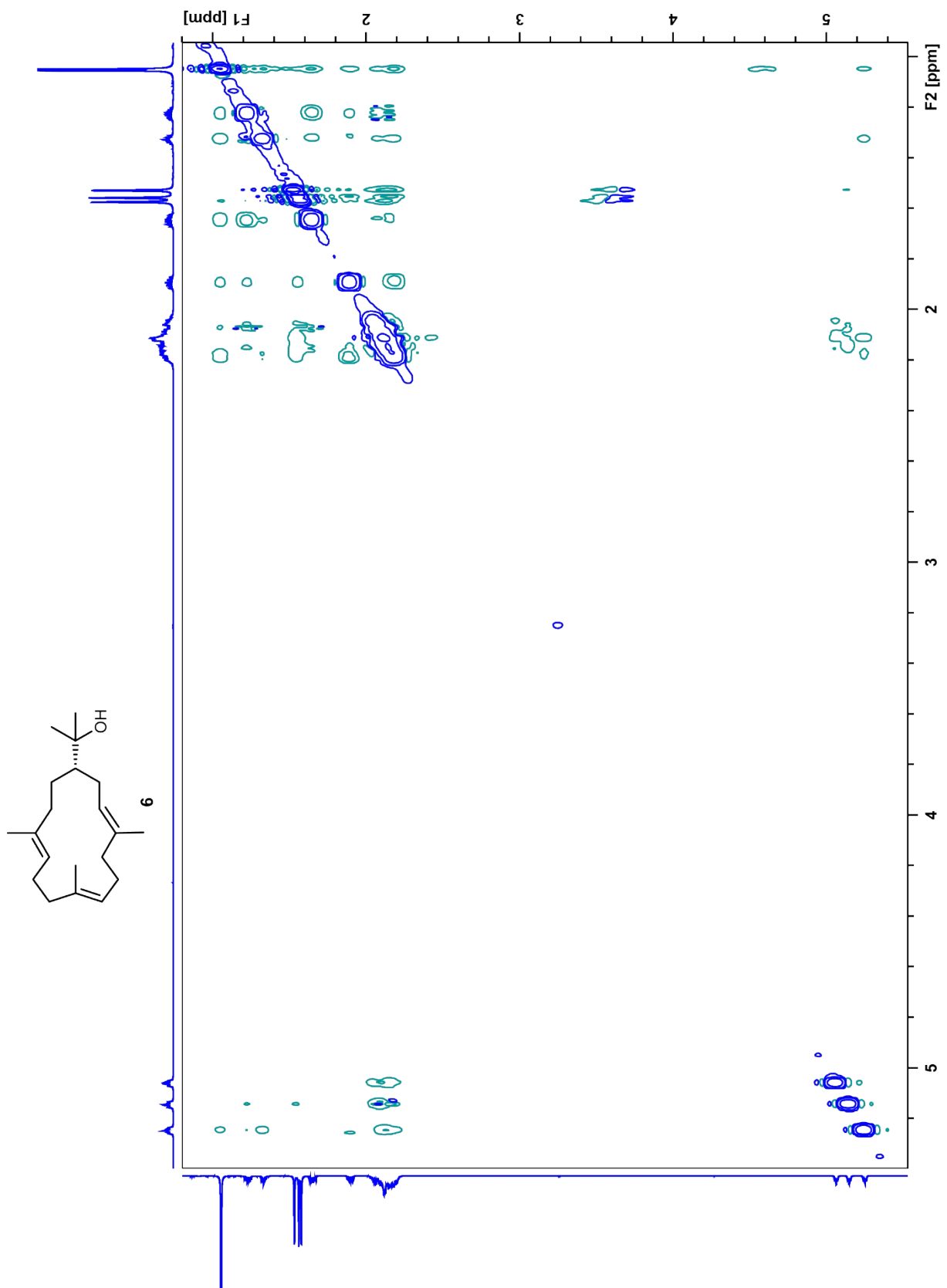


Figure S33. NOESY spectrum of **6** (700 MHz, C_6D_6).

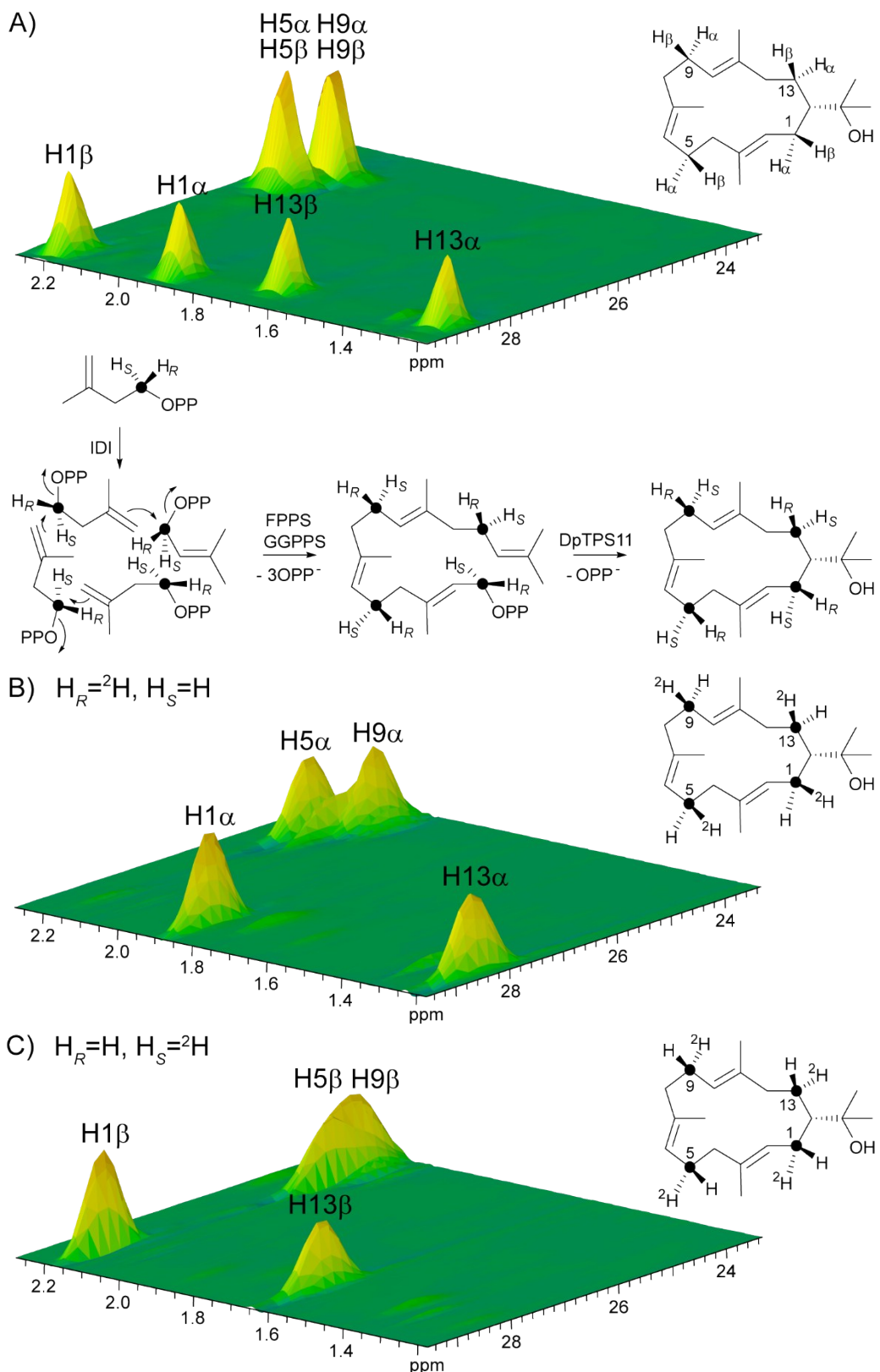


Figure S34. Partial HSQC spectra of A) unlabelled **6**, B) an incubation of (*R*)-(1-¹³C,1-²H)IPP with IDI, FPPS, GGPPS and DpTPS11 and C) an incubation of (*S*)-(1-¹³C,1-²H)IPP with IDI, FPPS, GGPPS and DpTPS11 showing the selective incorporation of deuterium into the methylene positions C1, C5, C9 and C13. The observed outcome is in line with the shown absolute configuration of **6** for C1 and C13. Determination of the relative configuration of C5 and C9 by NOE correlations was not possible. Black dots represent ¹³C-labelled carbon atoms.

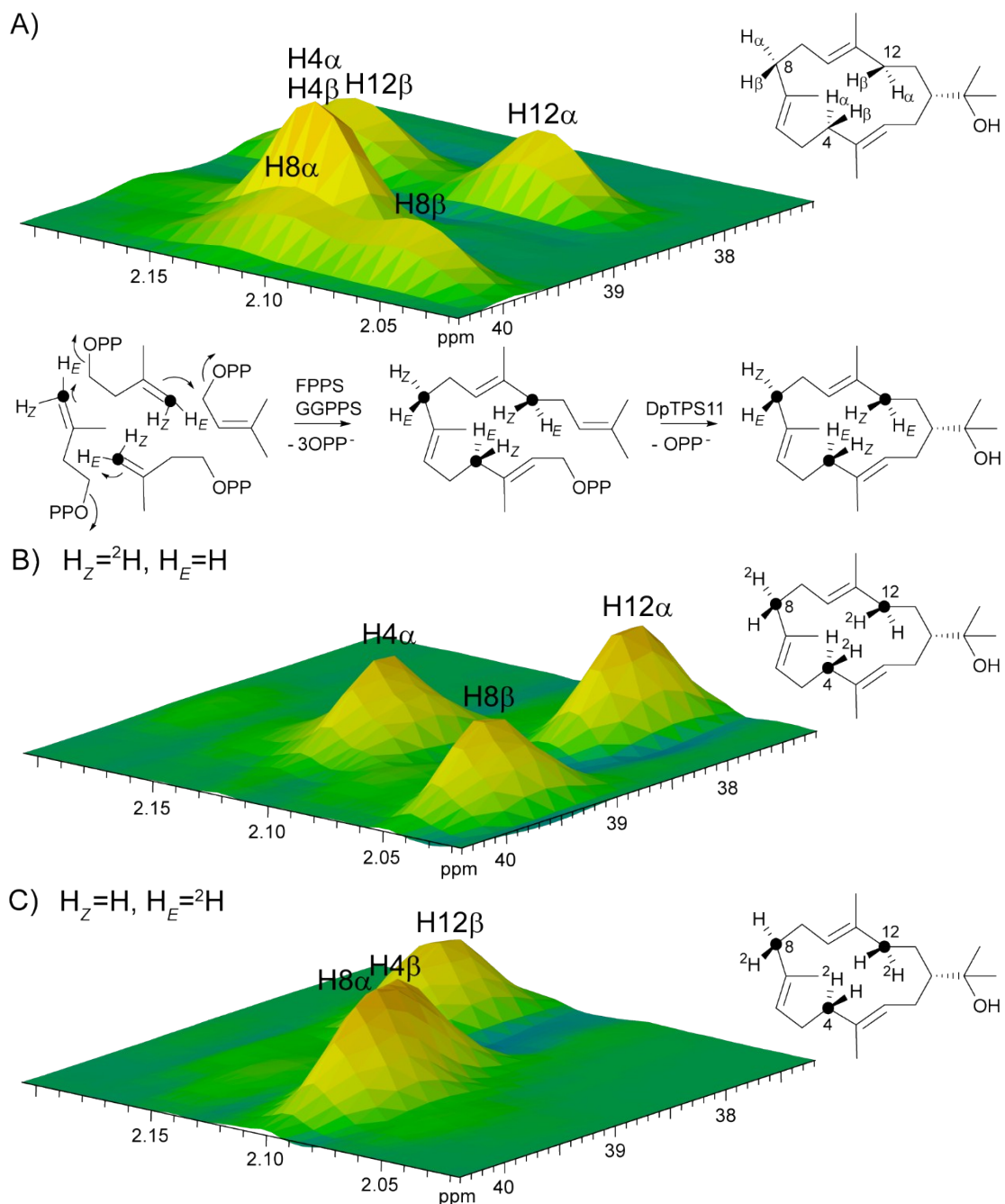


Figure S35. Partial HSQC spectra of A) unlabelled **6**, B) an incubation of (Z)-(4-¹³C,4-²H)IPP with DMAPP, FPPS, GGPPS and DpTPS11 and C) an incubation of (E)-(4-¹³C,4-²H)IPP with DMAPP, FPPS, GGPPS and DpTPS11 showing the selective incorporation of deuterium into the methylene positions C4, C8 and C12. Because of inconclusive NOE correlations on these positions, no conclusion on the absolute configuration was drawn. Black dots represent ¹³C-labelled carbon atoms.



Figure S36. Amino acid sequence alignment of DdTPS9, DpTPS10 and DpTPS11 with characterised bacterial and fungal terpene synthases.^{5,15-30}



Figure S36. Amino acid sequence alignment of DdTPS9, DpTPS10 and DpTPS11 with characterised bacterial and fungal terpene synthases.^{5,15-30}

XP_642260 (Dictyostelium discoideum AX4, (-)- <i>b</i> -Barbatene) XP_003289490 (Dictyostelium purpureum QSDP1, (-)- <i>b</i> -Araneosene) XP_003289235 (Dictyostelium purpureum QSDP1, (+)-Nephthenol) XP_645125 (Dictyostelium discoideum AX4, Asterisca-2(9),6-diene) XP_638489 (Dictyostelium discoideum AX4, Protoillud-7-ene) WP_039931950 (Streptomyces viridochromogenes DSM 40736, a-Amorphene) CCA53839 (Streptomyces venezuelae ATCC 10712, Isodauc-8-en-11-ol) WP_005317515 (Streptomyces pristinaespialis ATCC 25486, Selina-4(15),7(11)-diene) WP_003950762 (Streptomyces albus J1074, epi-Isozizaene) WP_042496076 (Streptomyces griseus NBRC 13350, Caryolan-1-ol) WP_003970379 (Streptomyces griseus NBRC 13350, epi-Cubenol) WP_003994861 (Streptomyces viridochromogenes DSM 40736, 7-epi-a-Eudesmol) Q55012 (Streptomyces exfoliatus UC5319, Pentalenene) WP_010981512 (Streptomyces avermitilis MA-4680, Avermitilol) AEM85259 (Streptomyces violaceusniger Tü 4113, Isoafricanol) WP_005320742 (Streptomyces pristinaespialis ATCC 25486, Pristinol) WP_014134444 (Kitasatospora setae KM-6054, Corvol ether) WP_012792334 (Chitinophaga pinensis DSM 2588, g-Cadinene) FFUJ_10353 (Fusarium fujikuroi IMI 58289, a-Acorenol) XP_023434772 (Fusarium fujikuroi IMI 58289, Koraiol) XP_023437750 (Fusarium fujikuroi IMI 58289, (-)-Guaiia-6,10(14)-diene) XP_006969402 (Trichoderma reesei QM6a, Trichobrasilenol) Q6WP50 (Botrytis cinerea B05.10, Presilphiperfolan-8-beta-ol)	241 250 260 270 280 290 300 -----GEKIEFFNQLKFIIIDWINSINPFNRADNL-----NNYD-SYNFFKR -----GRERLDAFNLLNIELVICLWTLVPFSKIHSK-----EKDFYPSYQ--LYRCIRT -----KYGNQSVNKFLKEEFFIKNVHSIHLKENA-----NYTNINFEEYTNTRS -----GEKRKSTFHRFNSSCVQWVDSIIPFKLKRN-----QKSLSDFNLHYIHHRK -----GKRKDKTFNRFISSLVQWVDSIIPFKLRLSA-----QGTSPHLE--LYSYLRK -----ERCTPAQAARWAWSNSREYVHGLLY-EAVAQA-----HPAPVESGLCRSIRS -----PPRLAWHRQEENLALAHYIDAGVQ-ELTNSR-----GGRVPHLI--EYAPFR -----RGFTAGQTARWVDALREYFFSVVV-EAHAHR-----AGTVPDLN--DYTLMLR -----GFLGPWNERFARHFHAIVGAYDQ-EFENRV----T-KVT-PKVA--EYIELRR -----RGRSPQWNRQFRRDTAAWLWTYYA-EAVERA-----AGQVPSRA--EFAKHRR -----PEAAPHWTRTRFAWHVLTATTWEAGNRA-----EDVVPSEE--TYIAKRR -----HGMSTLWQSRAFWASWGRFLAEHCE-EVDLAA-----RGLEGTLGLVEFTEFR -----EGMTPAWCARSARHWRNRYFDGYWD-EAESRF-----WNAPCDSAAQYLAMRR -----DGAHPGWARTAHEWEYYFAAQAH-EAINRL-----RGTPGDME--SYLQVRR -----SGRPQVWRDRFRHHWLEYLHSYHREALERTGALPGAGGDAPRSVE--AVLALRR -----AGAPYAWRLRFRDHQAYLAAHVG-EAHHRN-----ADRLPSLE--QFLEVRR -----AYLSDEHFQRFQAHGMRMWAATAGL-QIANHL-----GADTVDVA--PYETIRR -----ALGDTAQWTRFIRSMEEYFTSCH-EAGNRA-----ADIVPTVA--EYVITMRP -----ECDPILGPGLLAIRAGLFLVNAGRKKSPFKQD-----KYATLA--EYLDYRR -----ERSSPSLQYRWKHKHTMYCVGVLQ-QVGVQH-----RATRPTIE--EYMDMRA -----GFYAGKPSSERFYRRWMWAHELYWEGLVA-QVRTNV-----EGRSFTRGPEEYLAMRR -----SGLGPVSTERLRLQELHDYVNGAAN-QQGVRE-----EDHLPDPW--VHFQMRA -----AVSSQEMQQRWIDQHKRYFDQLLV-QVDQQV-----GGENFTRDVEAYMDLRR
XP_642260 (Dictyostelium discoideum AX4, (-)- <i>b</i> -Barbatene) XP_003289490 (Dictyostelium purpureum QSDP1, (-)- <i>b</i> -Araneosene) XP_003289235 (Dictyostelium purpureum QSDP1, (+)-Nephthenol) XP_645125 (Dictyostelium discoideum AX4, Asterisca-2(9),6-diene) XP_638489 (Dictyostelium discoideum AX4, Protoillud-7-ene) WP_039931950 (Streptomyces viridochromogenes DSM 40736, a-Amorphene) CCA53839 (Streptomyces venezuelae ATCC 10712, Isodauc-8-en-11-ol) WP_005317515 (Streptomyces pristinaespialis ATCC 25486, Selina-4(15),7(11)-diene) WP_003950762 (Streptomyces albus J1074, epi-Isozizaene) WP_042496076 (Streptomyces griseus NBRC 13350, Caryolan-1-ol) WP_003970379 (Streptomyces griseus NBRC 13350, epi-Cubenol) WP_003994861 (Streptomyces viridochromogenes DSM 40736, 7-epi-a-Eudesmol) Q55012 (Streptomyces exfoliatus UC5319, Pentalenene) WP_010981512 (Streptomyces avermitilis MA-4680, Avermitilol) AEM85259 (Streptomyces violaceusniger Tü 4113, Isoafricanol) WP_005320742 (Streptomyces pristinaespialis ATCC 25486, Pristinol) WP_014134444 (Kitasatospora setae KM-6054, Corvol ether) WP_012792334 (Chitinophaga pinensis DSM 2588, g-Cadinene) FFUJ_10353 (Fusarium fujikuroi IMI 58289, a-Acorenol) XP_023434772 (Fusarium fujikuroi IMI 58289, Koraiol) XP_023437750 (Fusarium fujikuroi IMI 58289, (-)-Guaiia-6,10(14)-diene) XP_006969402 (Trichoderma reesei QM6a, Trichobrasilenol) Q6WP50 (Botrytis cinerea B05.10, Presilphiperfolan-8-beta-ol)	301 310 320 330 340 350 360 TNSGTYVSLSVAM-LLYPNISKIDPKIWINPRFDLRTNGGYQMATNDCASTYAKEIRNNN INVGIIACCALNF-ILFK--DLDVKLWLNPLRFRKILRNRSIIVNDAVSYAKEILNEN IDFGFDLVLVSAAI-IDCE--EPSKEIRESSLFLNTKSSIIICVLVNDIYSFVKESKR-P FNIGAIPCPFLVSEIILDPMSNIECFIWLDSRWIJKMSEIICEITALVNDCVSYEKEIKENG VNIGAYPCVLT-EVMDH-EIEYYIWSDPKWIKMNEDIAIITTLINDLVSYEKEVNDQA LIAGVEPFYPLCE-AAQRC-ELAPEELHHPAMRRLSRLSADAADVWIPDLFSAVKEQRA-G ESFAAHTAATPSVE-LATGA-RIPEQLRHTRTVHALLDAFMVGLANDVASYEREVHEER YDGATSVLPMLE-MGHGY-ELQPYERDRTAVRAEAMASFIIITWDNDIFSYHKERRG HTFGHSVWIDL-E-PTAGR-EIPADLRTSGPFLAAARHCQDFSAWYNDLCSLPKELAG-D DSVAMQPFLCLHE-ITAGI-DLPSDARSLSPAYIALRNAVTDHSGLCNDICSFEKEAL-G HTGAIHVCMGLIE-IVAGI-DAPESVHNDPFRITALEAACNHVCWANDVYSFEKEQVL-G RTVGIIHHSIDAGE-RSRGF-EVPAQAMAHPVMERMRDLAADTIGFMNDIHSFEREKRR-G HTIGVQPTVDAE-RAGR-EVPHRFVDSAVMSAMQIAVDDVNLNNDIASLEKEEAR-G GIAGTDLPLSLGE-RAAGI-TVPAAFHSPQLRIMREAAIDVTLMCNDVYSLEKEEAR-G HSIGVQPCLDINE-PFGGY-TLPPALHGGFPMARCREATDDVVVFTNDIASLDEKLAV-G HSIGVQPCLDFTE-RCGGY-ALPDELYRSFPLREMREITGDDVVFVNDIVSLVKELAA-G HTSGTNPCPLAD-AAKHG-PVTPAEYHSPPVQRLVLHANNVVCWSNDVQSLKMEILNQPG YTGALFADVEAIE-IIIEKV-YLPAHILQHFTIVORLVLACNNIVCWANDIFSCAKEARQ-G HDIAKPFMIAAIR-FGSGVRQTPEE---TAPFAELEDLYVQHSILINDLYSYDKEMYE-A GCVGAYPCIGLMF-FAEGI-DI PQNVMHDPSMQAISRITCDLVLQNDLCSYRKDLIQ-G GSLGAYPALVNNE-WAYGI-DLPEEEVADHPLVFEIMIIMSDQILLVKDILSYEKDLRL-G DDVGVIPISTQNE-YAMEF-ELPEWIRRHEAMEEIVLECTKLILLNEVLSLQKEFRV-S GTIGVYPAISLSE-YGAGV-NVPQHVVYDHPQLQECMKVSADLVTLVNDVLSYRKDLEL-G

Figure S36. Amino acid sequence alignment of DdTPS9, DpTPS10 and DpTPS11 with characterised bacterial and fungal terpene synthases.^{5,15-30}

XP_642260 (Dictyostelium discoideum AX4, (-)- <i>b</i> -Barbatene) XP_003289490 (Dictyostelium purpureum QSDP1, (-)- <i>b</i> -Araneosene) XP_003289235 (Dictyostelium purpureum QSDP1, (+)-Nephthenol) XP_645125 (Dictyostelium discoideum AX4, Asterisca-2(9),6-diene) WP_638489 (Dictyostelium discoideum AX4, Protoillud-7-ene) WP_039931950 (Streptomyces viridochromogenes DSM 40736, a-Amorphene) CCA53839 (Streptomyces venezuelae ATCC 10712, Isodauc-8-en-11-ol) WP_005317515 (Streptomyces pristinaespialis ATCC 25486, Selina-4(15),7(11)-diene) WP_003950762 (Streptomyces albus J1074, epi-Isozizaene) WP_042496076 (Streptomyces griseus NBRC 13350, Caryolan-1-ol) WP_003970379 (Streptomyces griseus NBRC 13350, epi-Cubenol) WP_003994861 (Streptomyces viridochromogenes DSM 40736, 7-epi-a-Eudesmol) Q55012 (Streptomyces exfoliatus UC5319, Pentalenene) WP_010981512 (Streptomyces avermitilis MA-4680, Avermitilol) AEM85259 (Streptomyces violaceusniger Tü 4113, Isoafricanol) WP_005320742 (Streptomyces pristinaespialis ATCC 25486, Pristinol) WP_014134444 (Kitasatospora setae KM-6054, Corvol ether) WP_012792334 (Chitinophaga pinensis DSM 2588, g-Cadinene) FFUJ_10353 (Fusarium fujikuroi IMI 58289, a-Acorenol) XP_023434772 (Fusarium fujikuroi IMI 58289, Koraiol) XP_023437750 (Fusarium fujikuroi IMI 58289, (-)-Guaiia-6,10(14)-diene) XP_006969402 (Trichoderma reesei QM6a, Trichobrasilenol) Q6WP50 (Botrytis cinerea B05.10, Presilphiperfolan-8-beta-ol)	361 370 380 390 400 410 420 HLTNPLHFLQNQVG-----SFDNVYKVILKFNFDEIMNQICED-ERILLLECPIE---- AYCNTFYFLQKDST----KFSTFDQVCEYLNFNEANTYIKDIITD-EPLLHDFEDV---- DTMNYVKIMANKK-----SIQKALNHTNKIIINNTLKEIISI-ENQIKMQY---- APLNSLKFQIQIEKN----LNQESFEYISNYLNELINQYIEL-ETSFIKSYKPITSN- GDLNPLYFLQNQKN----IPLPDSYKQVVDLIDFWVKDYQTM-EQSLLNEMEFKDSK- GMINLALAYRTHR----CSLPAAVTLAVRHINSTIREFEDL-YGEVRPELSPSGIG- DVNNLVVVVGTSLG----ITLHQAVPAALHMVNARMRDFEHLRHELPPVDRFGLRP YYLNALRVLQEORG----LTPAQALDAASQRDRVMCLFTV-SEQLAEGQSP---- DQHNLGISLRHEG----LSLEEAVVEVRKRVCNVCTEFEVA-EKELRELLAGHLAAL YEHNRAVLRIQRDRG----STLQEAVDEAGIQLARIAERVQRA-ERELIEEIAAGIDG EIHNHLVHILVRHHRG----LGEQQALDHVAERLAMETERFLITA-EDELLELYPE---- DGHNLIAVLRERG----CSWQEATDEAYRMTIARLDEYLEL-QERVPQMCDELRLDE EQNNNMVILRREHG----WSKRSRSVSHMNEVRARLEQYILL-ESCLPKVGEIYQLDT DMDNVLVHARR----CTRDEAVTAARGEVARVIRFEQL-AREVPALCAQLGLSA DVHNSVIVQWERAG----GELEDRAVRHIADLANARYRWFEET-AARLPALLTEAGADP DINNSVVIERHKG----CTLEESVEHITALANARTARFARI-AASLPGTIADLGVPA QYWNMAAIYAH-RG----LSLQAVDVLVALVRGEIASFQSLALTLEPH---- DVHNLVLVQLHERN----STLQEAVNETARMHNEEVKLFAL-EKLLPSFGAE---- RTINGSVNAVHVIEKLMC-VPPHLAKTTIRTMFSFDVEKKYYAESERFMRDPA---- EESNIIFIL-KDQG----MTDQQAVDQIGEMLYDCYRRWHMA-LANLPFWGEG---- VDHNMVRLL-KAKG----LSTQQAINEVGVMINNCYRRYYRA-LSELPFCGEE---- QLENLCLLFMNTDN----VSIEEAIDKILGLLQEHYEICVAA-EARLPWSETDEK--- VDHNLMSLLMQRDN----LSAQQAVDVIGDMVNECYRRWYLA-LAELPSYGEK----
XP_642260 (Dictyostelium discoideum AX4, (-)- <i>b</i> -Barbatene) XP_003289490 (Dictyostelium purpureum QSDP1, (-)- <i>b</i> -Araneosene) XP_003289235 (Dictyostelium purpureum QSDP1, (+)-Nephthenol) XP_645125 (Dictyostelium discoideum AX4, Asterisca-2(9),6-diene) WP_638489 (Dictyostelium discoideum AX4, Protoillud-7-ene) WP_039931950 (Streptomyces viridochromogenes DSM 40736, a-Amorphene) CCA53839 (Streptomyces venezuelae ATCC 10712, Isodauc-8-en-11-ol) WP_005317515 (Streptomyces pristinaespialis ATCC 25486, Selina-4(15),7(11)-diene) WP_003950762 (Streptomyces albus J1074, epi-Isozizaene) WP_042496076 (Streptomyces griseus NBRC 13350, Caryolan-1-ol) WP_003970379 (Streptomyces griseus NBRC 13350, epi-Cubenol) WP_003994861 (Streptomyces viridochromogenes DSM 40736, 7-epi-a-Eudesmol) Q55012 (Streptomyces exfoliatus UC5319, Pentalenene) WP_010981512 (Streptomyces avermitilis MA-4680, Avermitilol) AEM85259 (Streptomyces violaceusniger Tü 4113, Isoafricanol) WP_005320742 (Streptomyces pristinaespialis ATCC 25486, Pristinol) WP_014134444 (Kitasatospora setae KM-6054, Corvol ether) WP_012792334 (Chitinophaga pinensis DSM 2588, g-Cadinene) FFUJ_10353 (Fusarium fujikuroi IMI 58289, a-Acorenol) XP_023434772 (Fusarium fujikuroi IMI 58289, Koraiol) XP_023437750 (Fusarium fujikuroi IMI 58289, (-)-Guaiia-6,10(14)-diene) XP_006969402 (Trichoderma reesei QM6a, Trichobrasilenol) Q6WP50 (Botrytis cinerea B05.10, Presilphiperfolan-8-beta-ol)	421 430 440 450 460 470 480 -----QRDDLKLL-TRSMKLILGGNYLW-SLQCSRVDINSPFIEQRSN----- -----EDRKVVQSSLNLNVHYLISGNGFVNWIENNRQYQSSISPFIETNKK----- -----KENNLYQY-IERLNSVISATIYL-HQNHKRYSVHNKNYINKNN----- -----YNSNFIAI-VEHLHNMSFANWS-STQTPRYLSQTQPFLELRRN----- -----QRSDMEFI-LEHLRLYLASGSKKW-SMQTPRYCSPTSPFIEMRTPKSTPV----- -----VEGMAGWIRGCYFW-SRTVPRYADLTAPAGL----- D-----EREELETW-LGGAASFSLGLHW-YTGAPRYAAPTDSVPEQRQGGSEG----- -----QLRQY-LHSLRCFIRGAQDW-GISSVRYTTPDDPANMPSVFTDVPT PGGAGTAEARSVAEAVGSA-VFNMRNWFFSVY-WFHESGRYRVDSWDD----- P-----TRTALERCV-RDYLGRVGDY-HARAERYTRPDVLEADER----- -----LSGMLVPY-LDGMRSWMRGNLDW-SRQTPRYNPADVGQYEEPEEYLEET A-----QRDGVRVLG-VEAIQHWINGNYEW-ALTSGRYAAAKEGAVATAE----- A-----EREALERYRTDAVRTVIRGYSWD-HRSSGRYDAEFALA----- V-----ERAHVDTY-LGVMEAWMMSGYHAW-QTQTRRYTGAPHVLP----- G-----THHAVGRY-VDGMRHMVTGNLHW-SVRTARYDERGTEAVSGGRQRPWAO P-----SREHVSHEY-VDGMRHMAGNLSW-SLATSRYDETGIAAVSGGRRRPWDG----- -----ASRPLRGF-VDGLRHWMRGYQDWVENDTLRYADAFIAE----- -----MDRELERF-MAVLRSWITANYDWSYHDTGRYQVKEVEVVINS----- -----LNDKQRTY-VIALFDCLTGNLFH-HATLGRYSSRYAEYVFDCKT----- -----IDRDVIKF-VTGCRNIALGNLHW-SLYTFRYLGNNDGPEVK----- -----ADRALLGY-LEVEKNHALGSLLW-SYNTGRYFKSKEDGARVR----- -----LNEDIREY-VRGANRLATGTACW-SYNCERYFKLSQVN----- -----IDYNVMKF-VEICRAVAQGNLYW-SFQTGRYILGPEGHEVH-----

Figure S36. Amino acid sequence alignment of DdTPS9, DpTPS10 and DpTPS11 with characterised bacterial and fungal terpene synthases.^{5,15-30}

	481	490	500	510
XP_642260 (Dictyostelium discoideum AX4, (-)- <i>b</i> -Barbatene)	-----DPNVIAYEKIVDKILLK-----			
XP_003289490 (Dictyostelium purpureum QSDP1, (-)- <i>b</i> -Araneosene)	-----ENKIEKYNTLISTIFKQ-----			
XP_003289235 (Dictyostelium purpureum QSDP1, (+)-Nephthenol)	-----KKIITKIYDLKNK-----			
XP_645125 (Dictyostelium discoideum AX4, Asterisca-2(9),6-diene)	MNSTKKQKIDHVPSQSFISTPIDLN-----			
XP_638489 (Dictyostelium discoideum AX4, Protoillud-7-ene)				
WP_039931950 (Streptomyces viridochromogenes DSM 40736, <i>a</i> -Amorphene)	AADRHAPAASSLARGAEAQTCGPTASAGSA-----			
CCA53839 (Streptomyces venezuelae ATCC 10712, Isodauc-8-en-11-ol)	DDSTEPLDI--PAVSWWWDLLAEDARSVRQRQVPAQRSA-----			
WP_005317515 (Streptomyces pristinaespiralis ATCC 25486, Selina-4(15),7(11)-diene)	RSTPPYVSDLAGDA-----			
WP_003950762 (Streptomyces albus J1074, epi-Isozizaene)	DSLSRHFAA-----			
WP_042496076 (Streptomyces griseus NBRC 13350, Caryolan-1-ol)	VLGVPPA---RSETAAPAPCGAEAPRAR-----			
WP_003970379 (Streptomyces griseus NBRC 13350, epi-Cubenol)	LAGRGGSVDDLLTV-----			
WP_003994861 (Streptomyces viridochromogenes DSM 40736, 7-epi- <i>a</i> -Eudesmol)	AGAQGYLEELGSSAH-----			
Q55012 (Streptomyces exfoliatus UC5319, Pentalenene)	STGPGYFDEVLP-----			
WP_010981512 (Streptomyces avermitilis MA-4680, Avermitilol)	LTGAELIR--AGRGAAPLPLGSGSGSR-----			
AEM85259 (Streptomyces violaceusniger Tü 4113, Isoafricanol)	L-----TTATGTASPRHPRRA-----			
WP_005320742 (Streptomyces pristinaespiralis ATCC 25486, Pristinol)	DADDTAVRT-----			
WP_014134444 (Kitasatospora setae KM-6054, Corvol ether)	-----			
WP_012792334 (Chitinophaga pinensis DSM 2588, <i>g</i> -Cadinene)	-----			
FFUJ_10353 (Fusarium fujikuroi IMI 58289, <i>a</i> -Acorenol)	-----RTRMMKLP-----			
XP_023434772 (Fusarium fujikuroi IMI 58289, Koraiol)	-----KTRELLIPKMAAL-----			
XP_023437750 (Fusarium fujikuroi IMI 58289, (-)-Guaiia-6,10(14)-diene)	-----EKRELLLDLSYR-----			
XP_006969402 (Trichoderma reesei QM6a, Trichobrasilenol)	-----ETGIMYLPPAANLVVA-----			
Q6WP50 (Botrytis cinerea B05.10, Presilphiperfolan-8-beta-ol)				

Figure S36. Amino acid sequence alignment of DdTPS9, DpTPS10 and DpTPS11 with characterised bacterial and fungal terpene synthases.^{5,15-30}

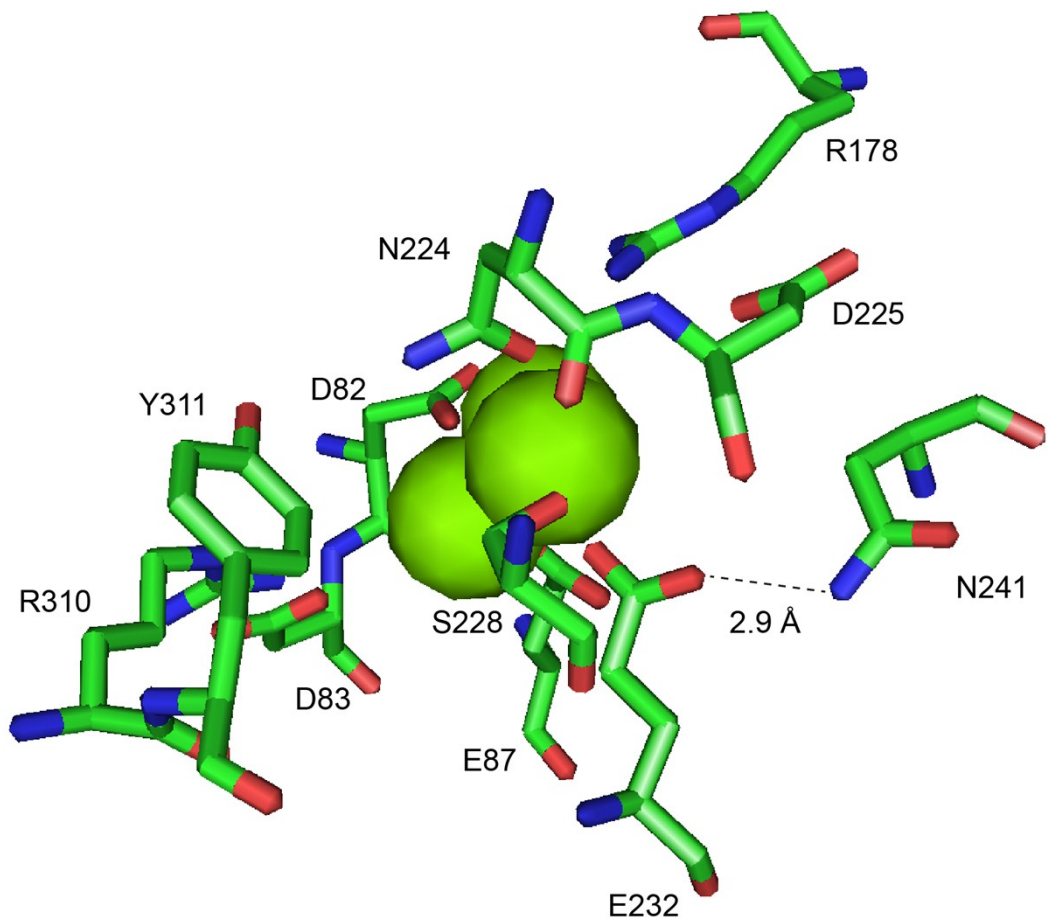


Figure S37. Active site residues observed in the crystal structure of selinadiene synthase (SdS, PDB: 4OKZ).³¹ Green spheres represent Mg^{2+} cations.

Qualitative conversion assay with TPS variants

For comparing the constructed enzyme variants with their corresponding wild types, small scale reactions were conducted using 0.2 mg of diphosphate substrate (FPP or GGPP) dissolved in 100 μ L substrate buffer. The solutions were diluted with incubation buffer (300 μ L) and the reactions were started adding TPS elution fraction (600 μ L, protein concentrations were adjusted to 0.2 mg/mL by Bradford assay, cf. Figure S1). The reactions were incubated for 30 min at 28 °C with shaking, before the mixtures were extracted with hexane (150 μ L). The extracts were dried with MgSO₄ and analysed by GC/MS. All reactions were conducted in triplicates.

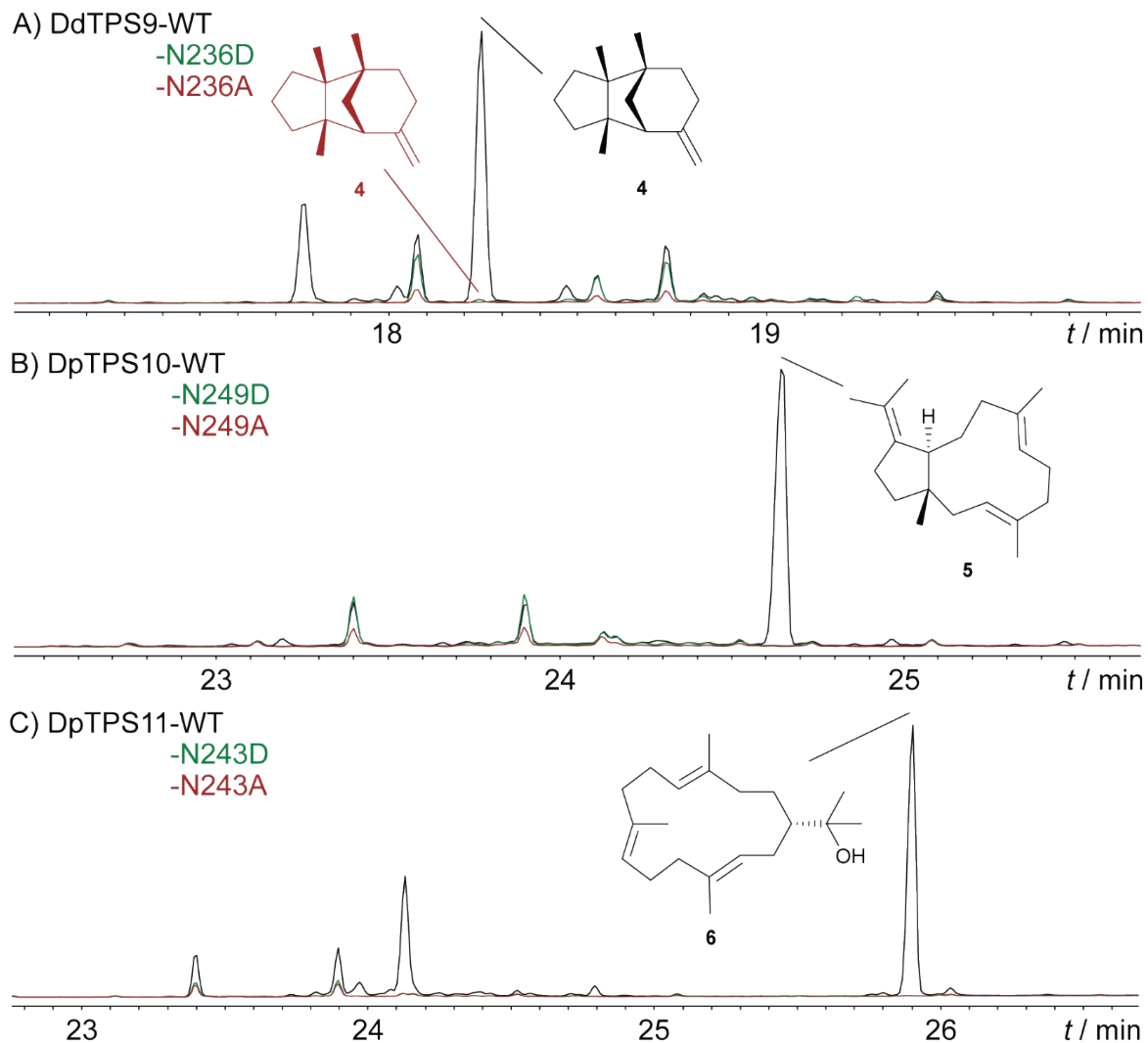


Figure S38. Comparing total ion chromatograms from incubation experiments using wild-type (WT) TPSs (black) and their corresponding Asn to Asp (green) and Asn to Ala (red) variants for A) DdTPS9 with FPP, B) DpTPS10 with GGPP and C) DpTPS11 with GGPP. Only for the variant DdTPS9-N236A, residual conversion to the native product was observed ($3.0 \pm 1.0\%$) compared to normalised WT conversion ($100.0 \pm 15.3\%$). Standard deviations were calculated from triplicates.

HPLC conditions

Analytical scale HPLC purifications were carried out using an PLATINblue-series UHPLC system (Knauer, Berlin, Germany), equipped with a photo diode array detector PDA-1 (190-1000 nm) and a Macherey-Nagel (Düren, Germany) Nucleodur® 110-1.8 Gravity C18 column (1.8 μm ; 2.0 x 100 mm) using an isocratic solvent mixture of [acetonitrile/water (90:10)] with 0.5 mL min⁻¹ (334 bar). The UV-vis absorption was monitored at 220 nm. Observed elution times were: **12**: 11.39 min; **13**: 9.20 min; **14**: 8.43 min; **15**: 7.42 min.

Semi-preparative scale HPLC purifications were performed on an Smartline-series HPLC system (Knauer) with a UV-Vis detector S-2550 (190-900 nm) using a Macherey-Nagel (Düren, Germany) Nucleodur® 110-5 Gravity C18 column (5 μm ; 10 x 250 mm). The solvent mixture [acetonitrile/water (90:10)] was used at 8 mL min⁻¹ (113 bar) and monitoring was done at 220 nm.

Reaction of 5 with NBS

A stirred solution of **5** (5.4 mg, 19.8 μmol , 1.0 eq.) in dry dichloromethane (1 mL) was cooled to -78 °C, before *N*-bromosuccinimide (NBS, 3.5 mg, 19.8 μmol , 1.0 eq. was added in one portion. Stirring was continued for 20 min at the same temperature and the solution was allowed to warm to room temperature over 1 h. After stirring for 30 min at room temperature, saturated NH₄Cl solution (2 mL) was added and the mixture was extracted with pentane (3x 3 mL). The organic extracts were dried with MgSO₄, concentrated under reduced pressure, fractionated by column chromatography on silica gel [pentane] and further purified by HPLC (conditions are described above) to yield bromodolastadienes **12** (1.4 mg, 4.0 μmol , 20%) and **13** (0.5 mg, 1.4 μmol , 7%), and bromodolastatrienes **14** (0.6 mg, 1.7 μmol , 9%) and **15** (1.8 mg, 5.2 μmol , 26%) as colourless solids.

(2*S*,6*R*,7*R*,11*S*)-6-Bromodolasta-3,10(14)-diene, (3*aS*,4*aS*,8*R*,8*aR*)-8-bromo-1-isopropyl-3*a*,5,8*a*-trimethyl-2,3,3*a*,4,4*a*,7,8,8*a*,9,10-decahydrobenzo[*f*]azulene (**12**). *R*_f (pentane) = 0.70. $[\alpha]_D^{20} = +3.2^\circ$ (*c* 0.15, C₆H₆). HRMS (QTOF): *m/z* = 350.1606 (calc. for [C₂₀H₃₁Br]⁺ 350.1604). GC (HP5-MS): *I* = 2283. MS (EI, 70 eV): *m/z* (%) = 352 (13), 350 (14), 337 (25), 335 (26), 309 (42), 307 (43), 281 (2), 271 (4), 255 (9), 227 (23), 213 (7), 199 (9), 190 (23), 175 (25), 161 (17), 151 (55), 133 (77), 121 (100), 107 (55), 95 (84), 81 (56), 69 (16), 55 (16), 41 (16). IR (diamond ATR): ν / cm⁻¹ = 3033 (w), 2955 (s), 2926 (s), 2853 (m), 1460 (m), 1377 (w), 1174 (w), 853 (w), 795 (w), 749 (w), 596 (w). NMR data are given in Table S5 and Figures S40–S46.

(2*S*,6*R*,7*R*,11*S*)-6-Bromodolasta-3(20),10(14)-diene, (3*aS*,4*aS*,8*R*,8*aR*)-8-bromo-1-isopropyl-3*a*,8*a*-dimethyl-5-methylene-2,3,3*a*,4,4*a*,5,6,7,8,8*a*,9,10-dodecahydrobenzo[*f*]azulene (**13**). *R*_f (pentane) = 0.56. $[\alpha]_D^{20} = +11.3^\circ$ (*c* 0.05, C₆H₆). HRMS (QTOF): *m/z* = 350.1597 (calc. for [C₂₀H₃₁Br]⁺ 350.1604). GC (HP5-MS): *I* = 2249. MS (EI, 70 eV): *m/z* (%) = 352 (13), 350 (14), 337 (44), 335 (45), 309 (82), 307 (85), 281 (7), 271 (13), 255 (16), 241 (2), 229 (19), 227 (36), 201 (14), 187 (14), 175 (16), 161 (38), 149 (51), 133 (71), 121 (100), 107 (80), 93 (83), 79 (58), 69 (26), 55 (33), 41 (33). IR (diamond ATR): ν / cm⁻¹ = 3083 (w), 2953 (s), 2926 (s), 2853 (m), 1462 (m), 1379 (w), 1208 (w), 891 (w), 726 (w). NMR data are given in Table S6 and Figures S48–S54.

(2*S*,6*R*,7*R*,11*S*)-6-Bromodolasta-3,9,13-triene, (3*aS*,4*aS*,8*R*,8*aR*)-8-bromo-1-isopropyl-3*a*,5,8*a*-trimethyl-3*a*,4,4*a*,7,8,8*a*,9-octahydrobenzo[*f*]azulene (**14**). *R*_f (pentane) = 0.56. $[\alpha]_D^{20} = +8.6^\circ$ (*c* 0.07, C₆H₆). HRMS (QTOF): *m/z* = 348.1450 (calc. for [C₂₀H₂₉Br]⁺ 348.1447). GC (HP5-MS): *I* = 2309. MS (EI, 70 eV): *m/z* (%) = 350 (15), 348 (15), 281 (4), 269 (6), 225 (4), 207 (7), 185 (4), 175 (8), 159 (8), 148 (55), 133 (100), 119 (57), 105 (42), 95 (36), 91 (35), 79 (15), 69 (7), 55 (8), 41 (10). IR (diamond ATR): ν / cm⁻¹ = 3048 (w), 3027 (w), 2956 (m), 2923 (s), 2852 (m), 1459 (m), 1378 (w), 1173 (w), 998 (w), 849 (w), 821 (w), 795 (w), 751 (w). NMR data are given in Table S7 and Figures S56–S62.

(2*S*,6*R*,7*R*,11*S*)-6-Bromodolasta-3(20),9,13-triene, (3*aS*,4*aS*,8*R*,8*aR*)-8-bromo-1-isopropyl-3*a*,8*a*-dimethyl-5-methylene-3*a*,4,4*a*,5,6,7,8,8*a*,9-decahydrobenzo[*f*]azulene (**15**). *R*_f (pentane) = 0.49. $[\alpha]_D^{20} = +44.0^\circ$ (*c* 0.20, C₆H₆). HRMS (QTOF): *m/z* = 348.1446 (calc. for [C₂₀H₂₉Br]⁺ 348.1447). GC (HP5-MS): *I* = 2294. MS (EI, 70 eV): *m/z* (%) = 350 (39), 348 (39), 335 (4), 333 (5), 307 (10), 305 (10), 269 (27), 225 (9), 213 (7), 199 (6), 185 (7), 175 (9), 161 (24), 148 (45), 133 (100), 119 (36), 105 (43), 91 (40), 79 (19), 69 (7), 55 (9), 41 (11). IR (diamond ATR): ν / cm⁻¹ = 3086 (w), 3047 (w), 2954 (s), 2924 (s), 2851 (m), 1460 (m), 1379 (m), 1207 (w), 1172 (w), 1001 (w), 976 (w), 901 (w), 852 (w), 820 (w), 726 (w), 615 (w). NMR data are given in Table S8 and Figures S64–S70.

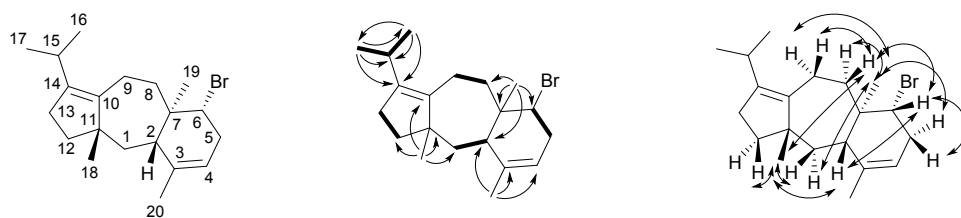


Figure S39. Carbon numbering and structure elucidation of **12**. H,H-COSY spin systems are represented by bold bonds, single headed arrows show HMBC correlations and NOESY correlations are depicted by double headed arrows.

Table S5. NMR data of (2*S*,6*R*,7*R*,11*S*)-6-bromodolasta-3,10(14)-diene (**12**) in C₆D₆ recorded at 298 K.

C ^[a]		¹³ C ^[b]	¹ H ^[b]
1	CH ₂	41.35	1.65 (m, H _α) 1.37 (m, H _β)
2	CH	46.97	2.06 (m)
3	C _q	136.35	—
4	CH	121.67	4.99 (br s)
5	CH ₂	36.39	2.65 (m, H _β) 2.50 (m, H _α)
6	CH	67.03	4.03 (dd, <i>J</i> = 11.4, 5.8)
7	C _q	41.72	—
8	CH ₂	37.41	2.29 (ddd, <i>J</i> = 14.7, 6.2, 4.2, H _β) 1.54 (m)
9	CH ₂	22.11	2.38 (m, H _β) 1.98 (m, H _α)
10	C _q	139.07	—
11	C _q	50.25	—
12	CH ₂	41.85	1.62 (m, H _α) 1.56 (m, H _β)
13	CH ₂	27.69	2.18 (m, 2H)
14	C _q	139.45	—
15	CH	27.09	2.54 (sept, <i>J</i> = 6.9)
16 ^[c]	CH ₃	20.79	0.941 (d, <i>J</i> = 7.0)
17 ^[c]	CH ₃	21.34	0.932 (d, <i>J</i> = 7.0)
18	CH ₃	24.66	1.04 (s)
19	CH ₃	11.39	0.924 (s)
20	CH ₃	22.80	1.46 (s)

[a] Carbon numbering indicates the origin of each carbon from GGPP by identical number as shown in Figure S39. [b] Chemical shifts δ in ppm, multiplicity: s = singlet, d = doublet, m = multiplet, br = broad, coupling constants J are given in Hertz. [c] Signals may be interchanged.

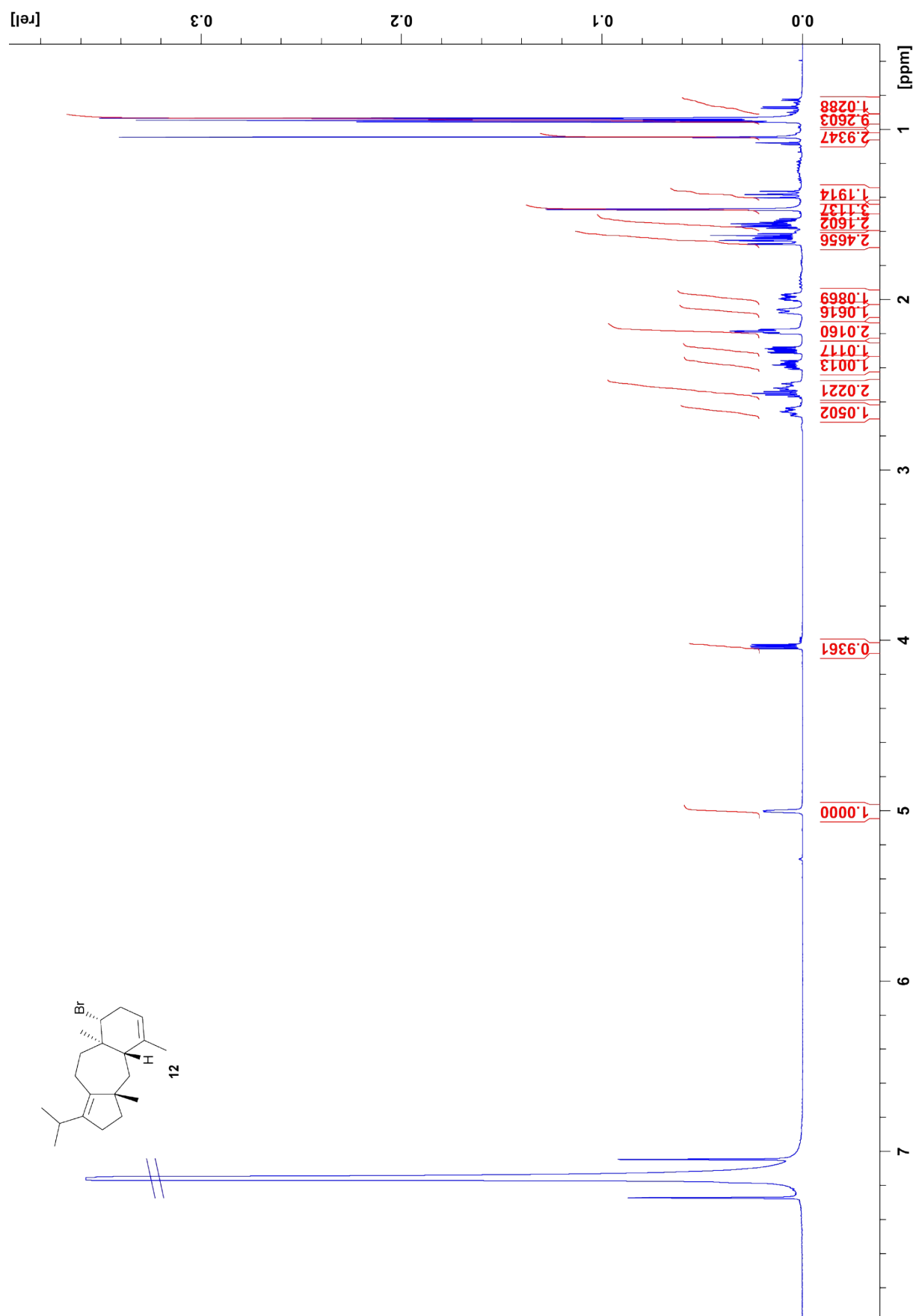


Figure S40. ¹H-NMR spectrum of **12** (700 MHz, C₆D₆).

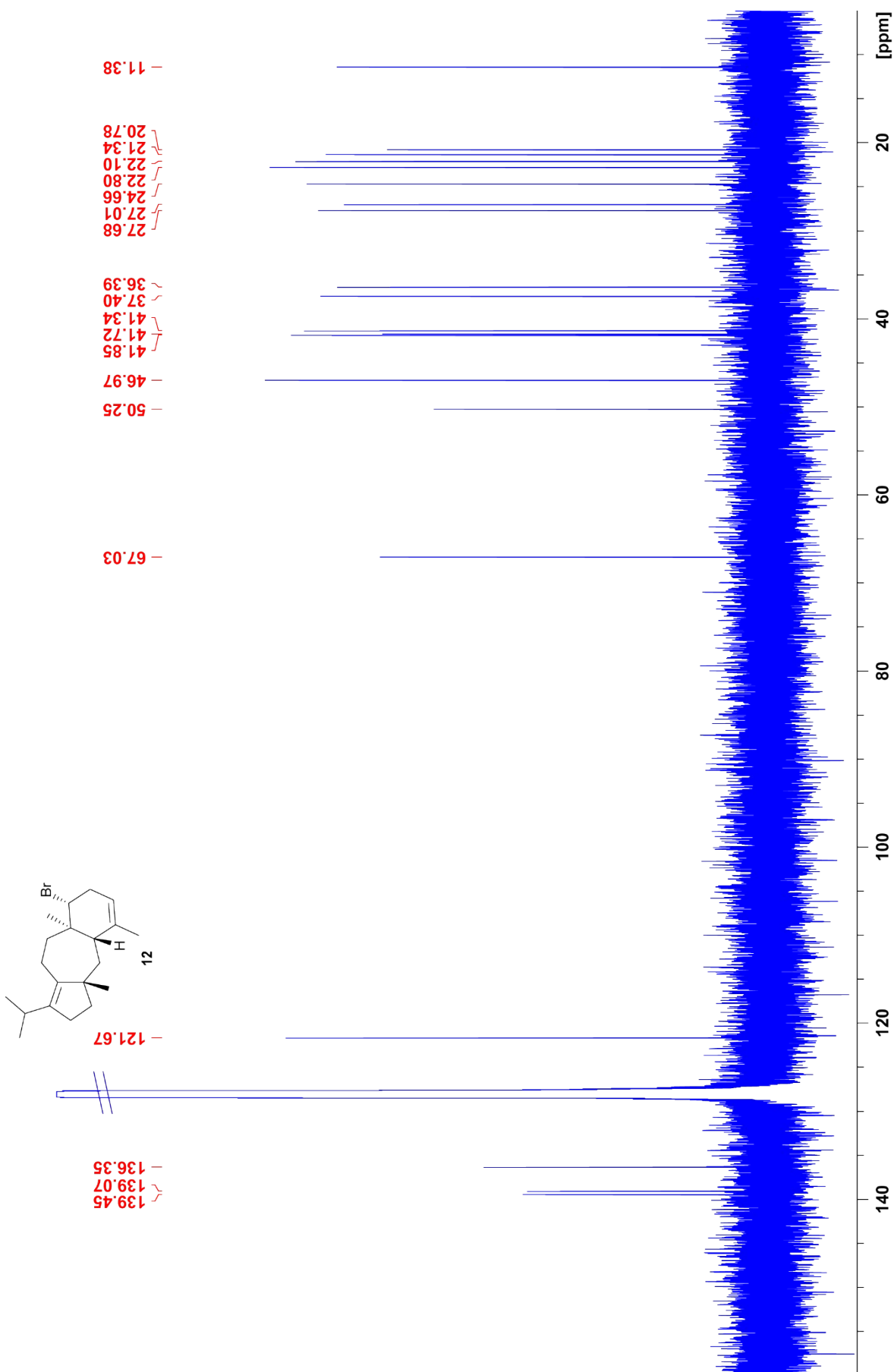


Figure S41. ^{13}C -NMR spectrum of **12** (175 MHz, C_6D_6).

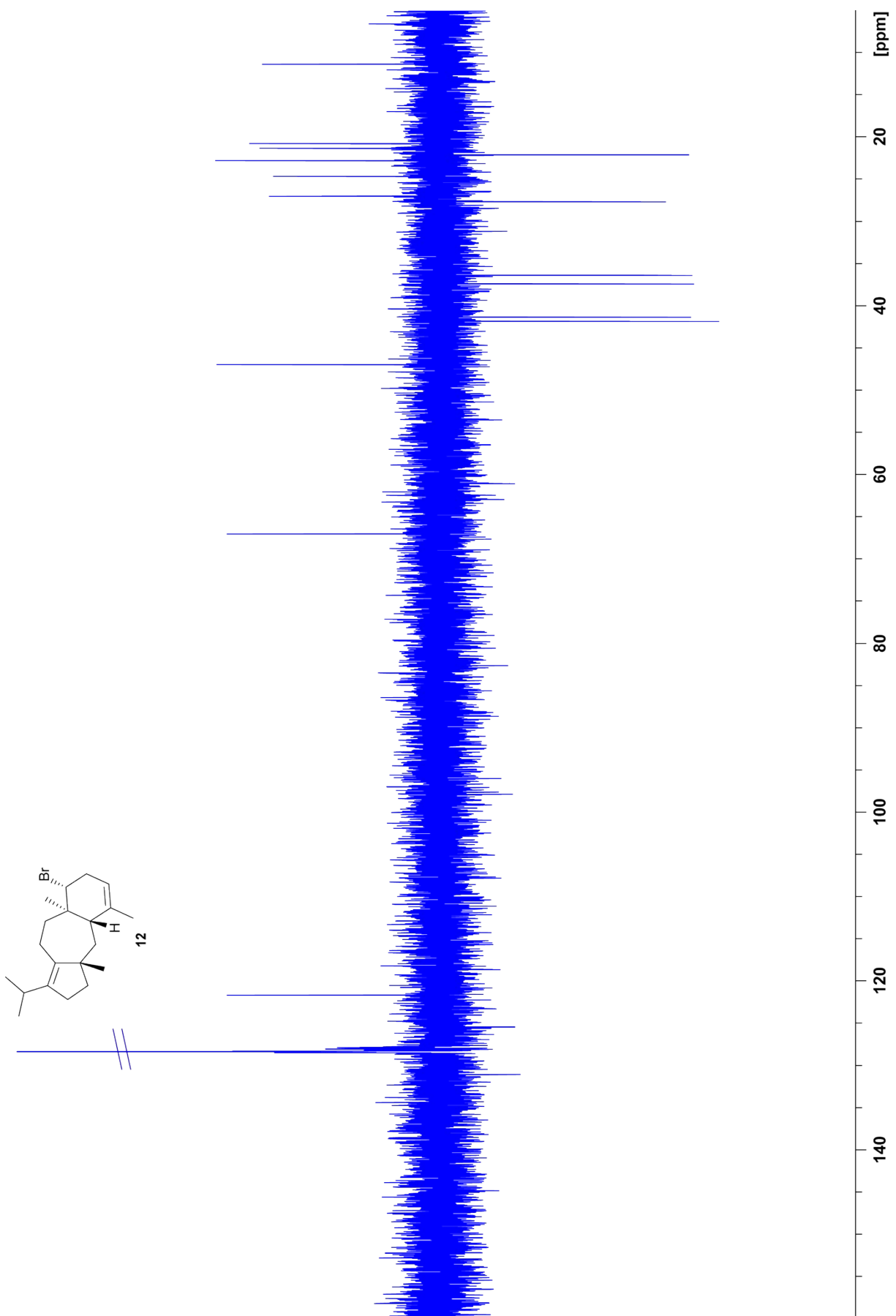


Figure S42. ^{13}C -DEPT spectrum of **12** (175 MHz, C_6D_6).

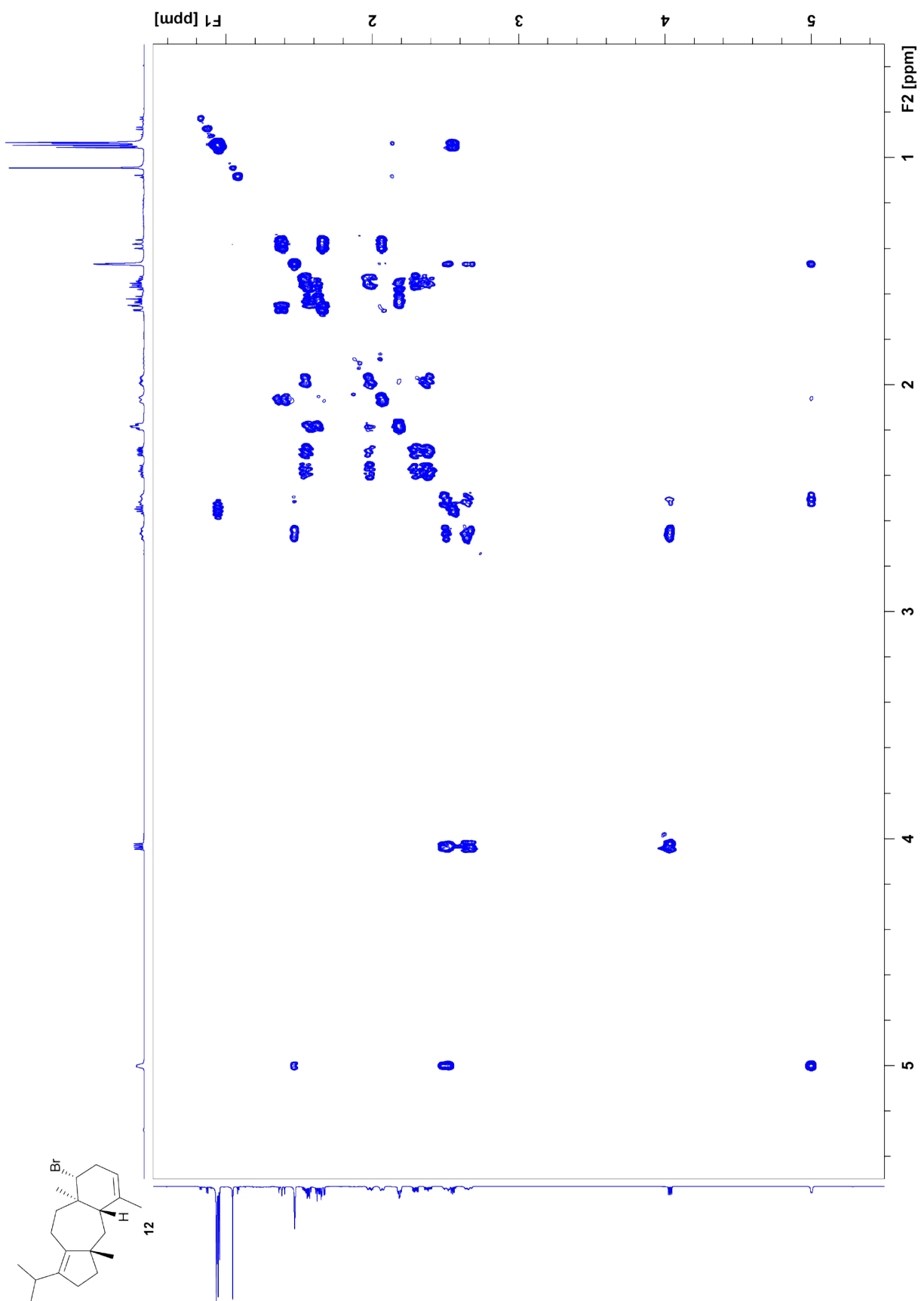


Figure S43. $^1\text{H},^1\text{H}$ -COSY spectrum of **12** (700 MHz, C_6D_6).

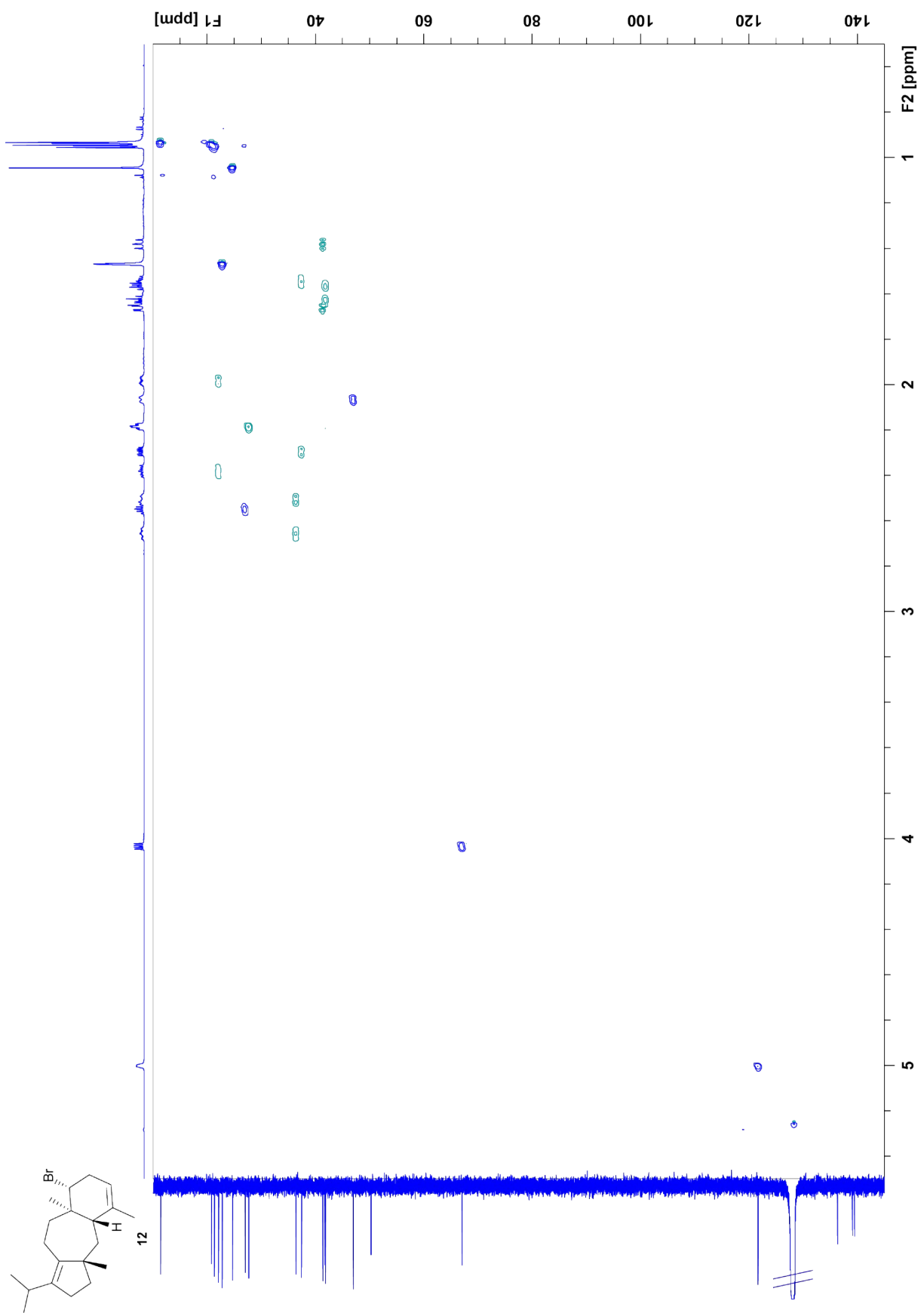


Figure S44. HSQC spectrum of **12** (700 MHz, C₆D₆).

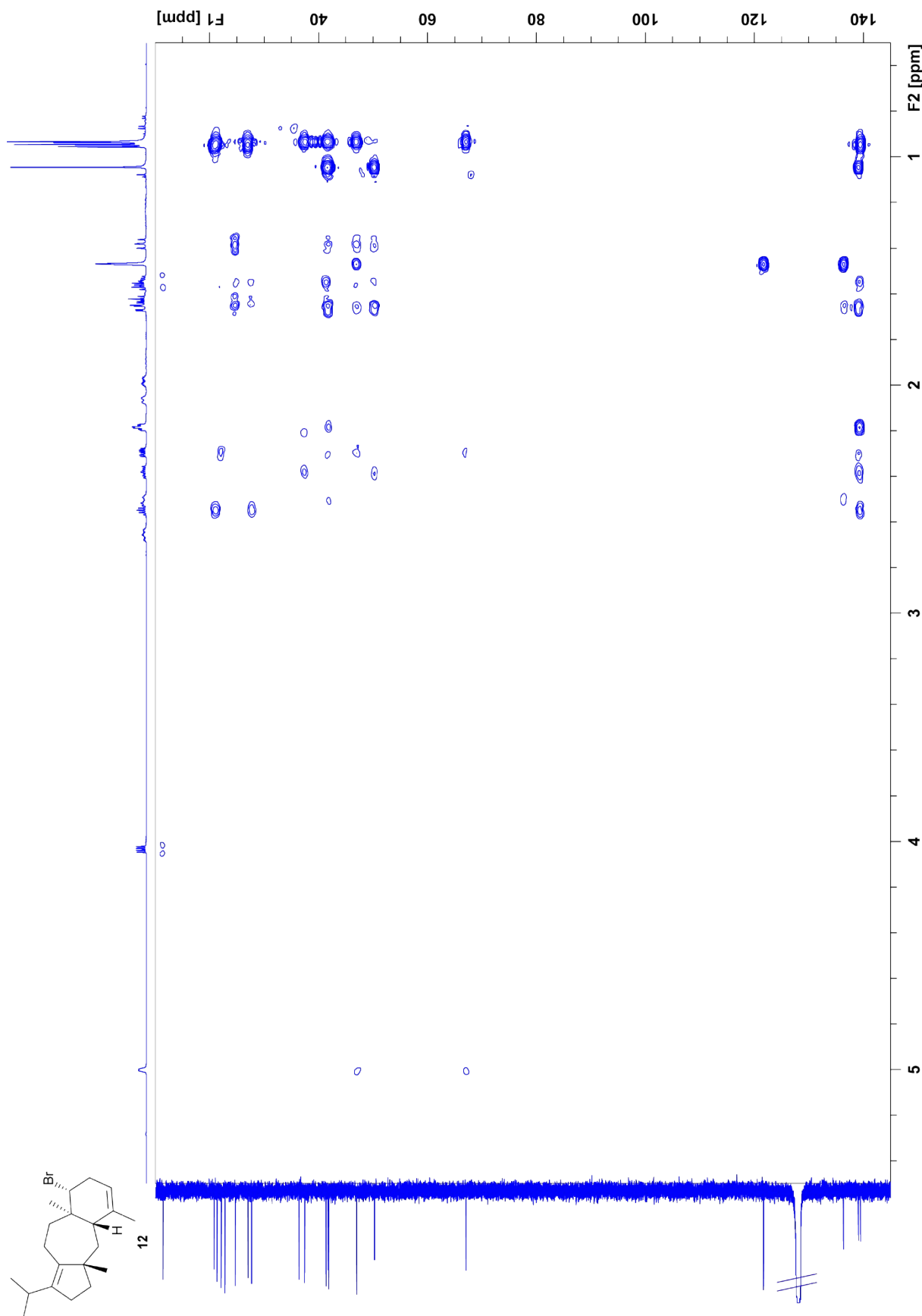


Figure S45. HMBC spectrum of **12** (700 MHz, C_6D_6).

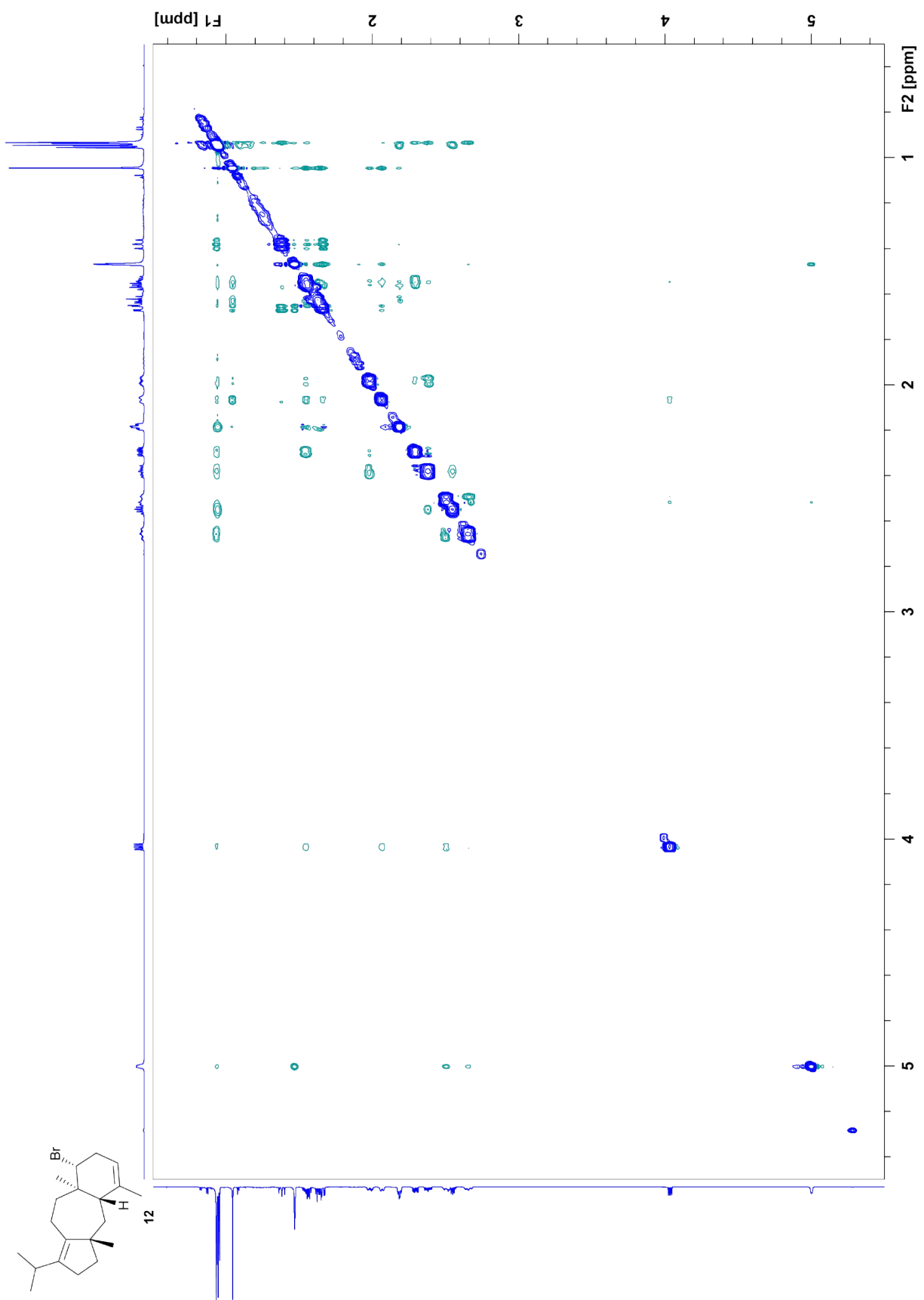


Figure S46. NOESY spectrum of **12** (700 MHz, C₆D₆).

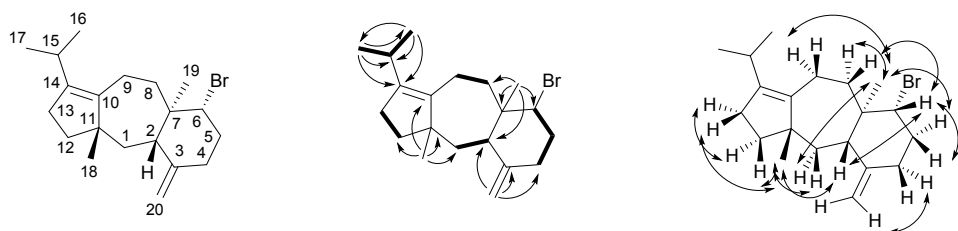


Figure S47. Carbon numbering and structure elucidation of **13**. H,H-COSY spin systems are represented by bold bonds, single headed arrows show HMBC correlations and NOESY correlations are depicted by double headed arrows.

Table S6. NMR data of (2*S*,6*R*,7*R*,11*S*)-6-bromodolasta-3(20),10(14)-diene (**13**) in C₆D₆ recorded at 298 K.

C[a]		¹³ C[b]	¹ H[b]
1	CH ₂	41.51	1.63 (m, H _α) 1.57 (dd, <i>J</i> = 13.9, 10.4, H _β)
2	CH	46.16	2.03 (m)
3	C _q	149.33	–
4	CH ₂	38.22	1.96 (ddd, <i>J</i> = 13.1, 4.9, 2.3, H _β) 1.72 (m, H _α)
5	CH ₂	36.11	2.10 (m, H _α) 2.08 (m, H _β)
6	CH	66.74	3.90 (dd, <i>J</i> = 12.0, 5.0)
7	C _q	44.97	–
8	CH ₂	38.38	2.03 (m, H _α) 1.72 (m, H _β)
9	CH ₂	20.51	2.25 (m, H _β) 1.87 (m, H _α)
10	C _q	140.85	–
11	C _q	49.59	–
12	CH ₂	41.68	1.63 (m, H _α) 1.52 (ddd, <i>J</i> = 11.9, 8.4, 8.4, H _β)
13	CH ₂	27.72	2.23 (m, H _α) 2.18 (m, H _β)
14	C _q	138.85	–
15	CH	26.83	2.56 (sept, <i>J</i> = 6.9)
16 ^[c]	CH ₃	21.38	0.96 (d, <i>J</i> = 6.9)
17 ^[c]	CH ₃	21.26	0.95 (d, <i>J</i> = 6.9)
18	CH ₃	23.68	1.00 (s)
19	CH ₃	14.25	0.88 (s)
20	CH ₂	108.16	4.73 (m, H _E) 4.59 (m, H _Z)

[a] Carbon numbering indicates the origin of each carbon from GGPP by identical number as shown in Figure S47. [b] Chemical shifts δ in ppm, multiplicity: s = singlet, d = doublet, m = multiplet, br = broad, coupling constants *J* are given in Hertz. [c] Signals may be interchanged.

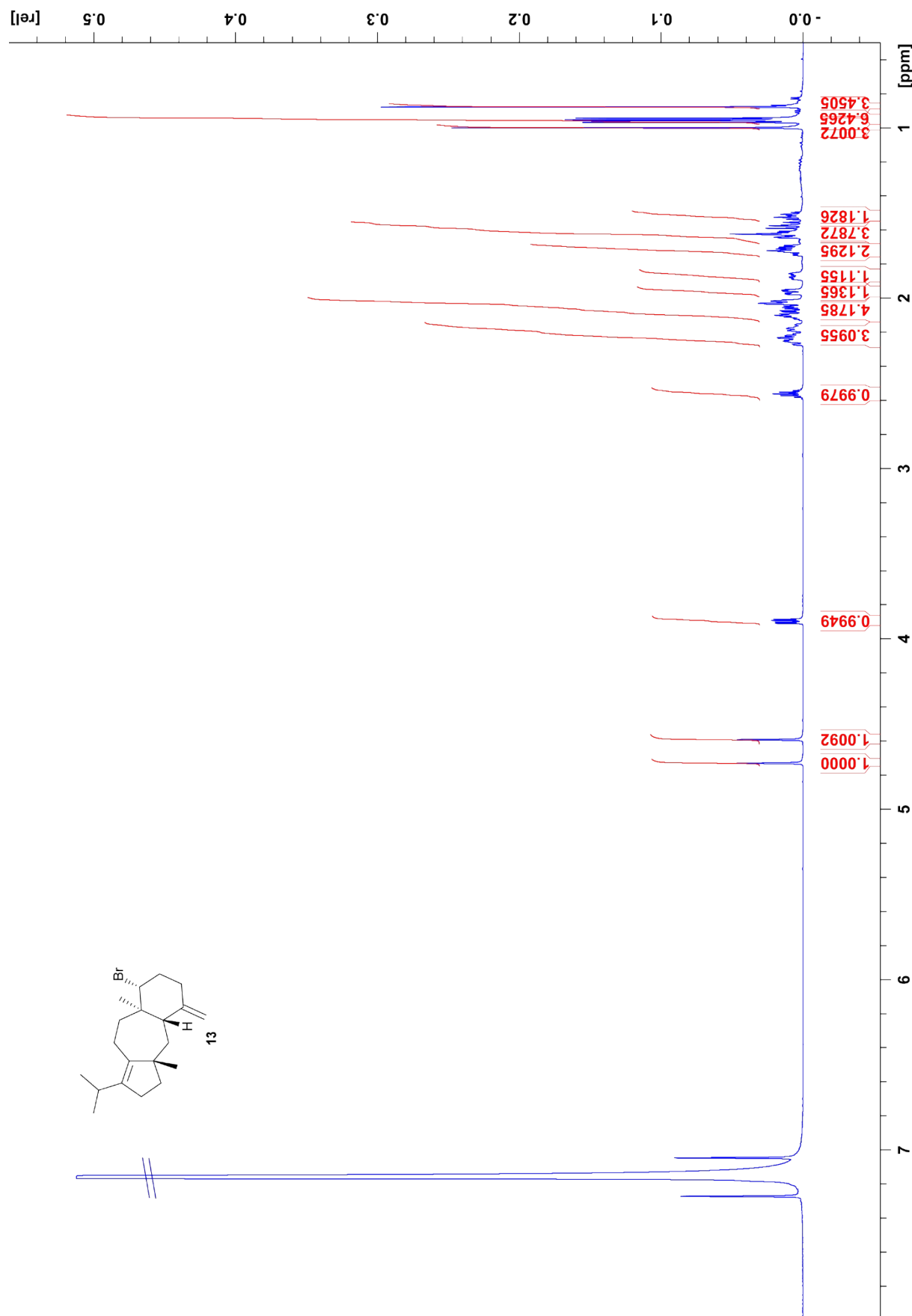


Figure S48. ¹H-NMR spectrum of **13** (700 MHz, C₆D₆).

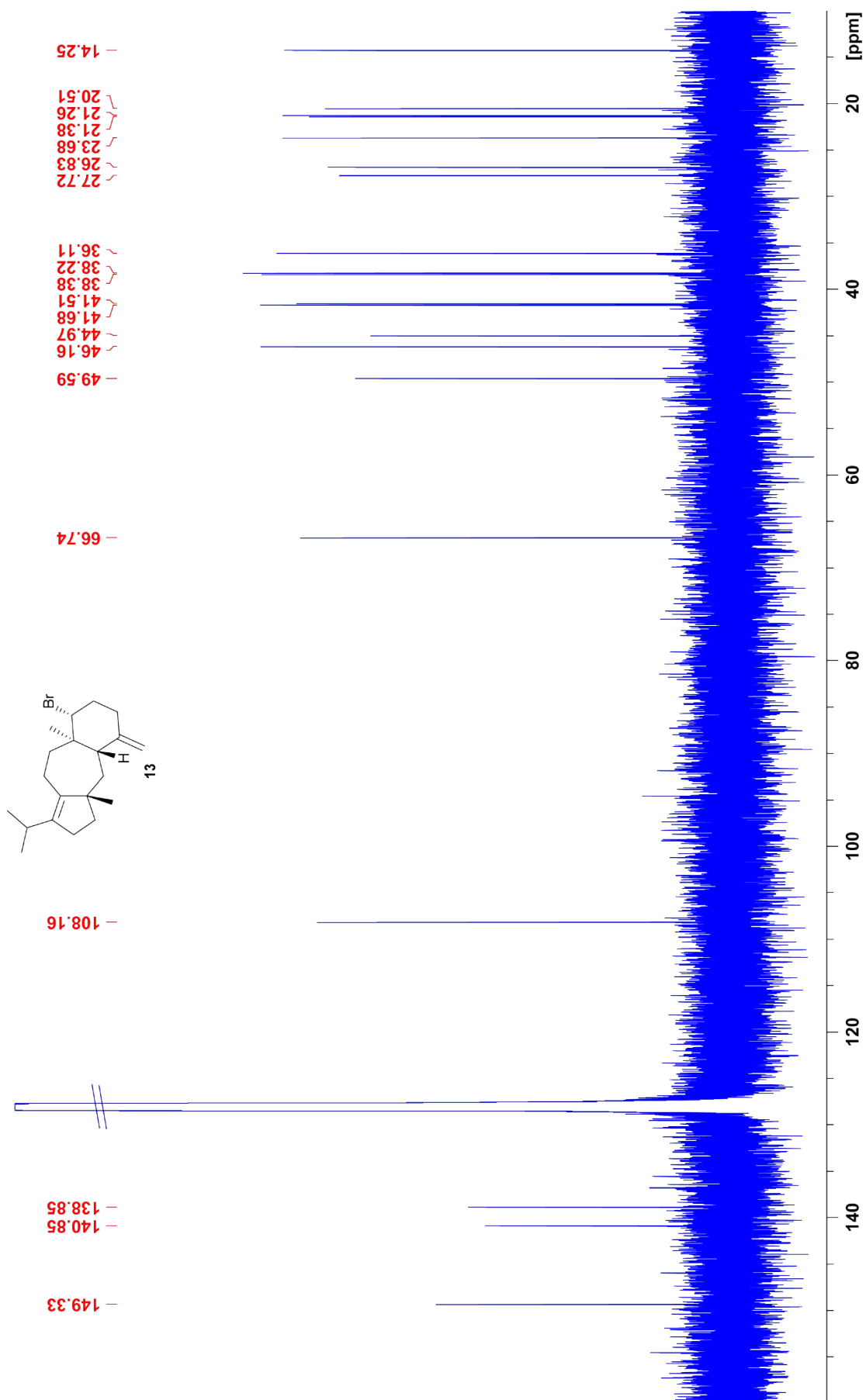


Figure S49. ¹³C-NMR spectrum of **13** (175 MHz, C₆D₆).

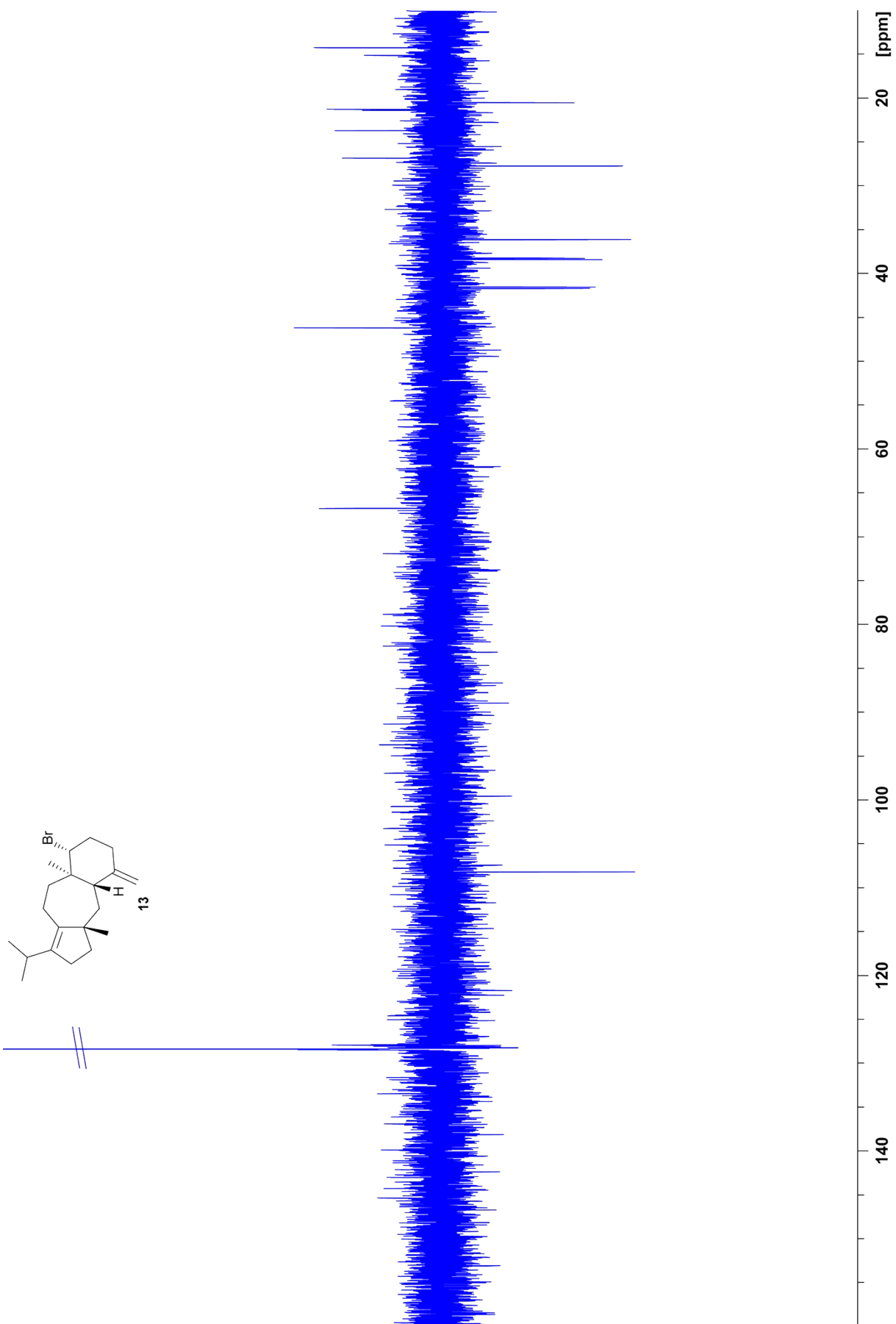


Figure S50. ^{13}C -DEPT spectrum of **13** (175 MHz, C_6D_6).

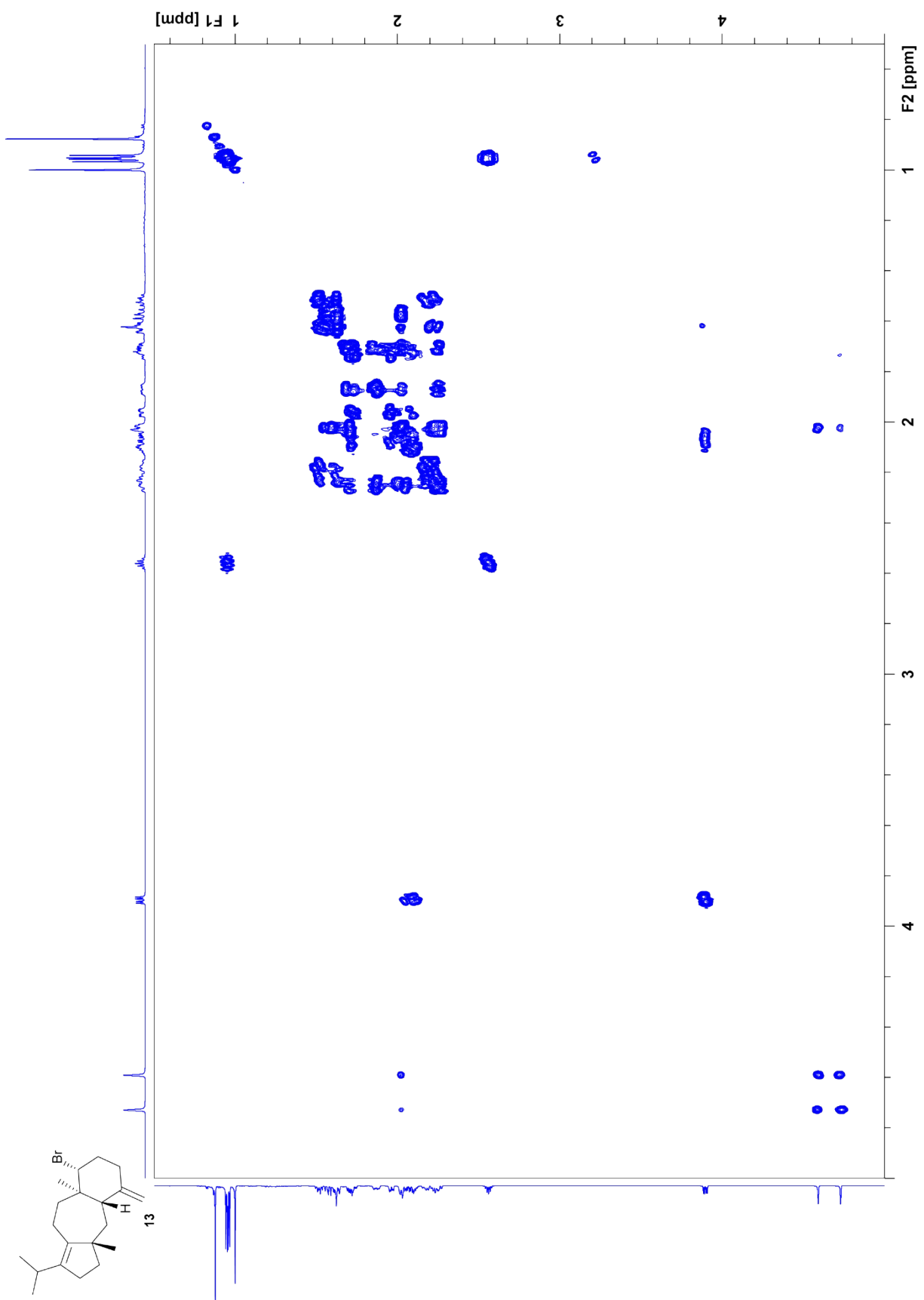


Figure S51. $^1\text{H},^1\text{H}$ -COSY spectrum of **13** (700 MHz, C_6D_6).

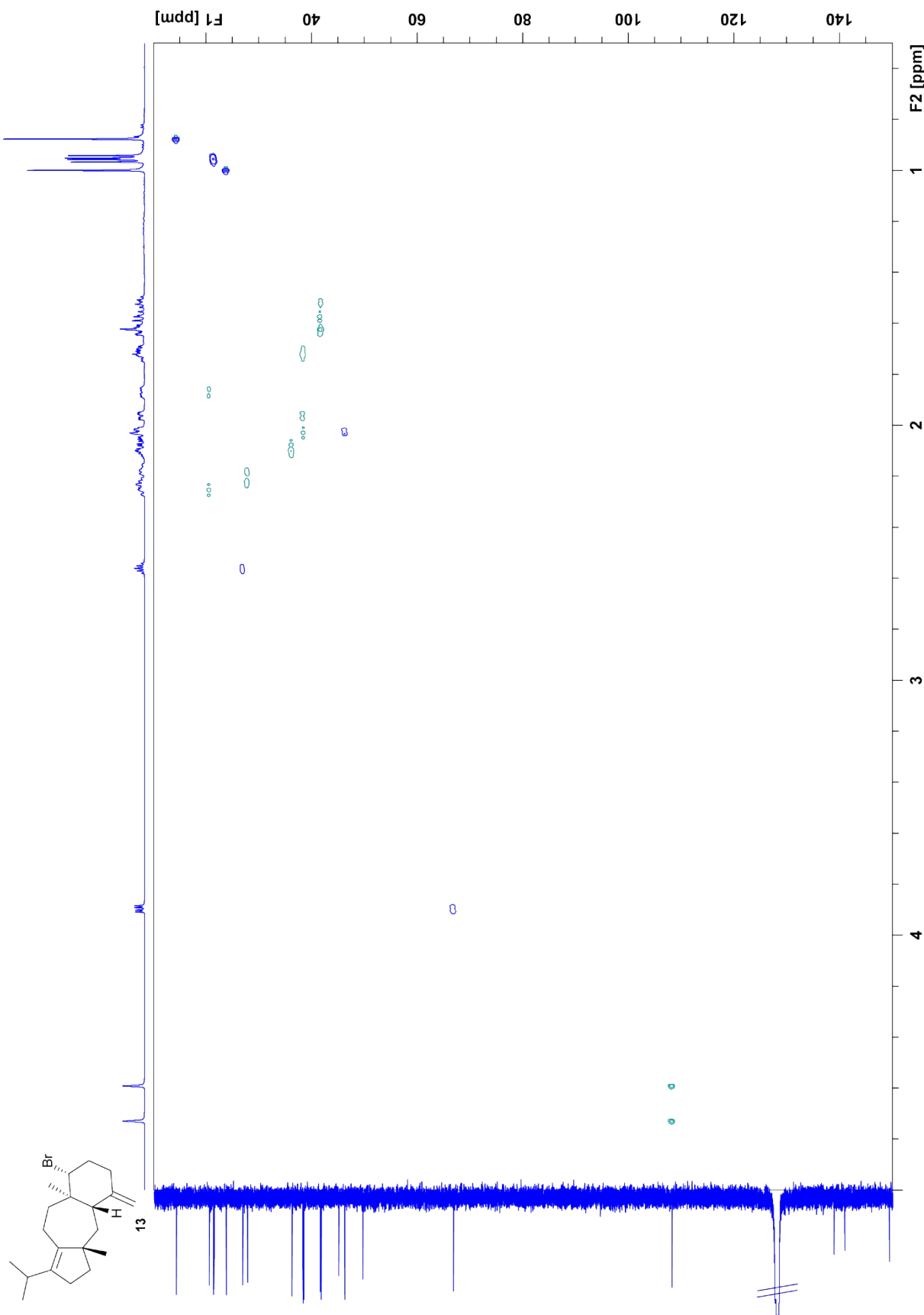


Figure S52. HSQC spectrum of **13** (700 MHz, C_6D_6).

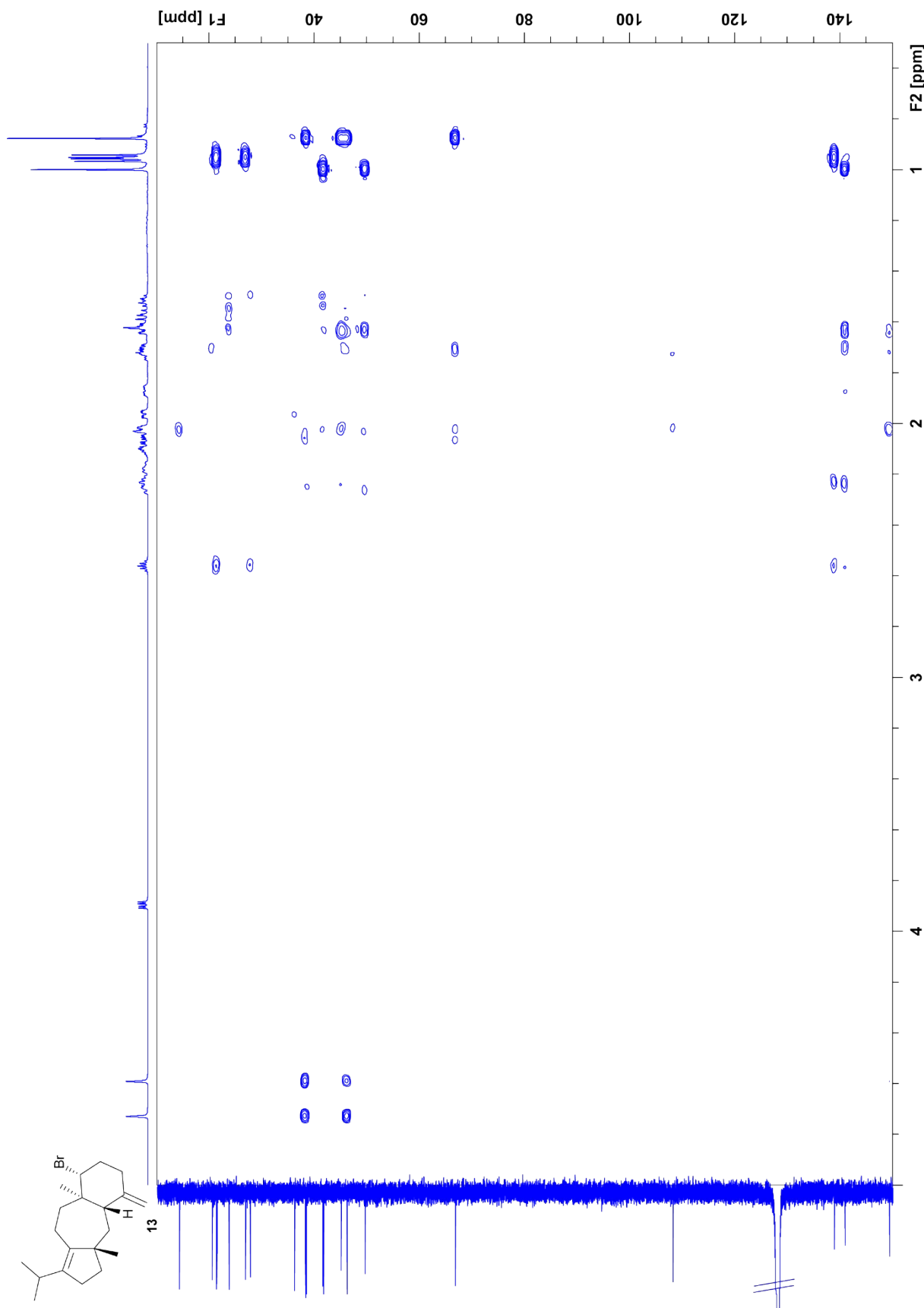
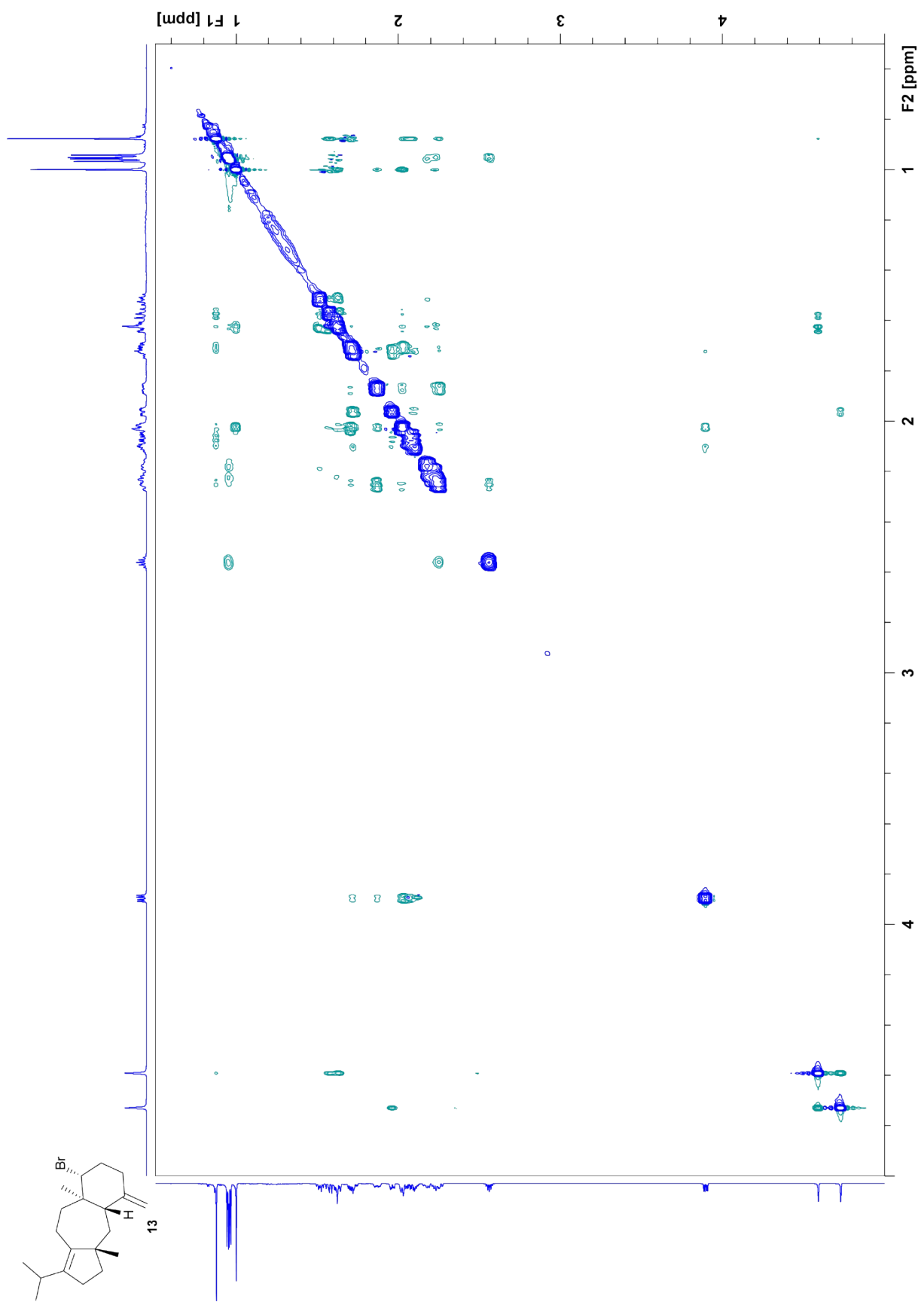


Figure S53. HMBC spectrum of **13** (700 MHz, C₆D₆).



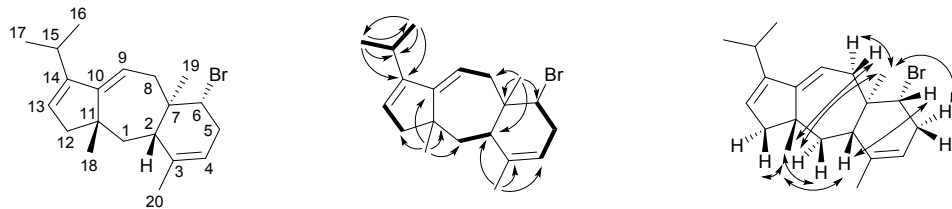


Figure S55. Carbon numbering and structure elucidation of **14**. H,H-COSY spin systems are represented by bold bonds, single headed arrows show HMBC correlations and NOESY correlations are depicted by double headed arrows.

Table S7. NMR data of (2*S*,6*R*,7*R*,11*S*)-6-bromodolasta-3,9,13-triene (**14**) in C₆D₆ recorded at 298 K.

C[a]		¹³ C[b]	¹ H[b]
1	CH ₂	37.38	1.71 (dd, <i>J</i> = 14.1, 2.0, H _α) 1.48 (dd, <i>J</i> = 14.1, 12.9, H _β)
2	CH	47.87	2.25 (m)
3	C _q	136.27	–
4	CH	122.04	5.02 (m)
5	CH ₂	36.47	2.66 (m, H _β) 2.51 (m, H _α)
6	CH	66.28	4.00 (dd, <i>J</i> = 10.4, 5.8)
7	C _q	41.41	–
8	CH ₂	39.33	2.99 (dd, <i>J</i> = 15.3, 9.8, H _β) 2.02 (dd, <i>J</i> = 15.4, 4.0, H _α)
9	CH	113.53	5.36 (dd, <i>J</i> = 9.8, 4.2)
10	C _q	154.90	–
11	C _q	45.46	–
12	CH ₂	49.78	2.20 (d, <i>J</i> = 16.7, H _β) 2.09 (dd, <i>J</i> = 16.7, 2.7, H _α)
13	CH	125.80	5.53 (m)
14	C _q	150.30	–
15	CH	25.83	2.34 (sept, <i>J</i> = 6.8)
16 ^[c]	CH ₃	22.23	1.10 (d, <i>J</i> = 6.8)
17 ^[c]	CH ₃	22.29	1.07 (d, <i>J</i> = 6.8)
18	CH ₃	24.28	1.07 (s)
19	CH ₃	11.51	1.01 (s)
20	CH ₃	22.68	1.44 (m)

[a] Carbon numbering indicates the origin of each carbon from GGPP by identical number as shown in Figure S55. [b] Chemical shifts δ in ppm, multiplicity: s = singlet, d = doublet, m = multiplet, br = broad, coupling constants *J* are given in Hertz. [c] Signals may be interchanged.

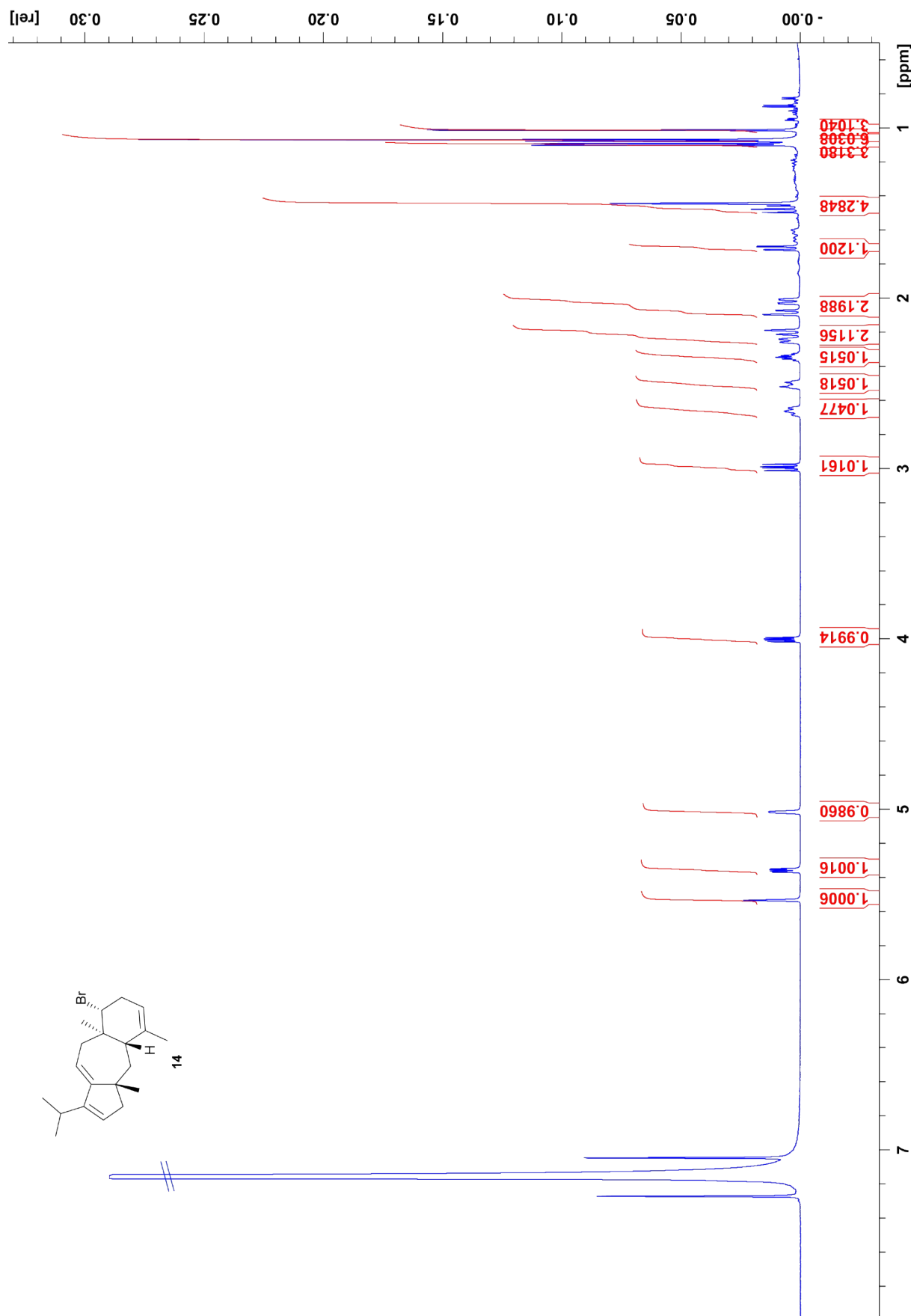


Figure S56. ^1H -NMR spectrum of **14** (700 MHz, C_6D_6).

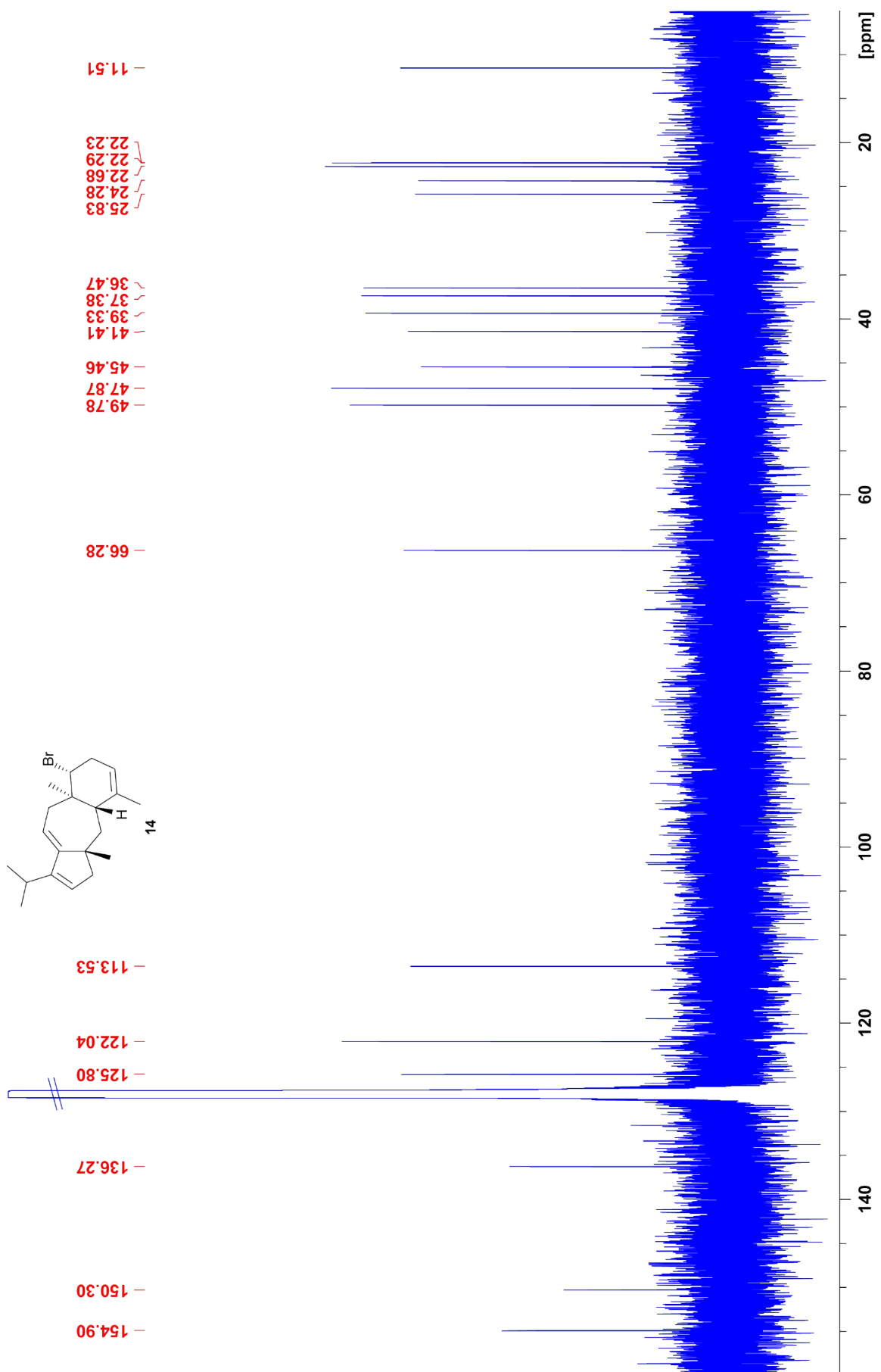


Figure S57. ^{13}C -NMR spectrum of **14** (175 MHz, C_6D_6).

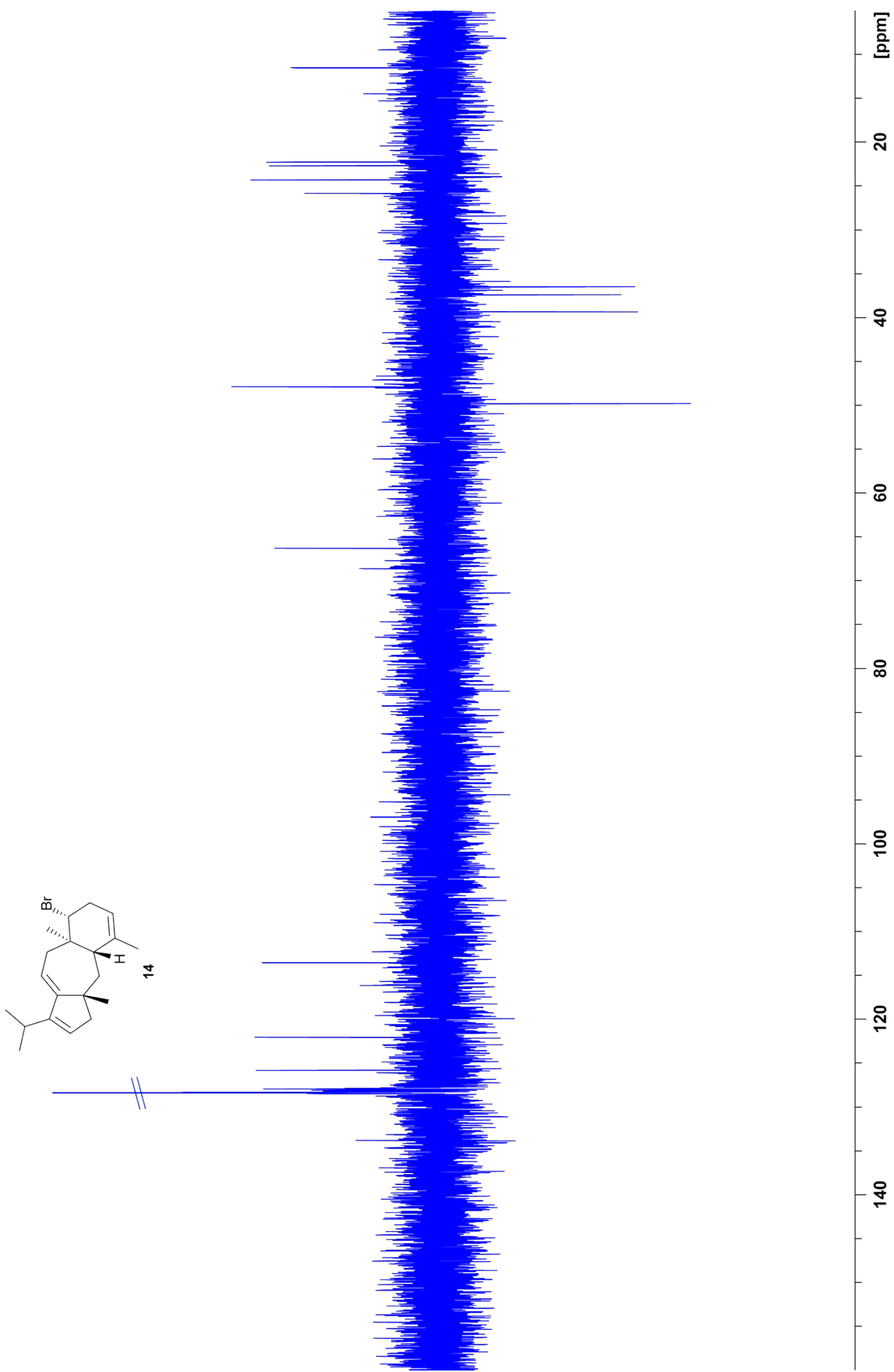


Figure S58. ^{13}C -DEPT spectrum of **14** (175 MHz, C_6D_6).

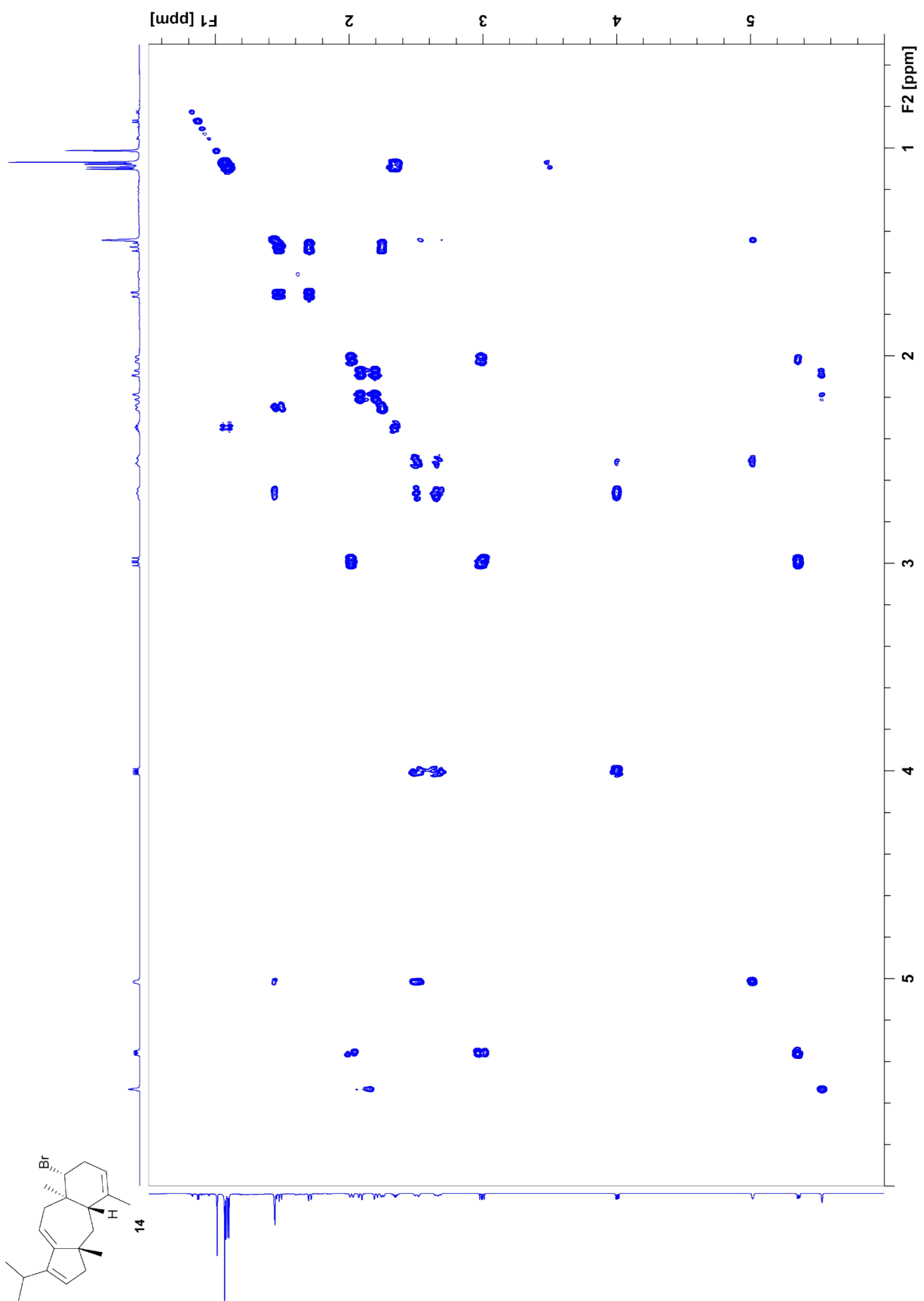


Figure S59. $^1\text{H},^1\text{H}$ -COSY spectrum of **14** (700 MHz, C_6D_6).

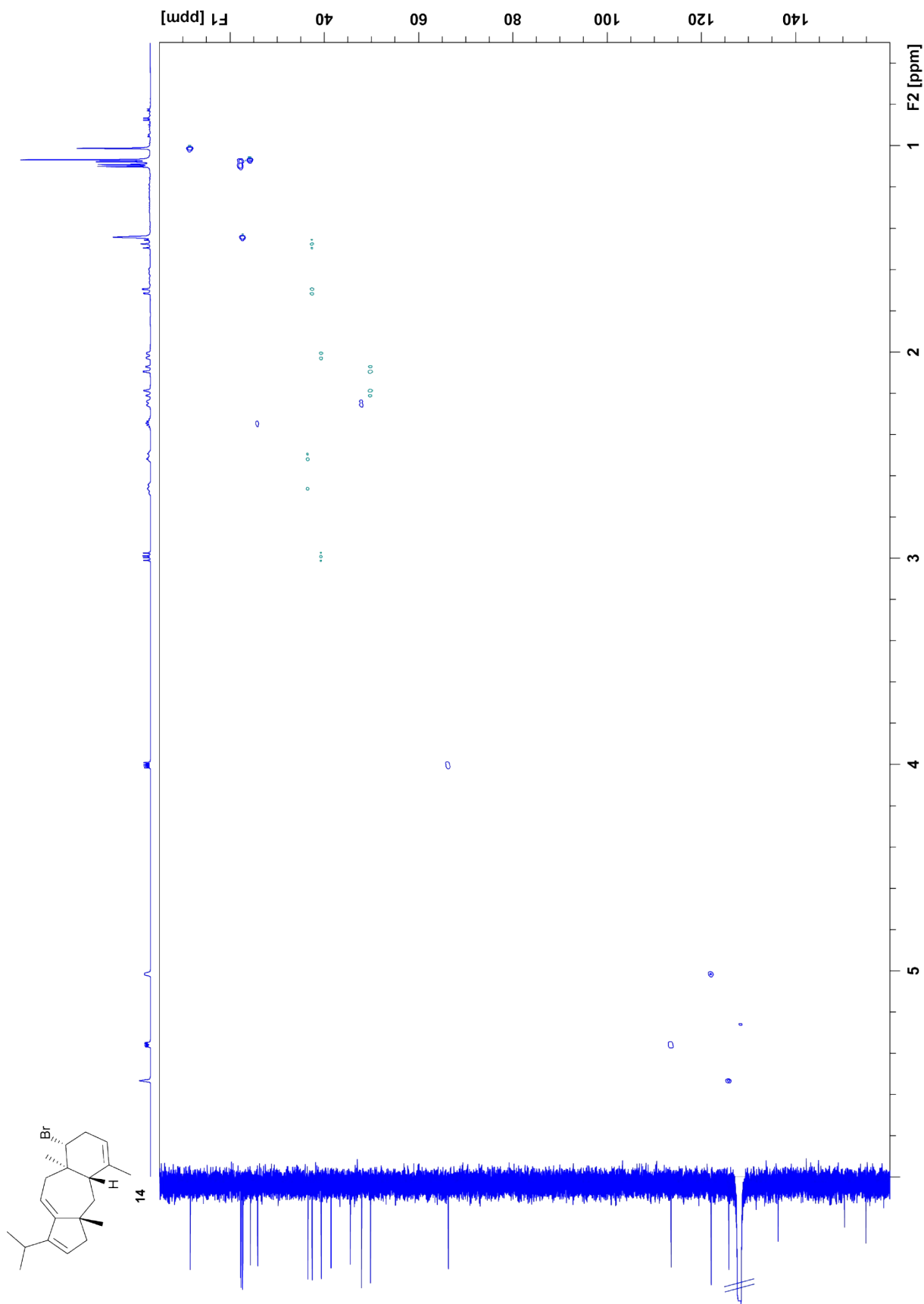


Figure S60. HSQC spectrum of **14** (700 MHz, C₆D₆).

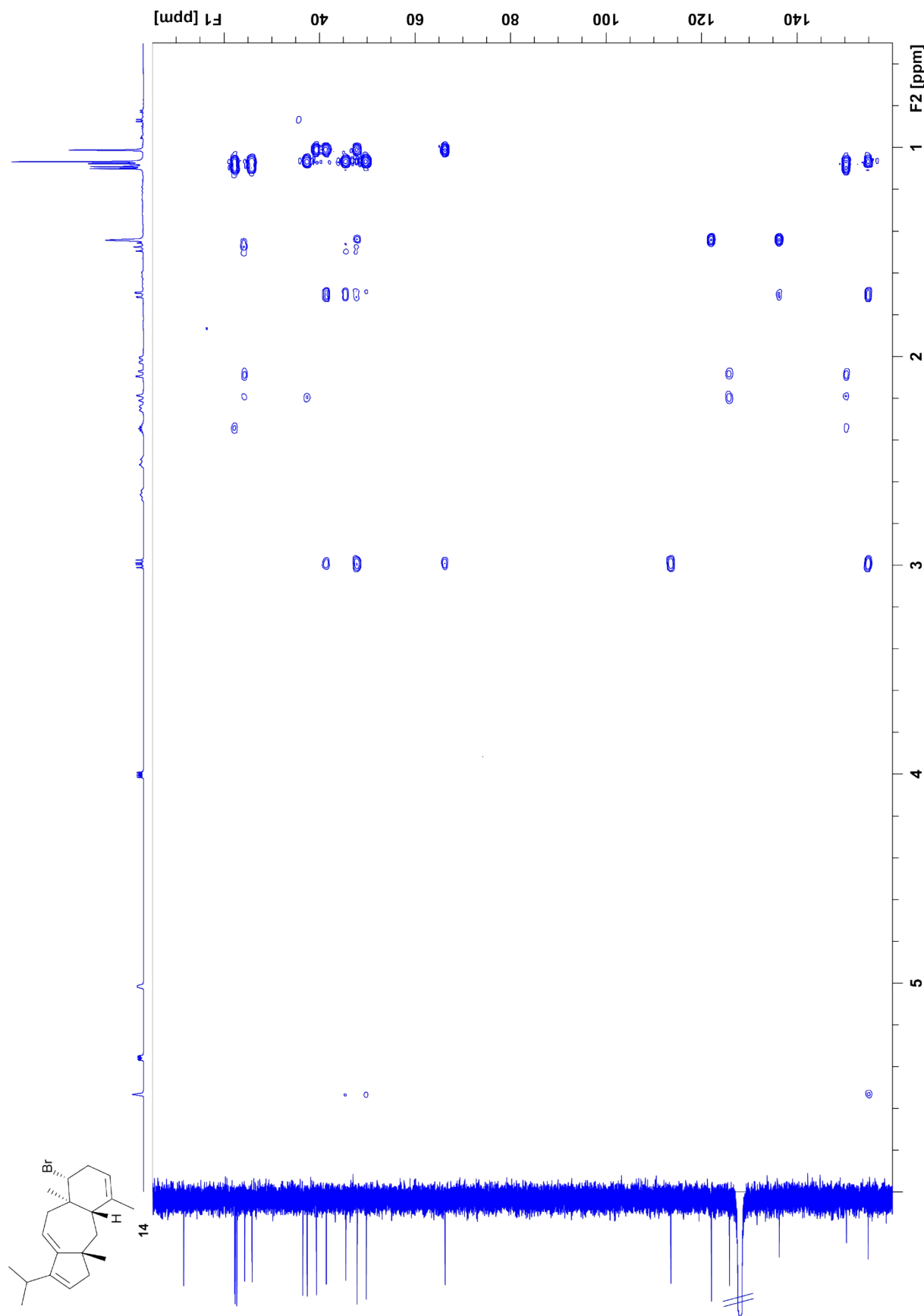


Figure S61. HMBC spectrum of **14** (700 MHz, C_6D_6).

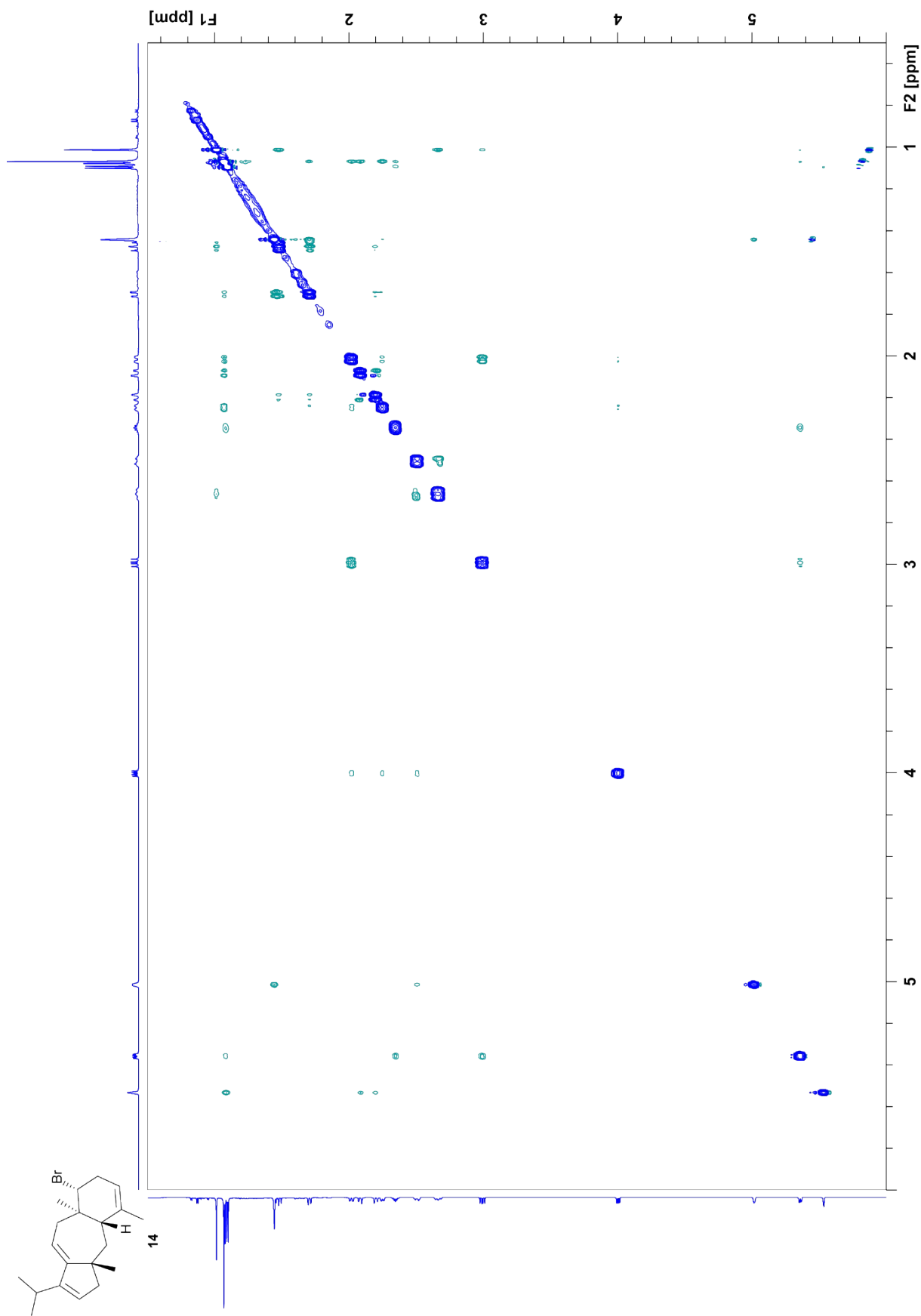


Figure S62. NOESY spectrum of **14** (700 MHz, C_6D_6).

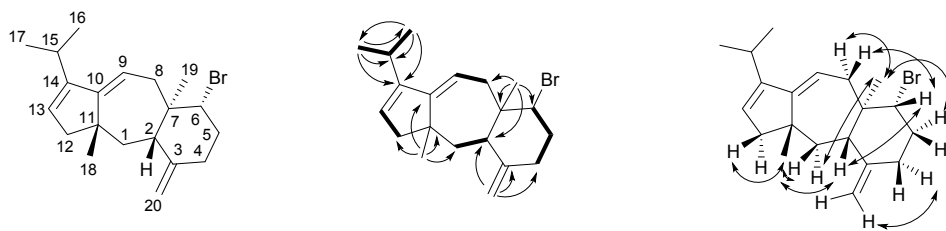


Figure S63. Carbon numbering and structure elucidation of **15**. H,H-COSY spin systems are represented by bold bonds, single headed arrows show HMBC correlations and NOESY correlations are depicted by double headed arrows.

Table S8. NMR data of (2*S*,6*R*,7*R*,11*S*)-6-bromodolasta-3(20),9,13-triene (**15**) in C₆D₆ recorded at 298 K.

		¹³ C ^[b]	¹ H ^[b]
1	CH ₂	39.24	1.71 (m, H _β) 1.57 (dd, <i>J</i> = 13.8, 2.3, H _α)
2	CH	48.45	2.12 (m)
3	C _q	149.55	–
4	CH ₂	38.57	1.96 (ddd, <i>J</i> = 12.9, 4.6, 2.6, H _β) 1.72 (m, H _α)
5	CH ₂	36.56	2.10 (m, H _α) 2.02 (m, H _β)
6	CH	68.19	3.75 (dd, <i>J</i> = 12.4, 4.5)
7	C _q	45.23	–
8	CH ₂	38.88	2.86 (dd, <i>J</i> = 14.8, 9.8, H _β) 2.18 (dd, <i>J</i> = 14.8, 4.6, H _α)
9	CH	112.98	5.33 (dd, <i>J</i> = 9.8, 4.7)
10	C _q	155.69	–
11	C _q	44.70	–
12	CH ₂	50.26	2.21 (d, <i>J</i> = 18.4, H _β) 2.09 (m, H _α)
13	CH	126.26	5.54 (br s)
14	C _q	149.85	–
15	CH	25.84	2.33 (m)
16	CH ₃	22.26	1.07 (d, <i>J</i> = 6.8)
17	CH ₃	22.34	1.09 (d, <i>J</i> = 6.8)
18	CH ₃	23.06	1.12 (s)
19	CH ₃	11.92	0.96 (s)
20	CH ₂	109.00	4.71 (m, H _E) 4.50 (br s, H _Z)

[a] Carbon numbering indicates the origin of each carbon from GGPP by identical number as shown in Figure S63. [b] Chemical shifts δ in ppm, multiplicity: s = singlet, d = doublet, m = multiplet, br = broad, coupling constants *J* are given in Hertz.

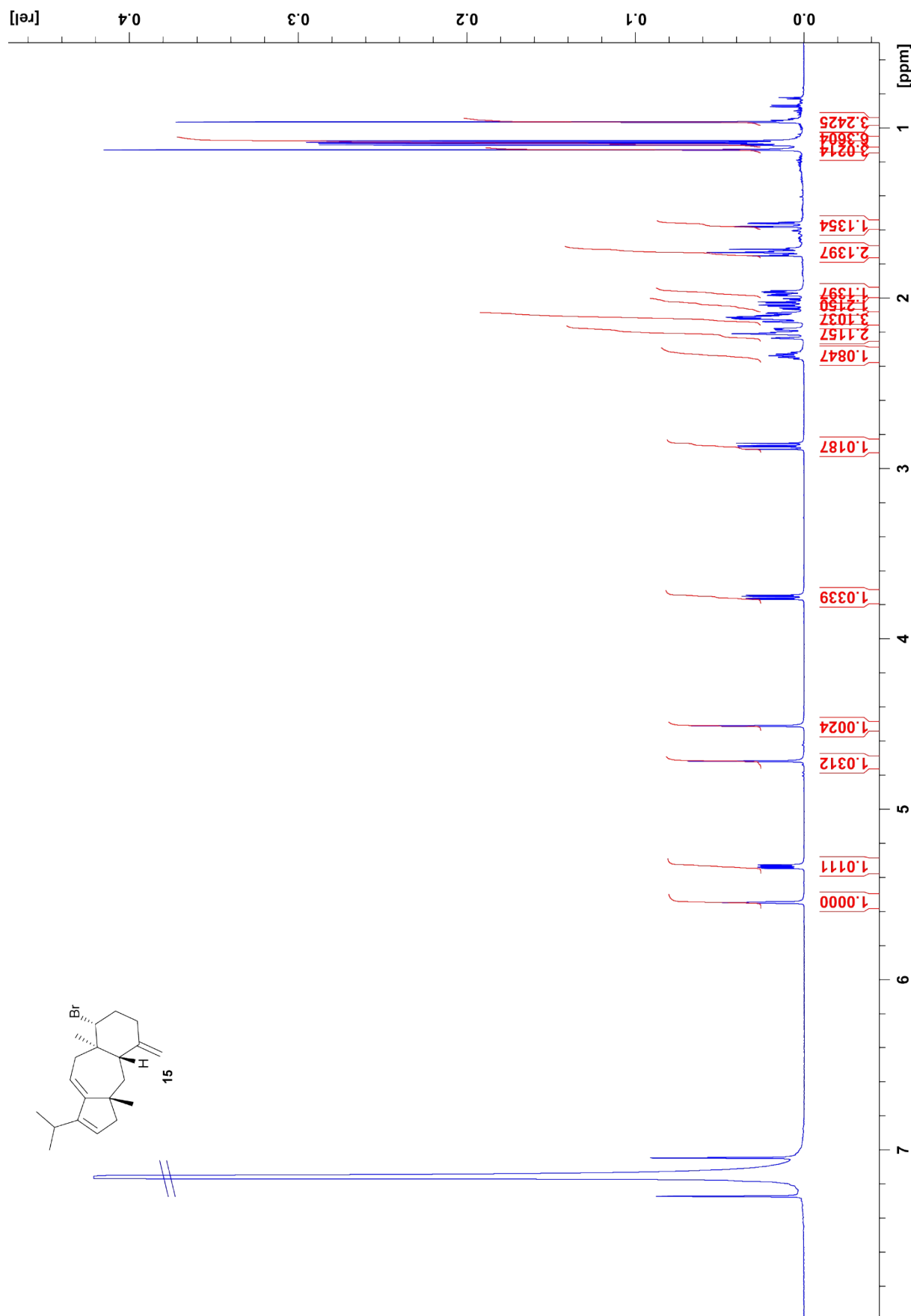


Figure S64. ¹H-NMR spectrum of **15** (700 MHz, C_6D_6).

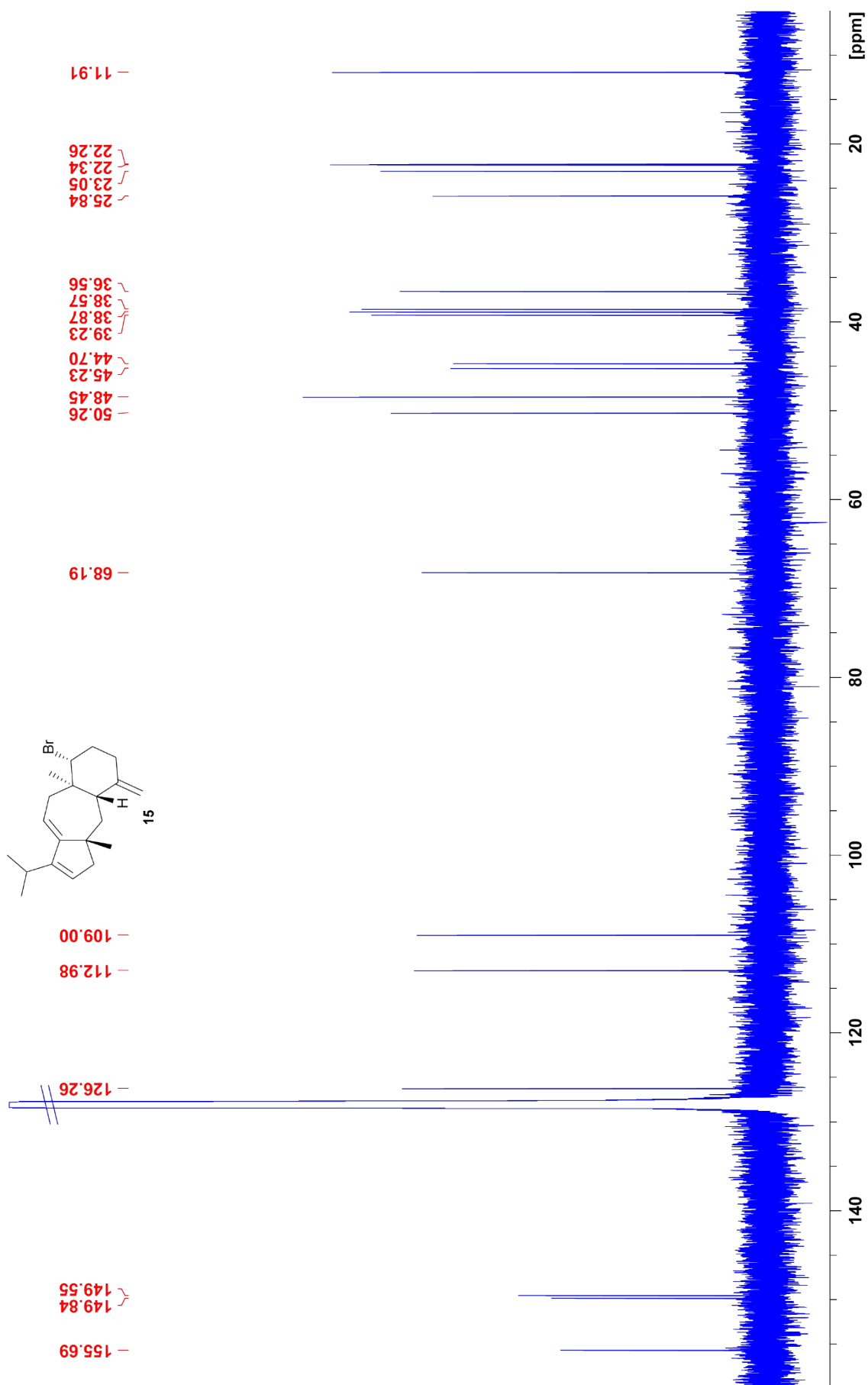


Figure S65. ^{13}C -NMR spectrum of **15** (175 MHz, C_6D_6).

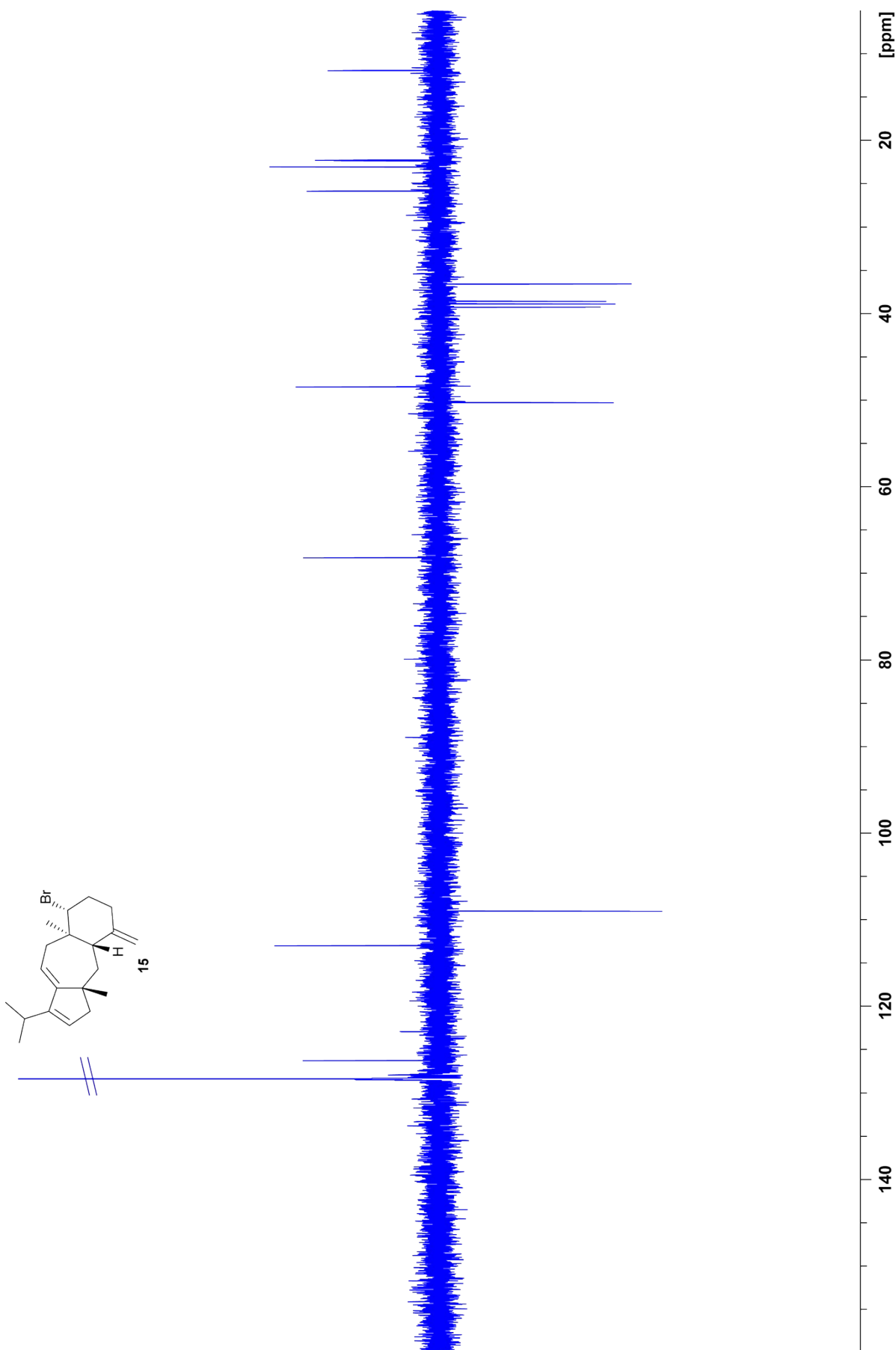


Figure S66. ^{13}C -DEPT spectrum of **15** (175 MHz, C_6D_6).

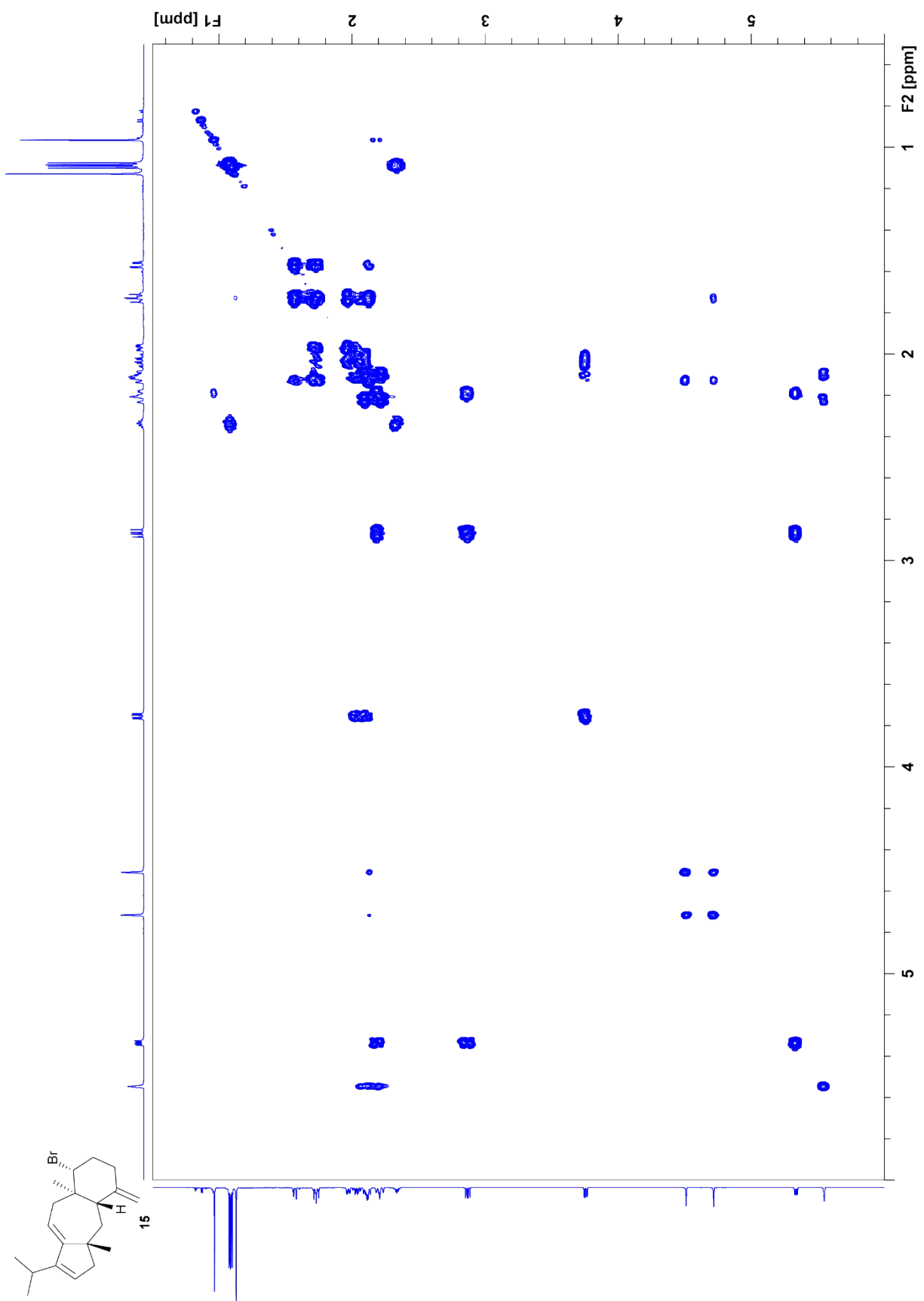


Figure S67. $^1\text{H},^1\text{H}$ -COSY spectrum of **15** (700 MHz, C_6D_6).

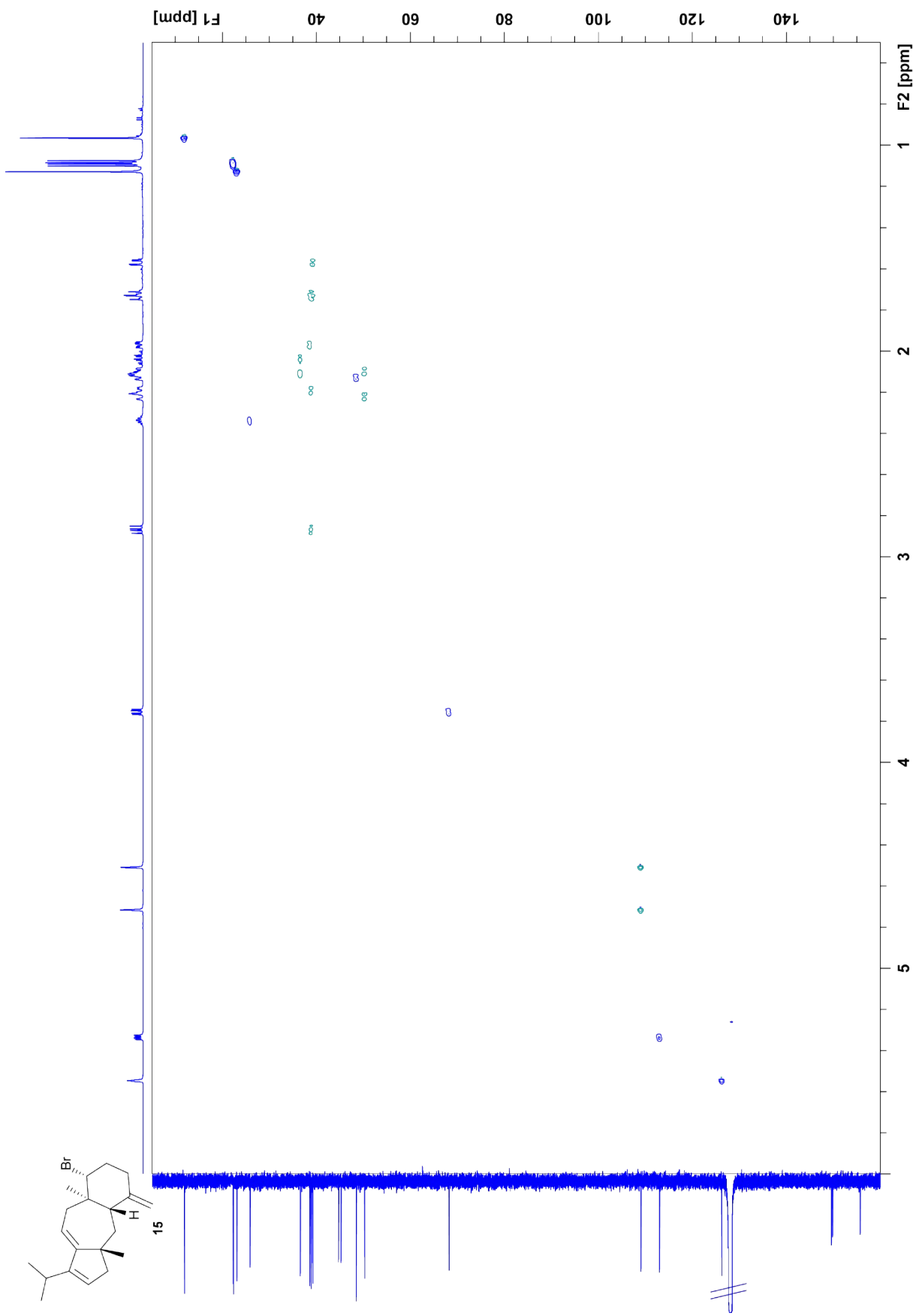


Figure S68. HSQC spectrum of **15** (700 MHz, C₆D₆).

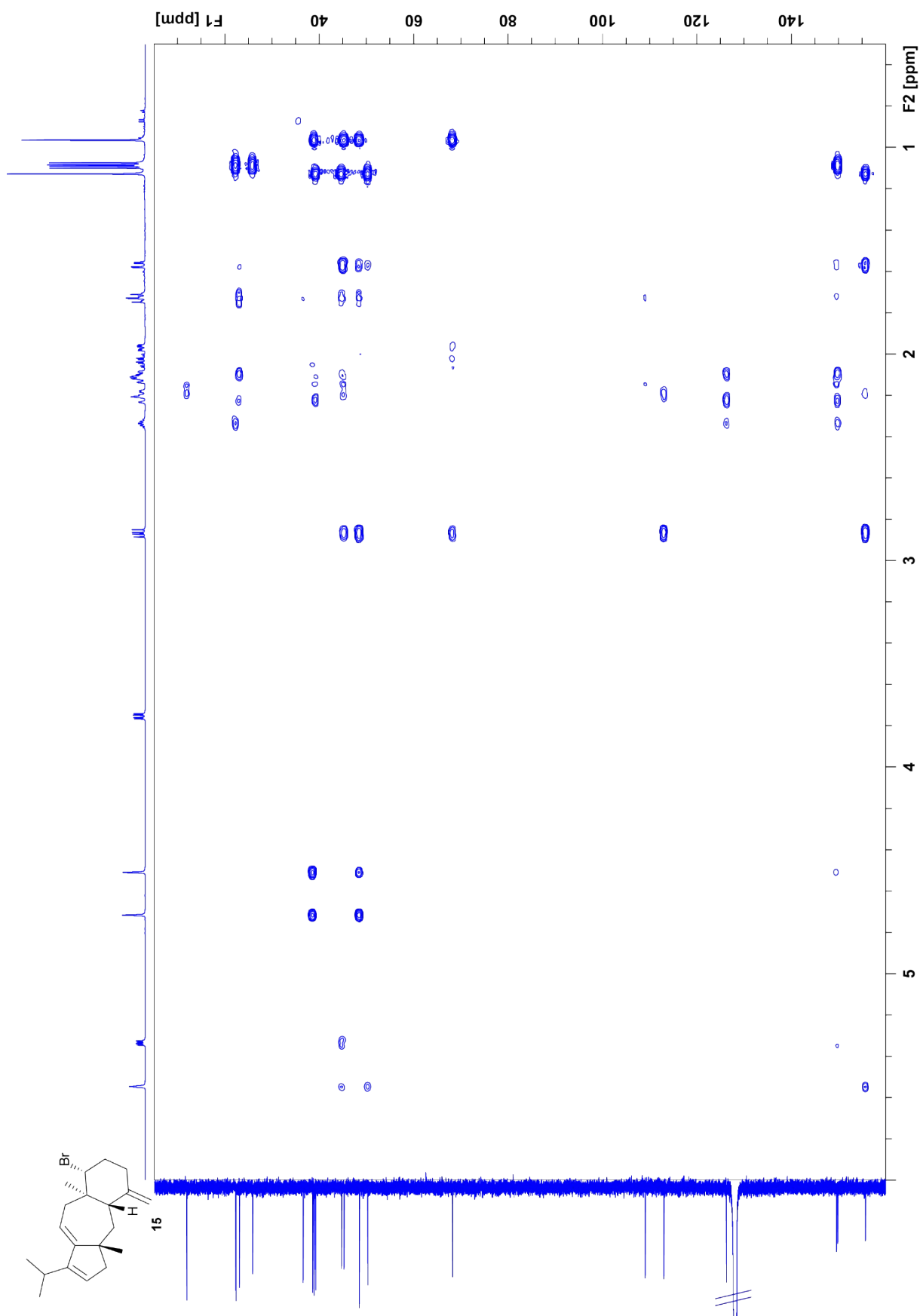


Figure S69. HMBC spectrum of **15** (700 MHz, C₆D₆).

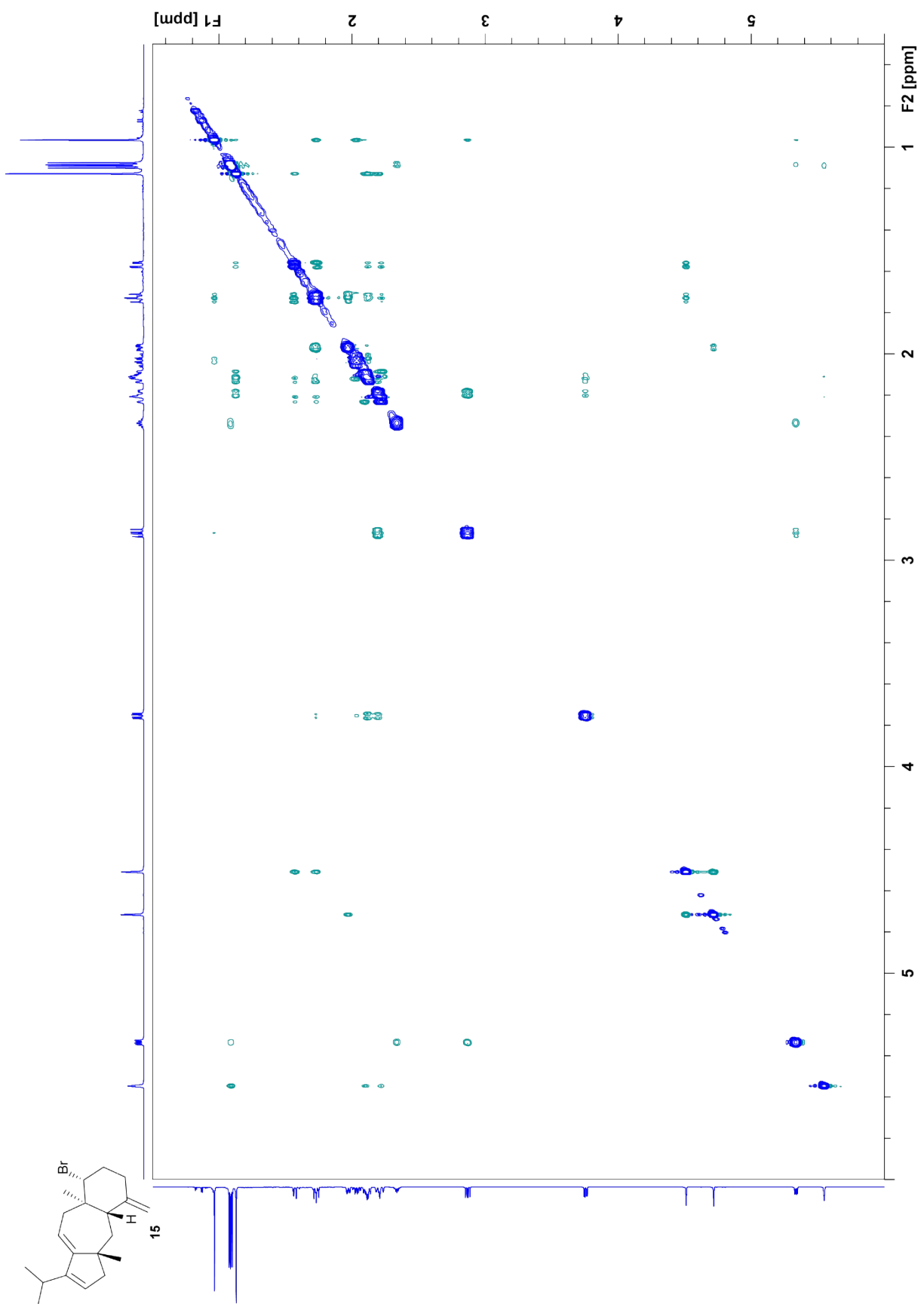


Figure S70. NOESY spectrum of **15** (700 MHz, C_6D_6).

References

- [1] M. M. Bradford, *Anal. Biochem.*, 1976, **72**, 248.
- [2] G. R. Fulmer, A. J. M. Miller, N. H. Sherden, H. E. Gottlieb, A. Nudelman, B. M. Stoltz, J. E. Bercaw and K. I. Goldberg, *Organometallics*, 2010, **29**, 2176.
- [3] J. Fälldt, M. Jonsell, G. Nordlander and A.-K. Borg-Karlson, *J. Chem. Ecol.*, 1999, **25**, 567.
- [4] J. Rinkel and J. S. Dickschat, *Org. Lett.*, 2019, **21**, 2426.
- [5] P. Rabe, J. Rinkel, B. Nubbemeyer, T. G. Köllner, F. Chen and J. S. Dickschat, *Angew. Chem. Int. Ed.*, 2016, **55**, 15420.
- [6] L. Lauterbach, J. Rinkel and J. S. Dickschat, *Angew. Chem. Int. Ed.*, 2018, **57**, 8280.
- [7] J. Rinkel and J. S. Dickschat, *Beilstein J. Org. Chem.*, 2019, **15**, 789.
- [8] J. Rinkel, P. Rabe, X. Chen, T. G. Köllner, F. Chen and J. S. Dickschat, *Chem. Eur. J.*, 2017, **23**, 10501.
- [9] J. Rinkel and J. S. Dickschat, *Beilstein J. Org. Chem.*, 2019, **15**, 1008.
- [10] P. Rabe, L. Barra, J. Rinkel, R. Riclea, C. A. Citron, T. A. Klapschinski, A. Janusko and J. S. Dickschat, *Angew. Chem. Int. Ed.*, 2015, **54**, 13448.
- [11] G. Bian, J. Rinkel, Z. Wang, L. Lauterbach, A. Hou, Y. Yuan, Z. Deng, T. Liu and J. S. Dickschat, *Angew. Chem. Int. Ed.*, 2018, **57**, 15887.
- [12] T. Sassa, H. Kenmoku, K. Nakayama and N. Kato, *Biosci. Biotechnol. Biochem.*, 2004, **68**, 1608.
- [13] P. Rabe, J. Rinkel, E. Dolja, T. Schmitz, B. Nubbemeyer, T. H. Luu and J. S. Dickschat, *Angew. Chem. Int. Ed.*, 2017, **56**, 2776.
- [14] K. H. Shaker, M. Müller, M. A. Ghani, H.-M. Dahse and K. Seifert, *Chem. Biodivers.*, 2010, **7**, 2007.
- [15] P. Rabe and J. S. Dickschat, *Angew. Chem. Int. Ed.*, 2013, **52**, 1810.
- [16] P. Rabe, T. Schmitz and J. S. Dickschat, *Beilstein J. Org. Chem.*, 2016, **12**, 1839.
- [17] P. Rabe, J. Rinkel, T. A. Klapschinski, L. Barra and J. S. Dickschat, *Org. Biomol. Chem.*, 2016, **14**, 158.
- [18] X. Lin and D. E. Cane, *J. Am. Chem. Soc.*, 2009, **131**, 6332.
- [19] P. Rabe, T. A. Klapschinski and J. S. Dickschat, *ChemBioChem*, 2016, **17**, 1333.
- [20] C. Nakano, S. Horinouchi and Y. Ohnishi, *J. Biol. Chem.*, 2011, **286**, 27980.
- [21] C. Nakano, T. Tezuka, S. Horinouchi and Y. Ohnishi, *J. Antibiot.*, 2012, **65**, 551.
- [22] D. E. Cane, J. K. Sohng, C. R. Lamberson, S. M. Rudnicki, Z. Wu, M. D. Lloyd, J. S. Oliver and B. R. Hubbard, *Biochemistry*, 1994, **33**, 5846.
- [23] W. K. W. Chou, I. Fanizza, T. Uchiyama, M. Komatsu, H. Ikeda and D. E. Cane, *J. Am. Chem. Soc.*, 2010, **132**, 8850.
- [24] P. Rabe, M. Samborskyy, P. F. Leadlay and J. S. Dickschat, *Org. Biomol. Chem.*, 2017, **15**, 2353.
- [25] T. A. Klapschinski, P. Rabe and J. S. Dickschat, *Angew. Chem. Int. Ed.*, 2016, **55**, 10141.
- [26] P. Rabe, K. A. K. Pahirulzaman, J. S. Dickschat, *Angew. Chem. Int. Ed.*, 2015, **54**, 6041.
- [27] N. L. Brock, K. Huss, B. Tudzynski and J. S. Dickschat, *ChemBioChem*, 2013, **14**, 311.
- [28] I. Burkhardt, T. Siemon, M. Henrot, L. Studt, S. Rösler, B. Tudzynski, M. Christmann and J. S. Dickschat, *Angew. Chem. Int. Ed.*, 2016, **55**, 8748.
- [29] K. Murai, L. Lauterbach, K. Teramoto, Z. Quan, L. Barra, T. Yamamoto, K. Nonaka, K. Shiomi, M. Nishiyama, T. Kuzuyama and J. S. Dickschat, *Angew. Chem. Int. Ed.*, 2019, **58**, accepted (doi: 10.1002/anie.201907964).
- [30] C.-M. Wang, R. Hopson, X. Lin and D. E. Cane, *J. Am. Chem. Soc.*, 2009, **131**, 8360.
- [31] P. Baer, P. Rabe, K. Fischer, C. A. Citron, T. A. Klapschinski, M. Groll and J. S. Dickschat, *Angew. Chem. Int. Ed.*, 2014, **53**, 7652.